Spring 2020

# Experimental and modeling studies using packed bed reactors: Liquid phase ethylene production by hydrogenation of acetylene

Humayun Shariff



Department: Chemical and Biochemical Engineering

# EXPERIMENTAL AND MODELING STUDIES USING PACKED BED REACTORS: LIQUID PHASE ETHYLENE PRODUCTION BY HYDROGENATION OF ACETYLENE

by

HUMAYUN SHARIFF

A DISSERTATION

Presented to the Graduate Faculty of the

MISSOURI UNIVERSITY OF SCIENCE AND TECHNOLOGY

In Partial Fulfillment of the Requirements for the Degree

DOCTOR OF PHILOSOPHY

in

CHEMICAL ENGINEERING

2020

Approved by:

Muthanna Al-Dahhan, Advisor
Jee-Ching Wang
Xinhua Liang
Ali Rownaghi
Marcus Foston

## PUBLICATION DISSERTATION OPTION

This dissertation consists of the following four articles, formatted in the style used by the Missouri University of Science and Technology:

Paper I, Pages 17–43, is intended for submission to AIChE Journal in May 2020.

Paper II, Pages 44-64, is intended for submission to Industrial & Engineering Chemistry Research Journal in May 2020.

Paper III, Pages 65–93, is intended for submission to Chemical Engineering Journal in May 2020.

# ABSTRACT

Gas-phase catalytic hydrogenation of acetylene to produce ethylene, commonly practiced in industries, has green oil formation, which leads to catalyst deactivation and sometimes reactor runaway risks due to high exothermicity. To overcome these issues as well as to increase the selectivity and conversion, liquid-phase hydrogenation of acetylene was investigated in packed bed reactors (PBR) using a commercial catalyst. The reactor performance of two-phase flow PBRs was assessed experimentally complemented by a validated mathematical model at different scales.

The selective hydrogenation of acetylene in the liquid phase over a commercial 0.5 wt% $Pd/Al_2O_3$ catalyst was investigated in a slurry and basket stirred-tank reactor to extract the intrinsic and apparent kinetics respectively, and in packed bed reactors in trickle flow and upflow at selected operating conditions to study the reactor performance. The selective solvent, N-methyl pyrrolidone (NMP) with absorbed acetylene, was used as the liquid phase. Rate equation models were derived and fit to the experimental data to estimate the kinetic parameters. Using Residence Time Distribution (RTD) experiments at scaled-down operating conditions for different catalyst bed packings and types of reactors (with and without thermowell), the axial dispersion coefficient and dynamic liquid holdup were measured and correlated. The reactor performance was evaluated in the packed bed with the downflow and upflow of the reactants. Both the mode resulted in high conversion and ethylene selectivity while upflow performed better. The reactor scale model, integrating the kinetics and the hydrodynamic parameters along with the wetting and mass transfer correlations, was able to simulate the experimental data with good agreement.

# ACKNOWLEDGMENTS

First and foremost, I would like to thank and praise God for his kindness and blessing throughout my life. I would like to express my deepest gratitude to my advisor and mentor, Dr. Muthanna H. Al-Dahhan, for his constant support and guidance during the course of my Ph.D. His active and optimistic personality has inspired me greatly. His encouragement and freedom of thought enabled me to think creatively and be self-driven.

I would like to thank my advising committee, Dr. Jee-Ching Wang, Dr. Xinhua Liang, Dr. Ali Rownaghi, and Dr. Marcus Foston for their critical comments and interest in evaluating my Ph.D. research.

My special appreciation goes to my mentors during my internships at Abbvie Pharmaceuticals. I would like to thank them for their constructive comments, personal advice, and guidance, which helped me to develop critical thinking and industrial exposure.

I would like to thank my research group members and friends at S&T, whose cooperation and useful discussions helped my work. I would also like to thank the amazing technicians in our department, Dean, Rusty, and Michael, who helped in technical discussions and troubleshooting my unit, which made my experiments go smoothly. I extend my thanks to the Department office staff for their quick support.

Finally, I would like to thank my wife, Triya, who has been my pillar of strength throughout this Ph.D. journey. Her support and patience made this whole process a wonderful journey. I would like to thank my son Ayaan and my daughter Ariya, who have been my bundle of joy. I would also like to thank my dad, mom, and brothers, who kept me encouraged from home.

# TABLE OF CONTENTS

Page

# LIST OF ILLUSTRATIONS

PAPER I Page

PAPER II



PAPER III

# LIST OF TABLES

# NOMENCLATURE

| Symbol | Description |
|---|---|
| a | Reaction order with respect to acetylene |
| A | cross section area ($m^2$) |
| b | Reaction order with respect to hydrogen |
| Bi | Biot Number |
| $C_{Ae}$ | equilibrium concentration of component ($mol/m^3$) |
| Ci, [$C_i$] | Concentration of species ($mol/m^3$) |
| $D_{AL}$ | Axial dispersion coefficient ($m^2/s$) |
| $D_p$ | equivalent particle diameter (m) |
| $D_R$ | diameter of reactor (m) |
| $E_a$ | Activation Energy (kJ/mol) |
| H | Heat of adsorption (kJ/ mol) |
| K | Adsorption equilibrium constant ($m^3/mol$) |
| $k_{C2H2}$ | Power law rate constant ($(m^3)^{a+b}$ $mol^{1-a-b}$ /(g-cat.min)) |
| $(ka)_{GL}$ | Gas-liquid mass transfer coefficient |
| $k_{GS,A}$ | Gas –solid interface mass transfer coefficient |
| $k_{LS,A}$ | Liquid –solid interface mass transfer coefficient |
| k | Rate constant for LHHW model (mol/g-cat/min) |
| L | Length of reactor (m) |
| P | Pressure (psig) |

| | |
|---|---|
| $Pe_L$ | Peclet Number - $u_{sL}$*L /$D_{AX}$ (-) |
| R | Gas constant (J/mol/K) |
| *Re* | Reynold's number |
| r | Reaction rate (mol/g-cat/min) |
| T | Temperature (K) |
| $T_m$ | Mean temperature (K) |
| X | Conversion (%) |
| x | coordinate in the external shell to completely dry surface or plane where B is depleted (-) |
| y | coordinate in the external shell to actively wetted surface (-) |
| z | distance along the reactor (m) |

Greek Letters

| | |
|---|---|
| $\eta_{CE}$ | Wetting efficiency |
| $\varepsilon_L$ | Liquid Hold up |
| $\eta_o$ | Overall effectiveness Factor(-) |
| $\varepsilon_B$ | bed voidage (-) |
| $\varepsilon_p$ | particle porosity(-) |
| $\omega$ | the fraction of catalyst |

Subscripts

| | |
|---|---|
| d,dw,w | Dry, dry-wet and wet zones of catalyst pellet |
| G,L | Gas, Liquid phase |

# 1. INTRODUCTION

Ethylene is considered one of the primary raw materials and the most important building blocks in the petrochemical industry. The global yearly demand for ethylene is over 145 million tons, with an annual increase of 3% for the next five years [1, 2]. More than 60% of ethylene production was utilized for polyethylene production. The other major products are polyvinyl chloride, polyester, polystyrene, resins, fibers, and packaging materials. Additionally, Ethylene-to-liquid fuels (ETL) technology has also been under active research to convert ethylene to liquid fuel to meet the increasing energy crisis. This process is to oligomerize ethylene to higher hydrocarbons. A need for a cost-effective process along with an alternate source to produce ethylene is indispensable.

Ethylene ($C_2H_4$) is manufactured by different processes such as steam cracking of ethane/propane/naphtha, catalytic pyrolysis, fluid catalytic cracking, catalytic dehydrogenation, Fischer-Tropsch process, and the recently developed, oxidative dehydrogenation of ethane [1, 3]. The most common practice in the industry is the steam cracking of naphtha, which produces ethylene along with acetylene ($C_2H_2$) as the by-product. The concentration of acetylene impurities in the $C_2$-cut from the cracker needs to be reduced from 1% to less than 5 ppm to reach the polymerization grade purity of the effluent [4-7]. Small traces of acetylene can deactivate the catalyst used for polymerization of ethylene to manufacture polyethylene and other valuable products, i.e., the downstream processing of the steam cracker effluent. Although acetylene can be absorbed from the gas mixture, it is more economically beneficial to selectively hydrogenate acetylene to ethylene

as well as critically reducing the formation of ethane [5, 8]. The hydrogenation of acetylene must be catalytic, assuring high selectivity to ethylene formation.

## 1.1. GAS PHASE HYDROGENATION OF ACETYLENE

Acetylene, a triple-bond hydrocarbon, though considered as an impurity in olefins, has its utilities and highly pure acetylene is also in high demand. In industry, the acetylene hydrogenation scheme in the gas phase takes place majorly as two variants in industries: front end and tail end. The significant difference between these two variants is the location of the demethanizer and the hydrogenation reactor. The front end variant in the downstream treatment of a cracking unit has the acetylene hydrogenation reactor located before the demethanizer. In this variant, the feed to the reactor includes $H_2$, $CH_4$, and CO where the $H_2$:$C_2H_2$ ratio is very high compared to the tail end variant. When the acetylene hydrogenation reactor is placed after the demethanizer, it is considered the tail-end variant where the hydrogen content is close to the stoichiometric ratio concerning acetylene [9, 10]. The tail end variant is of the typical configuration used in the industries where the reaction involves only the $C_2$ cut [10]. The major disadvantage was the formation of ethane and higher hydrocarbons, along with the risk of thermal runaway during reactions. Although many studies have reported and tested this reaction in the gas phase, there has always been an area for process improvement and development.

In many investigations, Carbon monoxide (CO) was added in relatively small amounts to control the formation of ethane from ethylene. CO has better adsorption on the active site of the catalyst compared to ethylene but lower than acetylene. It can also be said that CO inhibits $C_2H_6$ formation, which can improve the selectivity towards ethylene.

Moreover, CO addition can prevent the ethylene hydrogenation at low concentrations of acetylene [4, 7, 11-18]. Hence, the effect of CO was accounted for in most of the kinetic studies, and CO was included in the rate models [19, 20]. It has also been studied that CO can affect the rate of acetylene conversion too, and excess addition of CO could lead to thermal runaway conditions. It was reported that the decrease in the rate of hydrogenation might be due to the blockage of the hydrogen adsorption sites by CO. However, at high fractional coverage of acetylene, the effect of CO poisoning the ethylene adsorption sites was insignificant on ethylene selectivity [16, 19].

**1.1.1. Palladium Based Catalyst.** The increase in the production of ethylene is directly related to the catalyst selectivity. Hence, the selective hydrogenation process used to convert acetylene to ethylene in a gas phase in industries is catalyst dependent.

Group VIII metals, in general, are effective catalysts for hydrogenating alkynes. High ethylene selectivity to Group VIII was typically explained as ethylene being easily displaced from the active site and low activity for ethylene hydrogenation. Palladium-based catalysts have been widely used to hydrogenate acetylene selectively. For many decades research has been done on this topic as found in the open literature [10, 19]. Bond and group investigated Pd catalyst supported on alumina after having compared many transition metals over alumina supports like iridium, osmium, platinum, rhodium, and ruthenium. Their comprehensive work to identify palladium as the better catalyst for selective hydrogenation, in terms of activity and selectivity, paved the way for its use in industries [21-26].

The acetylene hydrogenation is conducted typically in the gas phase using a palladium (Pd) catalyst supported on $\alpha$-$Al_2O_3$. Of those metals in Group VIII, Pd has the

highest ethylene selectivity, despite a high activity for ethylene hydrogenation, as competitive adsorption of acetylene assists in ethylene desorption [27-30]. Eggshell catalysts with 0.01 to 0.1% Pd on $\alpha$-$Al_2O_3$ support were also commonly used in the catalytic hydrogenation of acetylene where acetylene associatively and dissociatively adsorbs to the catalyst surface [4]. Dissociative adsorption contributes to oligomerization and the formation of green oil, which acts as a catalyst poison. In the gas phase reaction, carbon monoxide was used to occupy some active sites and minimize ethylene adsorption, inhibiting the over-hydrogenation of ethylene to ethane. A more detailed explanation of the active sites involved in the hydrogenation mechanism can be found elsewhere [10, 19, 28, 29].

The kinetics of the $Pd/Al_2O_3$ catalyst for selective hydrogenation was developed and studied by many researchers [7, 12-15, 20, 24, 28, 31]. Bos and Westerterp (1993) reviewed the kinetics and mechanism of the selective hydrogenation of acetylene in the presence of ethylene using different Pd-supported catalysts, primarily focusing on alumina supports. Borodziński and Bond (2006, 2008) comprehensively reviewed the selective hydrogenation of acetylene in ethylene-rich streams on Palladium catalysts. Pd catalysts have shown high activity along with high selectivity towards ethylene in comparison with other metal catalysts. For this reason, supported catalysts use a little amount of palladium. Their review also mentioned the addition of promoters to the $Pd/Al_2O_3$ catalysts.

Various studies have been conducted over the years to determine the ideal heterogeneous catalyst for selective hydrogenation. Many metal promoters like Ag, Au, Ni, Cu of different loading have been used to enhance selectivity by reducing the adsorption energy of ethylene on the surface of the catalyst, thereby controlling the Pd

activity [19]. To mention some promoters used along with Pd are Si, Ag, Ti, Cu, Ni, K, Co, Pb, Ce, Nb, Re, and Zn. Bimetallic Pd catalysts have been of keen interest for selective hydrogenation of acetylene, currently used in industries [32-36]. The bimetallic catalysts have also proven to be more efficient and conservative when it comes to selective for ethylene production. Considering the selection of the catalyst based on the ethylene selectivity and performance, the catalyst life is also significant.

**1.1.2. Green Oil Formation and Catalyst Deactivation.** Apart from ethane formation, another undesirable byproduct formed during acetylene hydrogenation is the hydro-polymerization (oligomerization) of acetylene into $C_4^+$ compounds commonly called as the 'green oil'. Green oil affects both selectivity and conversion of the reaction [12, 37-41].

Process conditions, such as $H_2$:$C_2H_2$ ratio and temperature influence the rate of green oil formation [4]. The green oil was majorly formed due to the surface acidity of the catalytic support [40]. The increase in the formation of green oil may lead to deactivation of the catalyst and at scale clogging of pipes leading to shut down. This further needs regeneration of catalyst which is expensive economically and time-consuming. It was very critical to limit the formation of green oil to maintain a good heat transfer during the reaction as well.

## 1.2. LIQUID PHASE HYDROGENATION OF ACETYLENE

Solvent extraction to separate acetylene from the gaseous mixture in a cracking process using an organic solvent such as N,N-dimethylformamide (DMF) or N-methyl pyrrolidone (NMP) is typically practiced industrial technique [6]. However, extractions

using organic solvents are disadvantageous in terms of the significant loss of the solvent after multiple operations and the low solubility selectivity of acetylene over ethylene. Therefore, it is beneficial to search for efficient solvent systems that selectively and reversibly interact with acetylene for the acetylene/ethylene separation. The use of volatile organic solvent for the gas storage reduces the purity of acetylene because it can exhaust together with the gas stream as acetylene was commonly available as a compressed gas dissolved in acetone [7]. Recently, the use of Ionic liquids (IL) as selective absorbents for acetylene was also studied [42]. It was mentioned that the basic anions in the ionic liquids could combine with the acidic hydrogen atom of acetylene. The acidic hydrogen atom or atoms in acetylene have a pKa value of 25. The ionic liquid used in their study was [DMIM][$MeHPO_3$], with a methyl-phosphite group carrying the negative charge. The solubility of acetylene and propyne were very high than ethene and propene, confirming the interchange between the hydrogen atom and the $MeHPO_3$ anion. The use of ILs not only increases the performance of the catalyst but also controls the formation of ethane and other oligomers [43]. On the other hand, scaling up a process using ILs may be a challenge due to the limited research available.

Utilizing the acetylene absorbed in a solvent will be effective to have high acetylene availability, controlled heat profile in the reactor, and reduce the formation of green oil, thereby improving the catalyst lifetime. A review of liquid-phase hydrogenation studies is shown in Table 1.

Men'shchikov et al. (1983) [6] first investigated the liquid phase hydrogenation of acetylene in pyrolysis gas. The motivation for his research was that by using liquid phase rather than a gas phase for acetylene hydrogenation, the thermal stability of the reactor

increases, preventing runaway conditions. In their study, the liquid phase was not used as a selective solvent for acetylene. The experiments were conducted in a reactor where the gas stream suspended the catalyst present in the liquid phase at atmospheric pressure at a temperature range of 17-40$^{o}$C. The experiments were performed using Pd on activated carbon (Pd/C) after testing on alumina and zirconium oxide supports. Acetone was identified was the ideal liquid phase amongst dimethylformamide (DMF), alcohols (ethanol, methanol), esters (amyl acetate, ethyl acetate, propyl acetate), and water. It was observed that for low Pd loading on the catalysts at high acetylene feed, hydrogenation stopped as acetylene acted as a poison to the catalyst. The poisoning was mainly due to the displacement of hydrogen atoms from the active sites by acetylene. Their study did not follow any pattern but was more random. For every catalyst loading, different gas flow rates were used, which failed to provide the consistency needed to prove the results. Using a volatile solvent like acetone may not be a good choice to conduct experiments at higher temperatures and pressures.

**1.2.1. Liquid Phase Hydrogenation in Monolith Reactors.** Irandoust's group investigated the liquid phase hydrogenation of acetylene in the presence of excess ethylene using a monolith catalyst reactor. Heptane was used as the liquid-phase but not as a selective solvent for acetylene. A liquid phase was used in their study for two main reasons. First, the continuous removal of green oil could be achieved. Second, the heat generated due to exothermic reactions could be absorbed in the presence of the inert liquid phase, eventually reducing the risk of thermal runaway [5, 8].

Edvinsson et al. (1995) [5] studied the effect of the liquid phase in the selective hydrogenation of acetylene using a monolith catalyst reactor. The operating conditions

were 30-40$^{o}$C at 1.3-2 MPa. The monolith catalyst was placed in a 100cm long and 1inch diameter stainless steel reactor operated in batch mode for 113 hours. A known volume of heptane was used every run with a known weight of the monolith catalyst. It was observed that both selectivity and the turnover number decreased with an increase in time of reaction. This decline in performance was mainly due to the deposit of the carbonaceous residues in the active metal sites. Although the liquid phase in their study was majorly used to absorb excess heat while removing the green oil, the formation of the oligomers was faster than its removal. This activity was observed mainly during the early period of the reaction. It can be understood that the removal of green oil by the liquid phase was equal to its formation when the behavior of the catalyst attains a steady-state or due to the non-availability of a large number of active metal sites. The GC-MS analysis showed that there were majorly $C_8$ and $C_{10}$ compounds, and traces of $C_{12}$. The influence of CO in the liquid phase hydrogenation of acetylene was also studied and the addition of CO decreased the rate of acetylene hydrogenation in the liquid phase [5]. This usage of CO was in stark contrast to the gas phase, where CO was actively used to increase selectivity.

Asplund et al. (1995) confirmed the deactivation of the monolith catalyst in the liquid phase due to the strongly bound coke that was formed, although it removed the majority of the hydrocarbon deposits. The primary reason was the intraparticle mass transport limitations. Regenerating this catalyst was more arduous compared to that formed during the gas-phase reactions [8].

**1.2.2. Liquid Phase Hydrogenation Using Selective Solvent.** Selective solvent to absorb acetylene from a mixture of gases and to maintain high acetylene solubility at operating conditions during liquid phase hydrogenation was desired. Few studies used

NMP as a selective solvent to improve acetylene availability for reaction, but acetylene was not fed to the reactor system as a liquid phase, which is our motivation.

Selective hydrogenation of acetylene using NMP as the liquid solvent was conducted in the presence of Carbon monoxide over a Pd/Sibunit catalyst in shaker type reactor [44]. Their temperature range was 50-90$^{o}$C at atmospheric pressure. The acetylene along with hydrogen was sent to the reactor as gases with the reactor preloaded with NMP and catalyst. On the other hand, this process in the presence of CO showed about 90% and 96% of high ethylene selectivity and acetylene conversion, respectively.

Similarly, the use of NMP as only a liquid phase in the system with acetylene and hydrogen coming in the reactor as gases were conducted by Hou et al. (2015) [43]. The experiments were conducted at atmospheric pressure and flask type reactors. The effect of gas hourly space velocity and the molar ratio of $H_2$: $C_2H_2$ at different temperatures were investigated along with solubility measurements of acetylene and ethylene in NMP. High selectivity and conversion were observed at a higher temperature of 80$^{o}$C and low gas space velocity.

Although this study investigates the liquid phase effects, the need for NMP as a selective solvent for acetylene to understand the phenomena of flowing acetylene to a reactor system in the liquid phase was not addressed, which is the case in industrial applications. The need to demonstrate the selective hydrogenation of acetylene in liquid phase in packed bed reactors was essential accounting for different flow patterns, kinetics, dispersion, wetting and gas-liquid-solid contacting.

Table 1.1. Review on Liquid phase hydrogenation of acetylene

| **Article/ Patent** | **Catalyst** | **Solvent** | **Conditions** | **Additional information** |
|---|---|---|---|---|
| Liquid-phase hydrogenation of acetylene in pyrolysis gas in presence of heterogeneous catalysts at atmospheric pressure [6] | Pd on Alumina/ Activated C/ Zirconium oxide | **Acetone**, DMF, Methanol, Ethanol, Ethyl acetate, propyl acetate, amyl acetate, and water | T = 25-35$^{o}$C | Pyrolysis gas |
| Liquid-phase hydrogenation of acetylene in a monolithic catalyst reactor[5] | Pd on Alumina Monolith | Heptane | T= 30-40$^{o}$C | Presence of excess ethylene |
| Catalyst deactivation in liquid-and gas-phase hydrogenation of acetylene using a monolithic catalyst reactor**[8]** | Pd on Alumina Monolith | Heptane | | Presence of excess ethylene |
| U.S. patent 7045670, 7408091, 7919431, 8247340, 8460937 **(2006-2013**) | Tried various catalysts (Different Pd wt% on alumina) | NMP | T-120-135$^{o}$C P-150 psig (other conditions were also studied) | Presence of CO (was also studied) |
| The ÉCLAIRS Process for Converting Natural Gas to Hydrocarbon Liquids [47] | | | | Info paper, Synfuels |

Table 1.1. Review on Liquid phase hydrogenation of acetylene (cont.)

| | | | | |
|---|---|---|---|---|
| Liquid-phase hydrogenation of acetylene on the Pd/Sibunit catalyst in the presence of carbon monoxide [44] | Pd/Sibunit catalyst | NMP | T=50-90$^{o}$C | Presence of CO |
| Enhanced Selectivity in the Hydrogenation of Acetylene due to the Addition of a Liquid Phase as a Selective Solvent [43] | $Pd/SiO_2$ | NMP | T=80-100$^{o}$C | |
| Selective hydrogenation of acetylene on $Pd/SiO_2$ in bulk liquid phase: A comparison with solid catalyst with ionic liquid layer (SCILL)[48] | $Pd/SiO_2$ | NMP, 1,3-dimethylimidazolium methyl phosphite ([DMIM][$MeHPO_3$]) | T=80-100$^{o}$C | |
| $Pd/Ga_2O_3–Al_2O_3$ catalysts for the selective liquid-phase hydrogenation of acetylene to ethylene [49] | $Pd/Ga_2O_3–Al_2O_3$ | NMP | 10 atm, 55$^{o}$C | |
| Highly efficient and selective catalytic hydrogenation of acetylene in N,N-dimethylformamide at room temperature [50] | Pd with Ni/Ag based catalysts on zeolite and alumina supports | DMF | 25$^{o}$C | Presence of ethylene |

## 1.3. TWO-PHASE FLOW PACKED BED REACTORS

Three-phase catalytic reactors have extensive applications in various industries like petroleum, hydrotreating, hydro-processing, hydrogenation, and in the manufacture of high-value products [51-53]. Likewise, in our study, we have acetylene gas in the liquid phase, a polar solvent, reacting with hydrogen gas over a selective catalyst. To execute this liquid-phase flow hydrogenation reaction towards process development over a catalyst bed, the evaluation of the reactor performance systematically is vital. The kinetics of the catalyst, hydrodynamics, and mass transfer needs to be understood for this assessment. The operating conditions (flow rate, pressure, temperature), physical properties of reactor and catalyst, flow mode (trickle or upflow) need to be optimized and validated by a reactor scale model to ensure proper scale-up. A clear understanding of the flow regime during the operation of packed bed reactors is essential. Many researchers have highlighted the importance of the operating conditions to be in a specific flow regime (trickle, bubbly, pulsing, or spray) [10]. The most commonly used flow mode in the operation of multiphase reactors in industries is downflow (co-current downwards flow of reactants, trickle regime) while upflow (bubbly regime) is also successfully used in hydro-processing and related industries for specific applications [51]. The irrigation/wetting efficiency of the catalyst due to the liquid phase is the key influencing factor between these modes. This gas-liquid-solid contacting, especially for porous catalysts, affects the liquid holdup, dispersion and eventually the reaction process. The mode of operation, trickle or upflow, was chosen to enhance ease of operation and improve the overall conversion and selectivity of the reaction. The flow regime of the operating velocities is very critical as it will affect the wetting efficiency and hence the mass transfer between the phases.

To predict the reactor performance of a scaled-down lab-scale reactor and develop it towards scaling up, it is important to decouple the hydrodynamics from kinetics. On the other hand, the size of the catalyst being investigated is also significant. This will affect the ratio of the reactor to particle diameter (DR/Dp), which generally needs to be higher than 20 [51,54,55]. Researchers suggested this ratio to avoid maldistribution of the flow in the form of wall effects, axial dispersion, and irregular wetting patterns. To account for the actual reaction kinetics in the lab-scale reactor the same catalyst used at a larger scale should be used. However, the DR/Dp ratio would be less than 20, which may lead to an increase in wall voids leading to an increase in the reactant velocity. To reduce this voidage and avoid deviations from plug flow, the most recommended way to be close to the operation of the large scale reactors was to dilute the catalyst bed of lab-scale reactors with fines [56-60]. These fines are small inert particles which are not a part of the reaction. This eliminates the maldistribution while improving the liquid holdup and still maintaining the kinetics of the catalyst. Proper scale-up of the process can be enabled by scaling down the velocities based on the reactor length/catalyst bed accompanied by diluting the catalyst bed with fines. Concerning the process development of this proposed study in flow reactors, not only the kinetics but also the geometric and hydrodynamic similarity should be maintained at scaled-down conditions.

## 1.4. MOTIVATION

The increasing demand for ethylene production and ethylene being studied as a potential raw material for ETL technology to produce liquid fuels, it is significant to assess any possible research which can improve ethylene production [61,62]. For the industrial

practice at scale, the acetylene source should be either from the cracker effluent or in bulk, either from the partial oxidation of natural gas and hydrolysis using calcium carbide. In all cases, the acetylene will be sent to a tower/unit with a selective solvent to dissolve acetylene. The acetylene molecules absorbed in the liquid solvent with high acetylene solubility is the liquid phase. This liquid reactant should be effectively sent to the reactor at ideal operating conditions in order to have good availability to the active sites of the catalyst.

For the investigation of acetylene hydrogenation in the liquid phase, choosing the solvent is very critical. The selective solvent should have high acetylene solubility compared to ethylene, hydrogen, and other gases. Moreover, the solvent should have a stable thermal conductivity at higher temperatures and pressures. These factors will help to improve ethylene yield and better heat transfer in the system. Additionally, the green oil formed during the reaction can also be minimized due to the continuous flow of the liquid phase.

Only a few studies have worked on liquid-phase hydrogenation of acetylene to ethylene as mentioned in Table 1. To our knowledge, there are no studies involving the kinetics of liquid-phase hydrogenation of acetylene in open literature at high temperature and pressure. Although in Patent literature, the effect of different catalysts in a fixed bed reactor at various operating conditions using NMP for liquid-phase hydrogenation was found, as mentioned in Table 1. Still, an understanding of the kinetics of this process is lacking. Furthermore, investigating the reactor performance for the liquid phase hydrogenation of acetylene using a selective solvent over a commercial catalyst in a packed bed reactor was necessary. These experimental data must be validated using a reactor scale

model for further scaling of this process. The model must be robust accounting of pellet effects, kinetics, hydrodynamics, wetting efficiency, and mass transfer phenomena.

N-methyl pyrrolidone (NMP), a polar solvent with high boiling point (204oC) and high acetylene solubility was chosen as the selective solvent [63,64]. This solvent was commonly used to absorb acetylene from the mixture of gases mainly due to its high selectivity towards acetylene [43-46,64]. A gas-phase hydrogenation catalyst (Palladium over Alumina supports) used in many studies and industries was used in our study [4, 10, 19, 33].

## 1.5. RESEARCH OBJECTIVES

The overall objective is to study the selective hydrogenation of acetylene to ethylene in a liquid phase. The performance of commercially available 0.5 wt% $Pd/Al_2O_3$ catalyst in fixed-bed reactors for trickle and upflow mode will be investigated. A reactor scale model will be integrated with pellet scale diffusional effects to understand and validate the performance of the reactor. The detailed objectives are as follows:

a) Design, develop, and test a high-pressure lab-scale facility to study the overall performance of a fixed bed reactor in both upflow and trickle flow modes. These include developing a detailed operating protocol for the experimental setup, testing the facility for safe operation.

b) Investigate the kinetics of selective hydrogenation of acetylene in the liquid phase over commercially available 0.5 wt% $Pd/Al_2O_3$ catalyst using a 300 mL slurry and basket stirred-tank reactor. The parameters to be studied to understand the liquid phase kinetics are temperature, catalyst loading, and operating pressure. A kinetic model will be

developed and fitted on simple power-law equations and Langmuir-Hinshelwood-Hougen-Watson (LHHW) approach to estimate the intrinsic kinetics. The selected conditions to conduct packed bed studies will be identified.

c) Investigate the residence time distribution in a packed bed reactor at selected scaled-down operating conditions and different reactor configurations to estimate the liquid dispersion and holdup values with and without the presence of thermowell. These values will be correlated empirically to be used in the reactor scale model.

d) Experimentally evaluate the overall performance of a 1-inch diameter reactor packed with 0.5 wt% $Pd/Al_2O_3$ catalysts in co-current downflow mode and upflow mode. The liquid phase hydrogenation of acetylene to ethylene will be studied by selectively absorbing acetylene using a polar solvent, NMP. Specifically, the goal is to investigate acetylene conversion and selectivity to $C_2H_4$, $C_2H_6$, and by-products as a function of temperature, flow rates (gas and liquid), and operating pressure.

e) Validate and assess a reactor scale model integrated with pellet scale effects to assess the reactor performance of the acetylene hydrogenation in the liquid phase.

# PAPER

## I. QUANTIFYING LIQUID DISPERSION AND LIQUID HOLDUP IN A LABORATORY SCALE TRICKLE BED REACTOR WITH AND WITHOUT THERMOWELL USING RESIDENCE TIME DISTRIBUTION STUDIES

Humayun Shariff, Premkumar Kamalanathan, and Muthanna H. Al-Dahhan

Department of Chemical and Biochemical Engineering, Missouri University of Science and Technology, Rolla, MO, 65409

## ABSTRACT

The axial dispersion coefficient and liquid holdup were estimated at scaled-down operating conditions for liquid-phase hydrogenation of acetylene process using Residence Time Distribution (RTD) experiments in a stainless-steel laboratory-scale trickle bed reactor (TBR). The effect of liquid and gas velocities on the liquid axial dispersion coefficient and liquid holdup was investigated for different types of catalyst shapes (spheres and extrudates) and packings of the catalyst bed for reactors with and without thermowell. The mean residence time and variance were evaluated from the RTD of the liquid phase by the moments' method using the conductivity measurements from the pulse-input liquid-tracer injection. The liquid holdup values were evaluated from the mean residence time. The liquid axial dispersion coefficient was estimated by the regressive fitting of the axial dispersion model to the experimental data. The liquid holdup values increased with the increase in liquid velocities and were higher when the catalyst bed was diluted with fines. The bed with porous spherical catalyst diluted with fines had lower

dispersion at the operating conditions for the liquid hydrogenation compared to the undiluted bed. Peclet numbers increased with an increase in liquid velocities. Empirical correlations as a function of the liquid and gas Reynolds number were proposed for Peclet numbers and liquid holdup to fit the experimental data.

**Keywords:** Trickle Bed Reactor**,** Residence time distribution, Axial dispersion, Liquid holdup

## 1. INTRODUCTION

Liquid maldistribution is ubiquitous in trickle bed reactors (TBRs), one of the most common reactors used in petrochemical and hydrotreating industries. TBRs are widely used due to their inherent advantages for gas-solid-liquid contacting at high-pressure operations, a high catalyst to liquid ratio, and ease of operation. When these industrial TBRs are not in plug-flow and generally exhibit gross flow maldistribution, their non-ideality needs to be analyzed. Due to the complex flow behavior in TBRs, the wettability of the liquid, mixing, holdups (gas and liquid), residence time, and local velocities along with kinetics affect the conversion and selectivity. For the process development in general and for our continuing effort of understanding the hydrogenation of acetylene in the liquid phase using a selective solvent for ethylene production, it was necessary to evaluate the liquid-phase dispersion and liquid holdup for the reactor scale modeling and to define the experimental conditions.

Moreover, this information becomes vital while assessing the reactor performance during scale-up. Studying the TBR efficiency forms the essential core in the larger picture

of the economics. The contacting of the phases, which in turn depends on the phase distribution (holdup), catalyst properties (shape and size), the arrangement in the reactor, and operating conditions can affect the efficiency.

One of the widely used techniques to quantify the non-ideal behavior is the residence time distribution (RTD). It was always significant to run tracer studies or any other proven experimental technique to understand the residence time distribution for the specific reaction system at different operating and reactor conditions to evaluate the system-specific axial dispersion coefficient [1]. Axial dispersion coefficient ($D_{ax}$) is a lumped parameter of the non-ideal behavior flow in a reactor such as material transport through the stagnant pockets, local channeling, and turbulent eddy diffusivities [1, 2]. This dispersion coefficient is evaluated experimentally from RTD measurements assuming the mixing process follows Fick's law. The RTD data are interpreted with the axial dispersion model (ADM) to understand the non-idealities using the fitted parameter, $D_{ax}$ [1, 3-5]. This parameter is generally expressed in terms of dimensionless form viz., liquid Peclet number, $Pe_{L,}$ or Bodenstein number, Bo. A review of a few different axial dispersion models for various scales and processes like hydrotreating, hydrogenation, and hydrodesulfurization can be found elsewhere [4, 6]. This review helps in understanding the importance of applying ADM during the scale-up of any reaction system.

The two significant parameters that explain the bed behavior in the ADM are total liquid holdup ($\varepsilon_L$) and $D_{ax}$. Evaluating the liquid holdup from the RTD data helps in interpreting the conversion and selectivity, along with the diffusional effects, especially when the reactants are in the liquid phase [7]. Many studies adopt the values of $\varepsilon_L$ and $D_{ax}$ from correlations available in the literature for their reactor system and operating

conditions. Using the axial dispersion coefficient from correlations may not be accurate or give the exact value for the current system, which may affect the scale-up process as most of the studies were conducted at atmospheric pressure or limited to their experimental conditions. While conducting reactor performance studies for this process, it is critical to evaluate the dispersion parameter from RTD studies for such laboratory-scale TBRs to enhance the reactor scale model for future scale-up of the process [8].

Different types and shapes of catalysts are commercially used for various reactions in packed bed reactors at scale. By evaluating the hydrodynamics of these different shapes and packings, the reactor performance can be estimated using intrinsic kinetics and provide more understanding of the system before conducting experiments. Since the ratio $D_R/D_P$ needs to be greater than or equal to 20, it becomes a challenge while investigating the reactor using commercial catalysts, especially during scale up and scale down due to the effect of maldistribution and irregular contacting of the reactants. Hence, packing the reactors plays a significant role in the performance, especially in lab-scale reactors. Overall, packing the bed with fines helps in improving the contact between gas-liquid and catalyst, thereby improving the catalyst utilization and liquid holdup and reducing the dispersion effects across the reactor axis [9-11]. Studies on the effect of different packing methods and the significance of diluting the bed with inert fines in lab-scale reactors are available elsewhere [9, 11-13].

Packed-bed reactors with thermowell were also investigated using commercial catalysts where the bed was diluted to understand the hydrodynamics [1, 11] and reactions [13, 14]. These studies were conducted to ensure the geometric similarity was maintained while using thermowell in the reactors. Only few works studying the effect of thermowell

in a packed bed reactor were available in the literature, while reactors with thermowell were used in industrial practice extensively. However, using thermowell in the reactor system, the inlet of the gas and liquid configuration changes in comparison to a reactor without thermowell. This affects the dispersion in the reactor and the efficiency of the process.

The primary motivation for this study is to quantify the dispersion coefficient and liquid holdup for a laboratory-scale TBR, which are significant while developing a robust reactor-scale model for liquid-phase hydrogenation of acetylene. In this work, residence time distribution was investigated to estimate the liquid dispersion and overall liquid holdup for laboratory-scale TBRs with and without thermowell using different catalyst beds to understand the global mixing at different operating and bed conditions in a lab-scale TBR. The estimated holdup and dispersion values were used to develop empirical correlations, which were used further in the reactor performance assessment for liquid-phase hydrogenation of acetylene.

# 2. EXPERIMENTAL SECTION

## 2.1. PROCEDURE

A stainless-steel reactor of 60 cm long with 2.54 cm internal diameter was used to quantify the liquid dispersion and holdup in trickle flow modes. Two different reactor configurations were used: 1) with the gas-liquid distributor on the top without thermowell with liquid from the top and gas on the side of the distributor; 2) with thermowell at the center of the reactor (length 54 cm) with gas and liquid entering from the top.

Table 1. Operating conditions and bed characteristics

| **Reactor** | **Catalysts** | **Bed porosity** |
|---|---|---|
| Reactor 1 :with distributor,(60 cm long and 2.54 cm internal diameter) | Spheres (3-4 mm diameter) | 0.38 |
| | Extrudates (2mm dia X 4mm L) | 0.33 |
| | Spheres (3-4 mm diameter)+ Silicon carbide ( 400-600 μ) | 0.23 |
| Reactor 2 :with thermowell (length 54cm with reactor length of 60cm and 2.54 cm internal reactor diameter) | Spheres (3-4 mm diameter) | 0.37 |
| | Spheres (3-4 mm diameter)+ Silicon carbide ( 400-600 μ) | 0.29 |
| Superficial Liquid velocity, $u_{sL}$ (m/s) | 0.0005 to 0.002 (0.5-2 kg/m$^2$/s) | |
| Superficial gas velocity $u_G$ (m/s) | 0.04 to 0.16 (0.05-2 kg/m$^2$/s) | |

The reactors were dry-packed with catalysts for a length of 30 cm with fines packed for 15 cm on the bottom and top of the catalyst bed [12]. Since the goal of the work was to understand the liquid phase hydrogenation process and not to develop a catalyst, a commercial catalyst was used. For extrudates, the reactor was loaded only with the catalyst without fines.

The bed was packed by vibration and tapping to ensure effective bed porosity. The bed voidage was measured by the water draining method. Figure 1 shows the complete experimental setup with the packing lengths. The catalyst properties, operating velocities, and packing characteristics are mentioned in Table 1. The air-water mixture at specific flow rates was fed to the reactor. The operating conditions were chosen based on literature to identify the conditions to conduct the actual acetylene hydrogenation reaction in the

liquid phase, and all the conditions were in the trickle flow regime. Potassium chloride (KCl) solution was used as the tracer. The tracer was injected as a pulse at the top of the reactor, and the output of the tracer concentration was measured at the exit of the reactor to avoid any dispersion in the piping by a sensitive conductivity probe. The corresponding measurements were recorded as a function of time using a LabView Program.

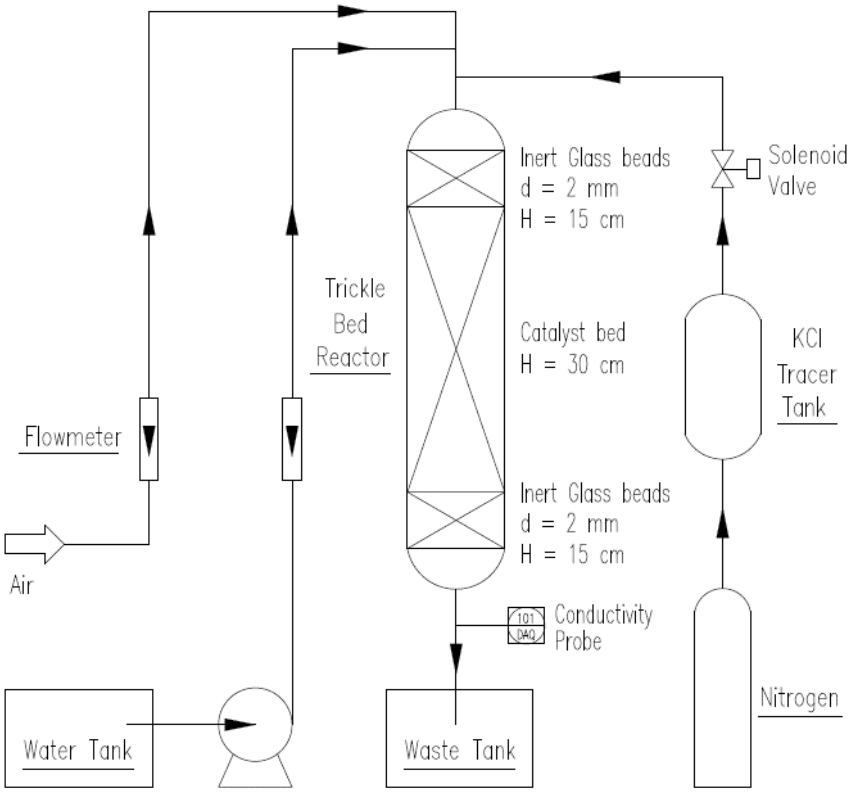


Figure 1. Experimental Setup for Liquid Tracer Technique with packing of the bed

## 2.2. DATA ANALYSIS

The conductivity data of the tracer was recorded by the LabView program at 25Hz. The output of the probe was in terms of voltage, which is linearly proportional to the

concentration of the tracer. The recorded voltage signals were filtered using the Butterworth filter to remove the non-biased noise like electrical signals. For each experiment, the conductivity signals were recorded for air-water (without KCl), and these signals were filtered. The average value of the initial filtered signals was considered as a base value. These base values were subtracted from the measured signals so that the processed signals only account for the tracer concentration and were further normalized by dividing by the maximum value of the measured signal of that experiment. These normalized values are equivalent to the dimensionless concentration.

The exit age distribution was calculated from the processed signal as follows.

$$E(t) = \frac{R(t)}{\int_0^\infty R(t)dt} \quad (1)$$

where R(t) represents the measured signal. The moments, first moment: mean residence time and second moment: variance were determined from the *E(t) vs t* curve. The mean residence time, $t_{mean}$ of the liquid in the reactor was calculated using the equation:

$$t_{mean} = \int_0^\infty t\, E(t)dt \quad (2)$$

The variance,$\sigma^2$, was estimated using the following relation:

$$\sigma^2 = \int_0^\infty (t - t_{mean})^2\, E(t)dt \quad (3)$$

To confirm if the dispersion was towards or away from plug flow (i.e., towards CSTR), dimensionless variance, $\sigma_\theta^2$ was evaluated

$$\sigma_\theta^2 = \frac{\sigma^2}{t_{mean}^2} \quad (4)$$

Once the moments were calculated, the liquid holdup, $\varepsilon_L$ in the reactor system was determined by

$$\varepsilon_L = \frac{u_{sL}}{L} t_{mean} \quad (5)$$

The total liquid holdup can include dynamic, static, and internal; however, in our case, only the dynamic holdup was obtained. This is due to the following reasons: a) the porous catalysts were flooded with the liquid phase before the experiments thereby prewetting them and filling the internal voids; b) the residence time required for the diffusion of the tracer into the catalyst pores is much larger than that of the tracer in the column due to the resistance of the liquid film around the catalyst; c) the static holdup, which is the holdup between the contact points of the catalysts, was considered significantly lower compared to the overall holdup due to high magnitudes of gas superficial velocities relative to the liquid velocities. Thus, the obtained holdup value is approximated as the dynamic holdup.

A one-dimensional axial dispersion model (ADM) was used to fit the model with the experimental measurements obtained. This model has been widely used to characterize packed beds with various assumptions. In our case, the following assumptions were used in order to use ADM as the model of choice: i) axial dispersion is more dominant, thereby neglecting the dispersion in other co-ordinates, ii) velocity of the liquid phase is consistent and is more prominent axially. The best fit curve to the experimental data determined the axial dispersion coefficient, $D_{ax,}$ which quantifies the degree of dispersion during the flow. Figure 2 shows typical experimental values with a corresponding predicted curve using the ADM with an error of 0.00063 for a bed with porous spheres with fines at $u_{sL}$ and $u_G$ of 0.001 m/s and 0.08 m/s respectively. The model was able to fit the measured signal data reasonably well for different operating conditions. The axial dispersion coefficient, $D_{ax,}$ was obtained by reducing the mean squared error of the measured signal values of the experimental and predicted curve obtained by solving Equations 6-9.

$$\varepsilon_L \frac{\partial C}{\partial t} = D_{ax} \frac{\partial^2 C}{\partial z^2} - u_{sL} \frac{\partial C}{\partial z} \quad (6)$$

The model equations were solved using the Danckwerts boundary conditions.

$$(C_o - C) + \frac{D_{ax}}{u_{sL}}\left(\frac{\partial C}{\partial z}\right) = 0 \text{ at z=0} \quad (7)$$

$$\frac{\partial C}{\partial z} = 0 \text{ at z=L} \quad (8)$$

$$error = \frac{1}{N}\sum_{i=1}^{N}[C_{expt}(t_i) - C_{sim}(t_i)]^2 \quad (9)$$

Further, using the $D_{ax}$, which gives the least error, the Peclet number was calculated using the relation:

$$Pe_L = \frac{u_{sL}\, L}{D_{ax}\, \varepsilon_L} \quad (10)$$

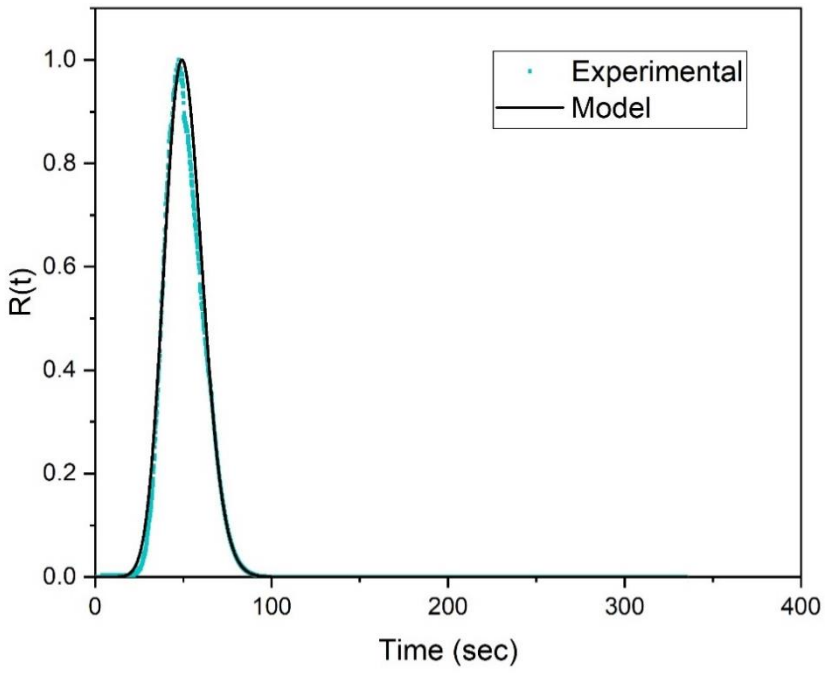


Figure 2. Representative experimental and model curve of the measured signal as a function of time

# 3. RESULTS AND DISCUSSIONS

## 3.1. EFFECT OF GAS AND LIQUID FLOWRATES

In this section, the effect of the liquid and gas superficial velocities on the axial dispersion coefficient and liquid holdup for different types of reactor configurations are discussed. The operating conditions and the bed properties are specified in the previous section. RTD studies were conducted for catalyst beds with spherical porous catalyst particles with and without fines in a reactor with and without thermowell and cylindrical extrudates in the reactor without thermowell to estimate the axial dispersion coefficient and liquid holdup values. The experiments were repeated for reproducibility, and the error for the holdup values was in the range of ±11%.

For the catalyst bed packed with only spherical particles without fines, it was observed that liquid holdup values increased with an increase in liquid velocities but were not in trend with the literature when the gas velocity was increased (Figure 3). Most of the studies reported an increase in the liquid holdup with an increase in liquid superficial velocity and decreased with an increase in gas velocity [15-19]. The holdup values were very close at 0.08 m/s and 0.16 m/s at a low and mid-range of liquid flow rates. This could be mainly due to the diffusional resistances in the porous particles at higher gas flow rates. Moreover, due to the low $D_R/D_P$ ratio (approximately 8) in the reactor, there could have been many pockets in the reactor leading to wall effects. At higher liquid superficial velocity, the holdup values generally decrease with the increase in the gas velocities. The values at a superficial gas velocity of 0.08 m/s were higher than the other holdup at different velocities, which was not in trend with the literature. A similar inconsistency was observed

with the $D_{ax}$ estimation, where the values were not decreasing at higher velocities [15-19]. This study helped to understand the axial dispersion and liquid holdup values before diluting the bed. Generally, it was recommended to dilute the catalyst bed for lab-scale TBRs to decouple hydrodynamics from kinetics and to overcome the wall effects while scaling down or scaling up. This way, the deviation from plug flow was restricted as scaled-up units operates close to plug flow conditions generally [10, 12, 20].

The fines were added along with porous spherical catalysts while packing the laboratory scale TBR to improve the contacting efficiency, which affects the pressure drop and liquid holdup [9, 12]. The bed voidage of the diluted bed, $\varepsilon_B^f = 0.23$ which was low compared to the bed without fines, $\varepsilon_B = 0.38$. In our effort to quantify the liquid holdup and axial dispersion coefficient, the pressure drop was not studied but estimated from correlations available in the literature. The dimensionless pressure drop estimated from the correlation by Al-Dahhan and Dudukovic (1994) [21] were in the range of 0.1-2. From literature, the bed with fines shows higher pressure drop mainly due to the low bed voidage due to an increase in the frictional surface area; on the other hand, it increases the liquid holdup [9, 15, 22]. The values of liquid holdup were high when the bed was diluted compared to the values to the catalyst bed with only spherical particles. The liquid holdup increased with an increase in liquid velocity and a decrease in gas velocity with the addition of fines (Figure 3). These high values can be attributed to the longer residence times of the tracer in the system, which in turn reflects on the residence time of the reactants. It can be added that high liquid holdup, especially at lower liquid flow rates, should enhance reaction selectivity and hence the conversion.

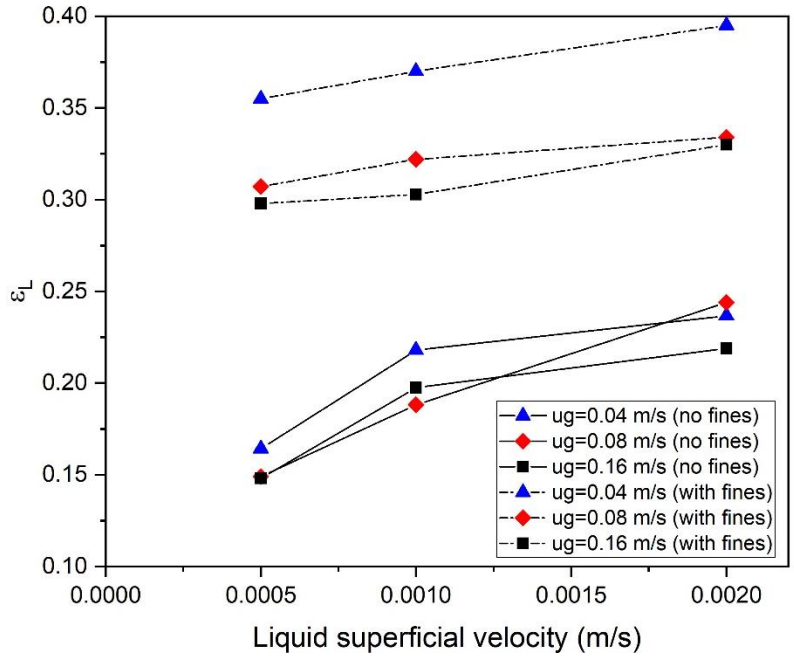


a

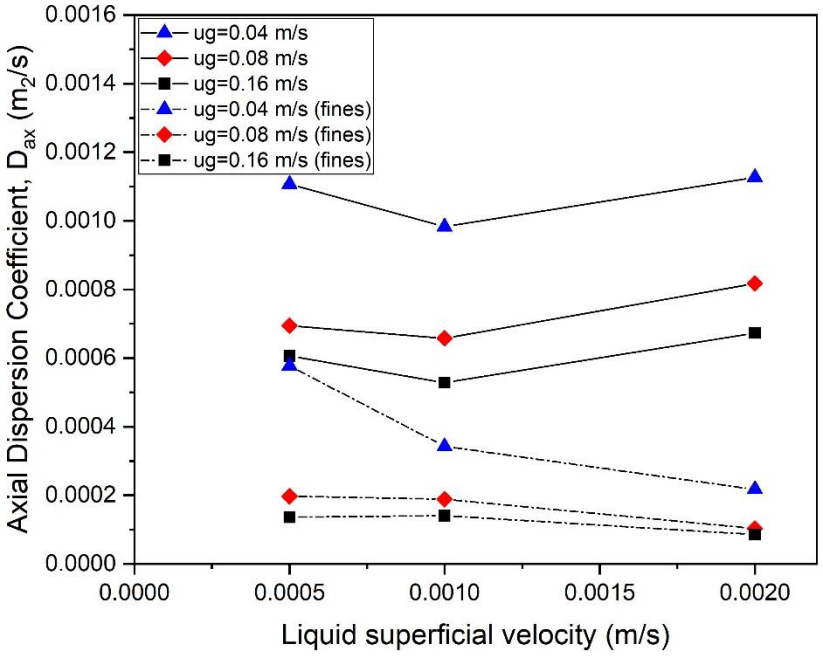


b

Figure 3. Effect of liquid and gas velocities on a) liquid holdup, b) axial dispersion coefficient in catalyst bed with porous spherical particles with and without fines (dashed lines – fines)

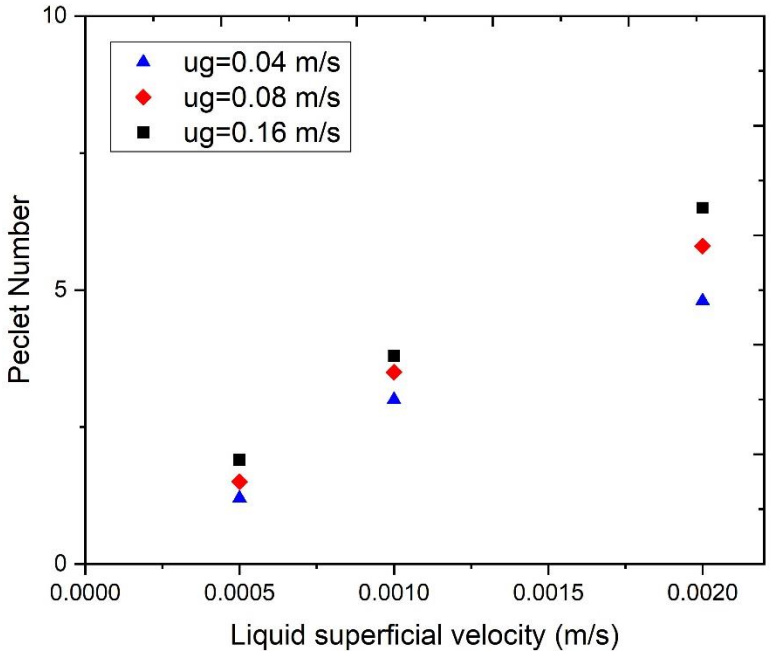


Figure 4. Effect of liquid and gas velocities on liquid Peclet number in catalyst bed with porous spherical particles with fines

At higher flow rates of liquid and gas, the liquid holdup values were almost similar due to gas interference in between the solid-to-solid contact points. The $D_{ax}$ values decreased with an increase in liquid velocities, as shown in Figure 3. Moreover, by diluting the bed, the axial dispersion was reduced which helps during scaling up the reactor [10]. The Peclet number values estimated were in the range of 1.2-7 as shown in Figure 4 and the values were increasing with liquid velocities while no significant change was seen due to the effect of gas velocity.

Similar studies at the scaled-down operating conditions using cylindrical extrudates catalysts were conducted to estimate the liquid holdup and dispersion values. The interest in conducting this study was to understand the hydrodynamics of the scaled-down reactor based on shapes of the catalyst as well as the effect of packing in a lab-scale TBR. The

packing technique was followed, as mentioned in Al-Dahhan et al. (1995) [12], and no fines were used while using the extrudates to pack the bed. The holdup values were similar while using spherical particles with fines with high reproducibility in the data. By the hydrodynamic phenomena, the values increased with an increase in liquid flow and decreased with an increase in gas flow. The packing of the bed should contribute to these high holdup values, even though the bed was not diluted. This is largely due to the cylindrical shape of the catalyst, which was able to settle in the bed with fewer voids. At low liquid superficial velocities, the holdup values were in the range of 0.31-0.35, confirming negligible film resistance on the catalyst surface (Figure 5).

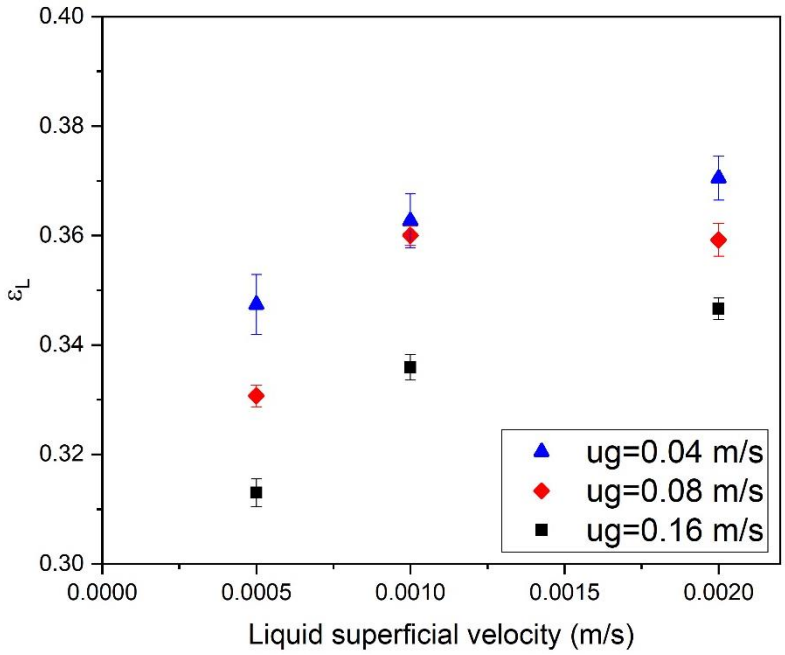


**a**

Figure 5. Effect of liquid and gas velocities on a) liquid holdup, b) axial dispersion coefficient, c) liquid Peclet number in catalyst bed with porous cylindrical extrudate particles

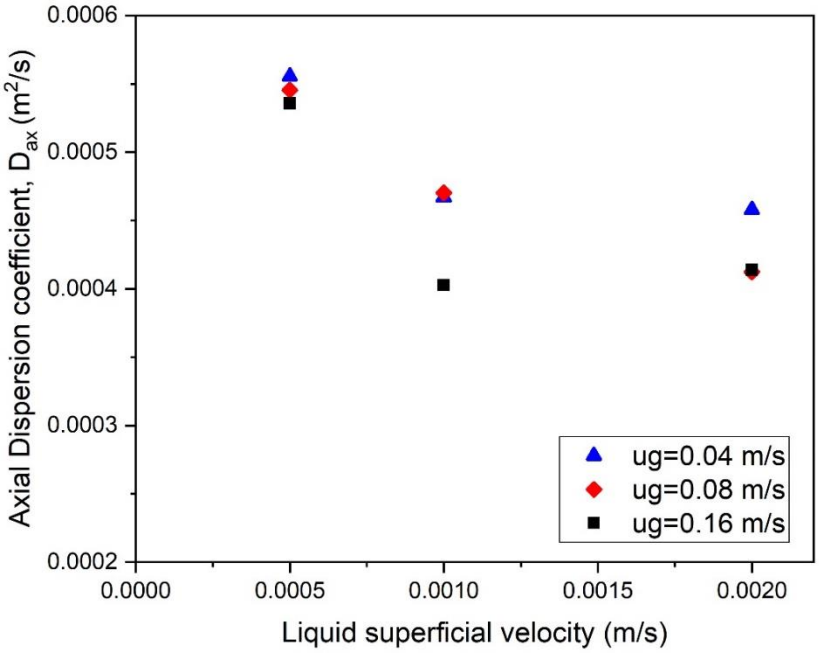


b

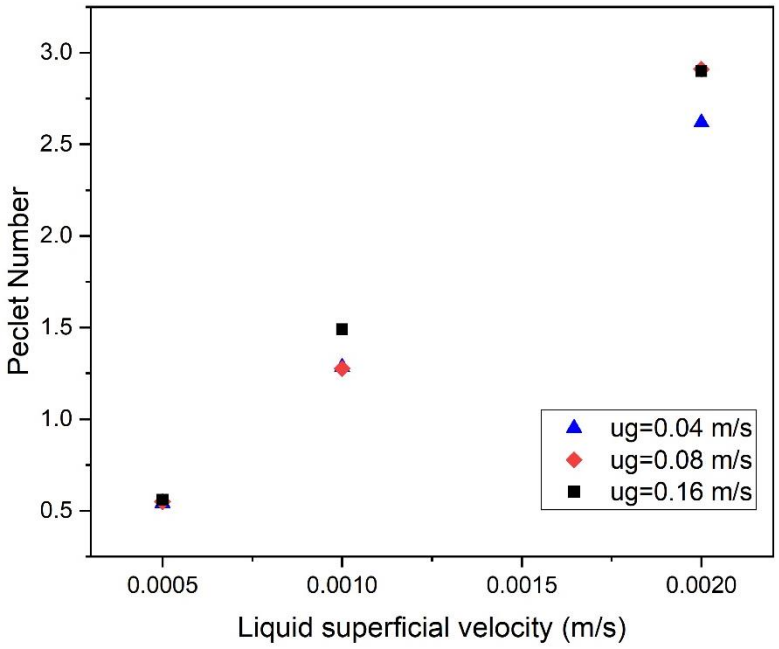


**c**

Figure 5. Effect of liquid and gas velocities on a) liquid holdup, b) axial dispersion coefficient, c) liquid Peclet number in catalyst bed with porous cylindrical extrudate particles (cont.)

The Peclet numbers were in the range of 0.5-3, which were lower than the values of the bed with spherical catalysts and fines. This was mainly due to an increase in $D_{ax}$ values. It could be inferred that diluting the bed with spherical catalysts tends towards plug flow in comparison with the bed with only extrudates.

### 3.2. EFFECT OF THERMOWELL

As the $D_R/D_P$ ratio was low, packing the bed with only the spherical catalysts in a reactor with thermowell wouldn't give adequate irrigation. From initial test experiments, the estimated liquid holdup and axial dispersion coefficient from the RTD information were inconsistent and not in trend [1]. This may be due to the wall effects near the thermowell during packing the bed, as seen in the results of packing the reactor with only spheres where more bed voidage led to inconsistent results. The bed was diluted with fines; this way, most of the wall effects will be reduced in the reactor. The inlet of the liquid and gas feed was at the top of the reactor while using the reactor with thermowell.

From the experimental results, the liquid holdup values increased while packing the reactor with thermowell with spherical particles and fines (Figure 6). It was evident that this is due to having less voidage in the packing, especially around the thermowell. The bed porosity was 0.29 against 0.37 without the fines. Moreover, the axial dispersion coefficient values decreased with an increase in the liquid velocities significantly at each gas velocity. At higher gas velocities, the $D_{ax}$ values did not have any significant change with an increase in liquid velocities. These results were similar to the trend observed by Tsamatsoulis and Papayannakos [1], where the bed was diluted while packing a reactor with thermowell.

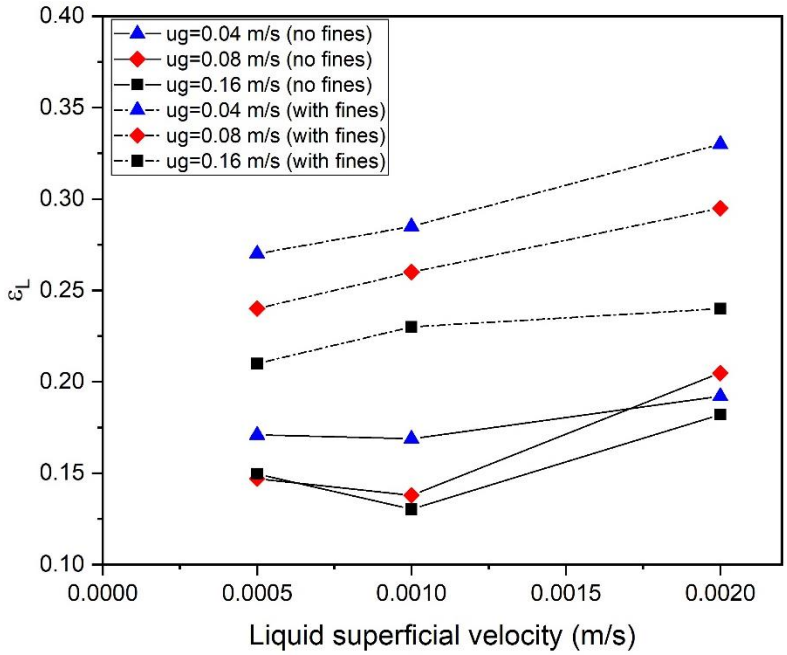


Figure 6. Effect of liquid and gas velocities on liquid holdup in catalyst bed with porous spherical particles with and without fines in a reactor with thermowell

The dispersion significantly reduces at lower liquid velocities, as shown in Figure 7. This effect may be due to the lower residence time leading to narrow distribution in the measured signal. The Peclet number values were observed to be increasing with liquid velocities. Figure 8 compares the liquid holdup axial dispersion coefficient values at different gas and liquid velocities in reactors, with and without thermowell packed using spheres with fines. It can be observed that the holdup values were higher in the reactor without thermowell because of lower bed voidage leading to higher irrigation in the bed. Similarly, dispersion values were low in the reactor without thermowell. This could be attributed to the walls effect, which is significantly negligible in the reactor without thermowell. With the increase in the gas flowrate, both the holdup and dispersion values reduced in both the reactor configurations.

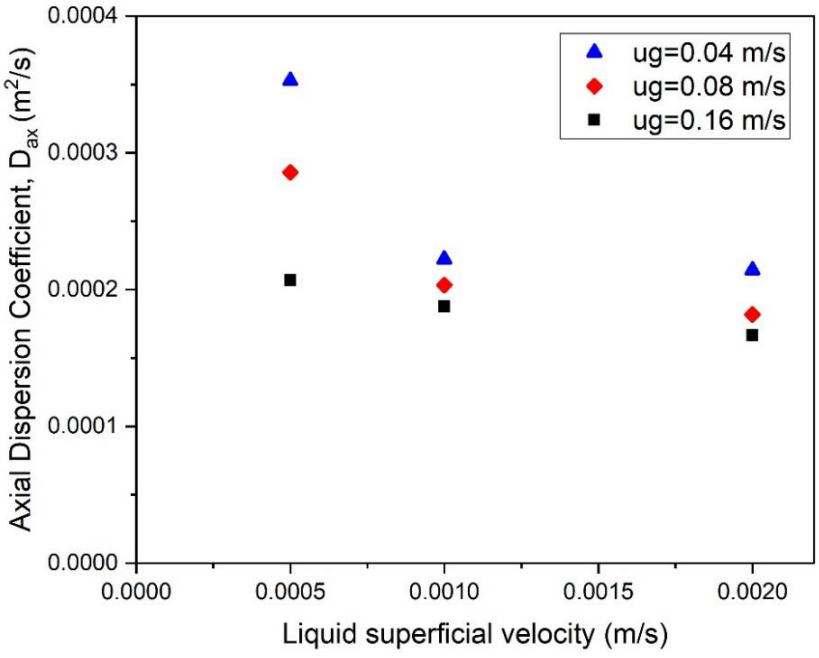


a

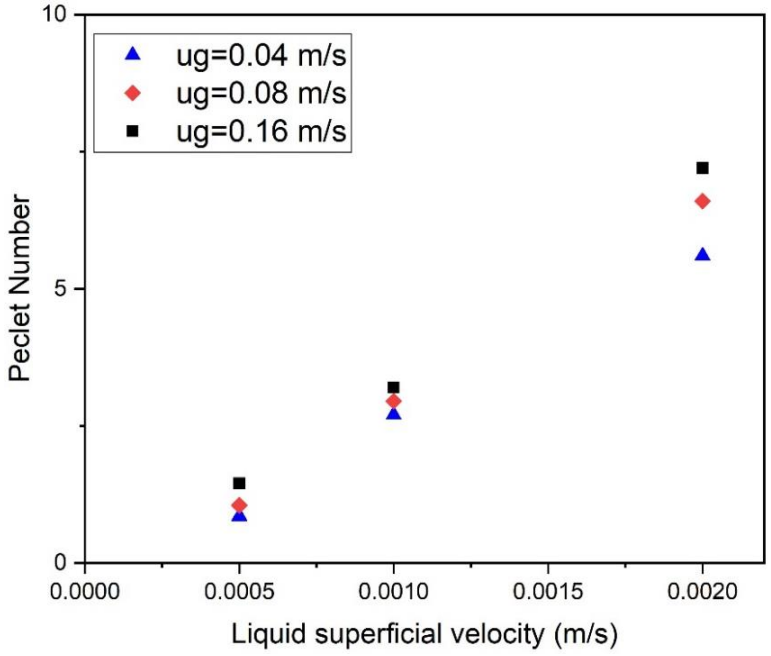


b

Figure 7. Effect of liquid and gas velocities on a) axial dispersion coefficient, b) liquid Peclet number in catalyst bed with porous spherical particles with fines in a reactor with thermowell

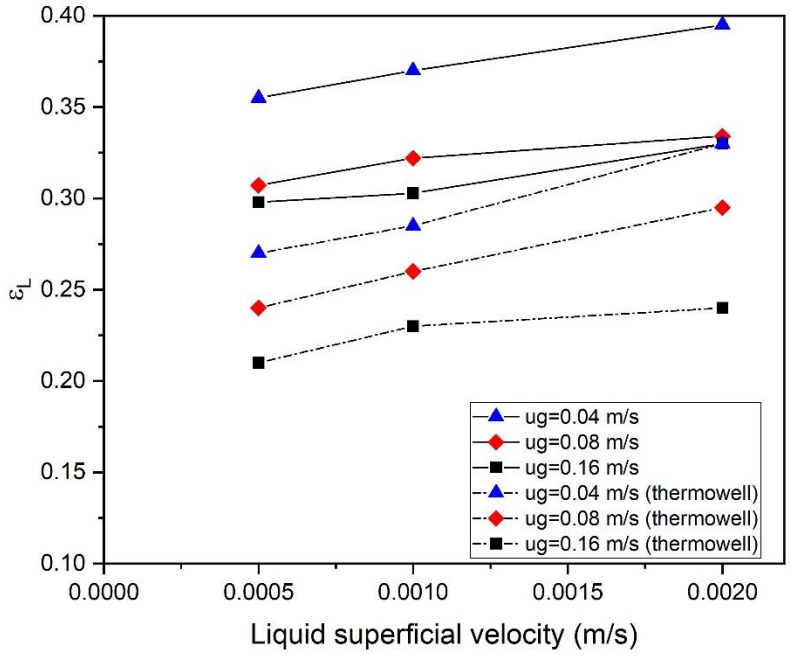


a

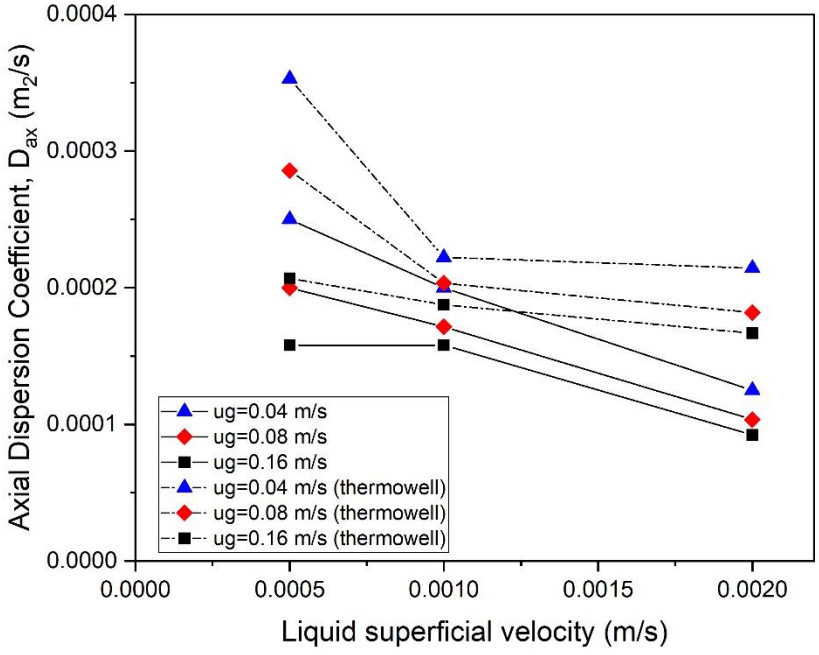


b

Figure 8. Comparing the liquid holdup and axial dispersion coefficient for the reactor with and without thermowell packed with porous spherical particles with fines

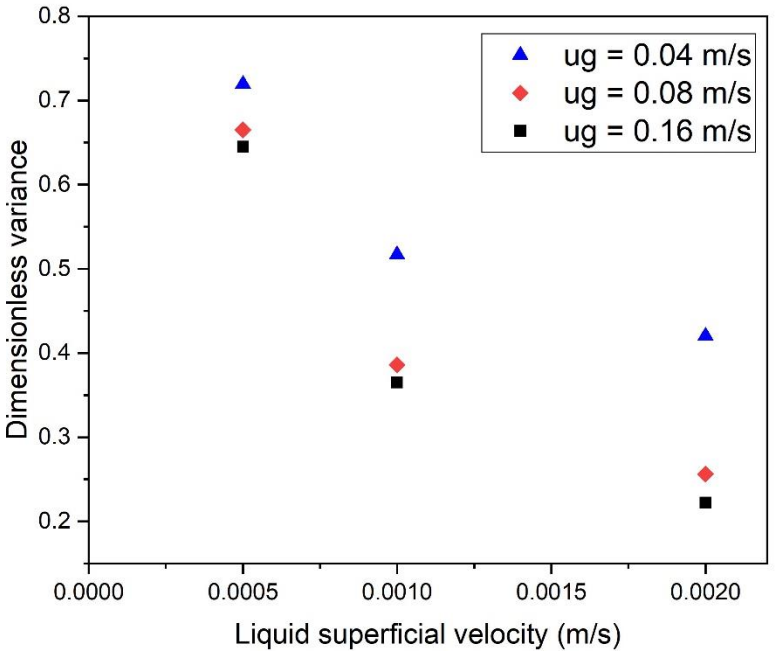


**a**

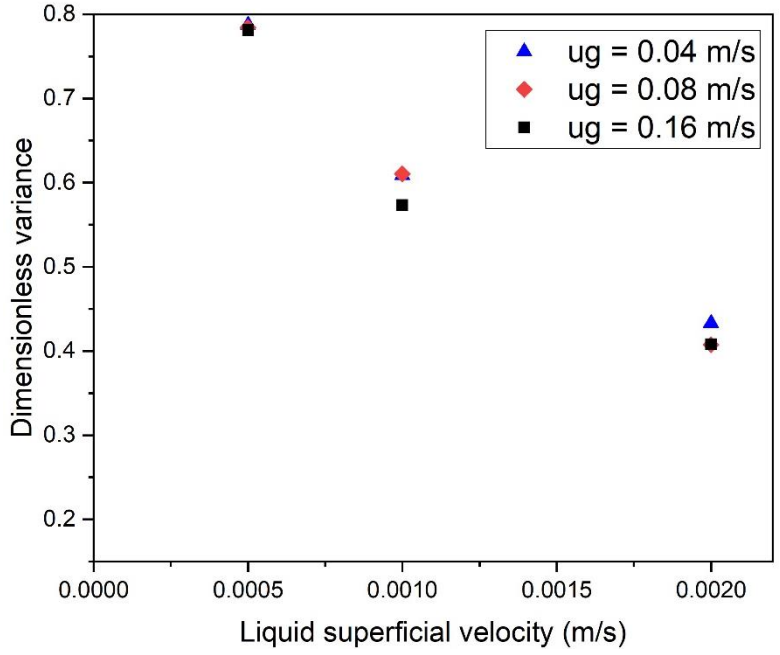


**b**

Figure 9. Effect of liquid and gas velocities on the dimensionless variance of the R-t curves for bed packed with a) spheres with fines, b) extrudates, c) spheres with fines in a reactor with thermowell

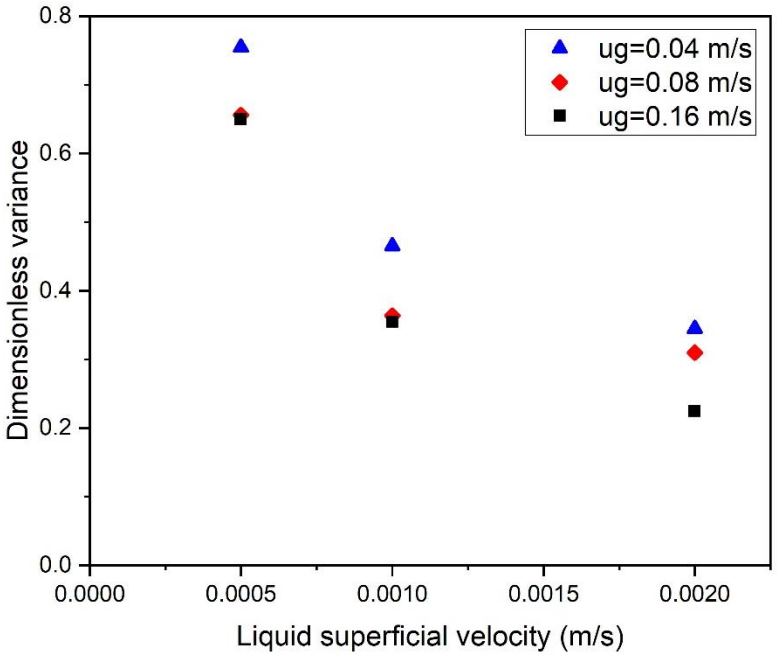


**c**

Figure 9. Effect of liquid and gas velocities on the dimensionless variance of the R-t curves for bed packed with a) spheres with fines, b) extrudates, c) spheres with fines in a reactor with thermowell (cont.)

From Figure 9, the dimensionless variance was estimated from the experimental data curves based on Equation 4. It was observed that the variance values decreased with an increase in liquid flow rates. This was due to the reactor's tendency to approach plug flow with less dispersion. In the case of extrudates, the variance values were independent of the change in gas velocities. Also, the Peclet number values were independent with the increase in the superficial gas velocity, as shown in Figure 10.

On the other hand, the values were higher in the case of reactor bed packed with spheres with fines compared to bed with extrudates due to the presence of fines reducing the dispersion in the system. From the three different effective packings of the bed, the liquid holdup values were improved by the addition of fines, and dispersion in the bed was

also reduced. The dependence of these parameters on the liquid superficial velocity was represented by correlations for this system, which will be used in the optimization of the hydrogenation process.

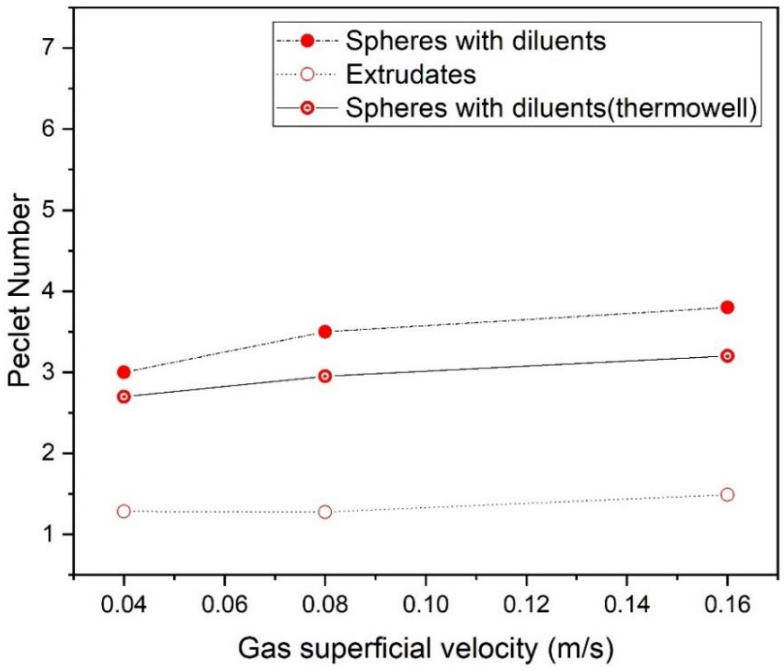


Figure 10. Effect of gas velocities on the Peclet number for different reactor configurations at $u_{sl}$ = 0.001 m/s

Since bed voidage and liquid and gas velocities, majorly affected liquid holdup and Peclet number values, these values were correlated in simple forms considering the physical properties of the reactor system investigated. These correlations will be used to estimate the Peclet number and liquid holdup parameters needed for the reactor scale model and its validation in our subsequent works.

Table 2. Constants of the $Pe_L$ and $\varepsilon_L$ correlations

| **Bed** | | **Peclet Number** | | **Liquid holdup** | | |
|---|---|---|---|---|---|---|
| | ***a*** | **α** | **β** | **b** | **γ** | **δ** |
| Extrudates | 2.614 | 1.1147 | -0.183 | 1.738 | 0.138 | -0.795 |
| Spheres with fines | 2.74 | 0.869 | -0.1456 | 1.71 | 0.198 | -0.113 |

Although the reaction experiments will have acetylene in liquid phase with hydrogen, the correlations were estimated from an air-water system as the same beds (packing with fines for the same bed length) were used during the reaction. It was assumed that the bed characteristics dominated the Peclet number and liquid holdup values. Although, at operating pressure and temperature, the densities of hydrogen and the solvent (N-methyl pyrrolidone) were very close to air and water respectively. Hence, these correlations were used to only estimate the needed parameters for the reactor scale model to make it more sensible to the actual operating conditions. The coefficients for the empirical correlations were estimated by regression of evaluating and plotting against the experimental values. The objective function was to minimize the average mean relative error to less than 10%. An empirical correlation to evaluate the Peclet number and liquid holdup for the packed bed reactor in our study for the investigation of liquid phase acetylene hydrogenation were proposed as

$$Pe_L = a\, Re_L^{\alpha} Ga_L^{\beta} \tag{11}$$

$$\varepsilon_L = \varepsilon_B \left(b\, Re_L^{\gamma} Re_G^{\delta}\right) \tag{12}$$

Table 2 gives the values for the correlations. The fitting error for the $Pe_L$ correlation was about 9.3% and for $\varepsilon_L$ correlation, it was 10.5%.

## 4. CONCLUSIONS

The liquid phase axial dispersion in terms of Peclet number and dynamic liquid holdup were measured for a trickle bed reactor with different bed and reactor configurations using residence time distribution studies. It was evident that the resistances of the tracer within the catalyst pores and diluting the bed had a strong effect on the liquid phase hydrodynamics. Packing the bed with fines was beneficial to enhance the dynamic liquid holdup at especially low gas flow rates. The effect of liquid superficial velocities significantly affected the axial dispersion coefficient in a reactor with a diluted catalyst bed of spherical particles. With an increase in the liquid superficial gas velocities, liquid holdup and Peclet number increases due to lower dispersion. Similarly, for an increase in the gas velocity, the liquid holdup decreases in all cases while the effect of gas velocity was insignificant on the Peclet number. From the results, it can be concluded that a combination of spheres with fines gives lower dispersion than extrudates or reactor bed without fines. The reactor with thermowell packed with spherical catalysts and fines had higher holdup values while packing with no fines. From the results, the correlation was developed to predict the Peclet number and liquid holdup, which will be further used in the reactor scale modeling of liquid-phase acetylene hydrogenation study.

## REFERENCES

1. Tsamatsoulis, D. and N. Papayannakos, *Axial-Dispersion and Hold-up in a Bench-Scale Trickle-Bed Reactor at Operating-Conditions.* Chemical Engineering Science, 1994. **49**(4): p. 523-529.

2. Sater, V.E. and O. Levenspiel, *Two-phase flow in packed beds. Evaluation of axial dispersion and holdup by moment analysis.* Industrial & Engineering Chemistry Fundamentals, 1966. **5**(1): p. 86-92.

3. Cassanello, M.C., O.M. Martinez, and A.L. Cukierman, *Effect of the Liquid Axial-Dispersion on the Behavior of Fixed-Bed 3-Phase Reactors.* Chemical Engineering Science, 1992. **47**(13-14): p. 3331-3338.

4. Ranade, V.V., R.V. Chaudhari, and P.R. Gunjal, *Trickle Bed Reactors: Reactor Engineering & Applications.* Trickle Bed Reactors: Reactor Engineering & Applications, 2011: p. 1-274.

5. Fogler, H.S., *Elements of chemical reaction engineering*. 1999.

6. Ancheyta, J., *Modeling and simulation of catalytic reactors for petroleum refining*. 2011: John Wiley & Sons.

7. Iliuta, I., F. Larachi, and B.P. Grandjean, *Pressure drop and liquid holdup in trickle flow reactors: improved Ergun constants and slip correlations for the slit model.* Industrial & engineering chemistry research, 1998. **37**(12): p. 4542-4550.

8. Shariff, H. and M.H. Al-Dahhan, *Analyzing the impact of implementing different approaches of the approximation of the catalyst effectiveness factor on the prediction of the performance of trickle bed reactors.* Catalysis Today, 2019.

9. Al-Dahhan, M.H. and M.P. Duduković, *Catalyst bed dilution for improving catalyst wetting in laboratory trickle-bed reactors.* AIChE journal, 1996. **42**(9): p. 2594-2606.

10. Sie, S., *Scale effects in laboratory and pilot-plant reactors for trickle-flow processes.* Revue de l'Institut français du pétrole, 1991. **46**(4): p. 501-515.

11. Van Klinken, J. and R. Van Dongen, *Catalyst dilution for improved performance of laboratory trickle-flow reactors.* Chemical Engineering Science, 1980. **35**(1-2): p. 59-66.

12. Al-Dahhan, M.H., Y. Wu, and M.P. Dudukovic, *Reproducible technique for packing laboratory-scale trickle-bed reactors with a mixture of catalyst and fines.* Industrial & engineering chemistry research, 1995. **34**(3): p. 741-747.

13. Carruthers, J.D. and D.J. DiCamillo, *Pilot plant testing of hydrotreating catalysts: Influence of catalyst condition, bed loading and dilution.* Applied Catalysis, 1988. **43**(2): p. 253-276.

14. Korsten, H. and U. Hoffmann, *Three-phase reactor model for hydrotreating in pilot trickle-bed reactors.* AIChE Journal, 1996. **42**(5): p. 1350-1360.

15. Guo, J. and M. Al-Dahhan, *Liquid holdup and pressure drop in the gas–liquid cocurrent downflow packed-bed reactor under elevated pressures.* Chemical Engineering Science, 2004. **59**(22-23): p. 5387-5393.

16. Saroha, A.K., et al., *RTD studies in trickle bed reactors packed with porous particles.* The Canadian Journal of Chemical Engineering, 1998. **76**(4): p. 738-743.

17. Stegeman, D., et al., *Residence time distribution in the liquid phase in a cocurrent gas− liquid trickle bed reactor.* Industrial & engineering chemistry research, 1996. **35**(2): p. 378-385.

18. Pant, H., A. Saroha, and K. Nigam, *Measurement of liquid holdup and axial dispersion in trickle bed reactors using radiotracer technique.* Nukleonika, 2000. **45**(4): p. 235-241.

19. Fu, M.-S. and C.-S. Tan, *Liquid holdup and axial dispersion in trickle-bed reactors.* Chemical Engineering Science, Elsevier, 1996. **51**(24).

20. Gierman, H., *Design of laboratory hydrotreating reactors: scaling down of trickle-flow reactors.* Applied Catalysis, 1988. **43**(2): p. 277-286.

21. Al-Dahhan, M.H. and M.P. Dudukovic, *Pressure drop and liquid holdup in high pressure trickle-bed reactors.* Chemical Engineering Science, 1994. **49**(24b): p. 5681-5698.

22. Wu, Y., et al., *Comparison of upflow and downflow two-phase flow packed-bed reactors with and without fines: experimental observations.* Industrial & engineering chemistry research, 1996. **35**(2): p. 397-405.

# II. KINETIC STUDIES OF LIQUID PHASE HYDROGENATION OF ACETYLENE FOR ETHYLENE PRODUCTION USING A SELECTIVE SOLVENT OVER A COMMERCIAL PALLADIUM/ALUMINA CATALYST

Humayun Shariff and Muthanna H. Al-Dahhan

Department of Chemical and Biochemical Engineering, Missouri University of Science and Technology, Rolla, MO, 65409

## ABSTRACT

The kinetics of selective hydrogenation of acetylene in the liquid phase over a commercial Pd/ $Al_2O_3$ catalyst was investigated in a stirred-tank basket reactor. The liquid phase was acetylene gas absorbed in a selective solvent, N-Methyl Pyrrolidone (NMP). The reactor was operated at a pressure range of 15-250 psig with temperature varying from 60-120$^oC$ using different catalyst loading to identify the suitable operating conditions. The liquid phase was operated in batch mode while the gas phase was continuous. The kinetic experiments were conducted in the absence of external mass transfer resistances. The initial rates varied linearly with catalyst loading at all temperatures. The parameters (80-100$^oC$, 3 g/L catalyst loading, and operating pressure of 250 psig) were used to investigate the intrinsic kinetics with the catalyst as a slurry. An intrinsic kinetic model was developed using simple power-law equations and Langmuir-Hinshelwood-Hougen-Watson (LHHW) approach. The surface reaction between the adsorbed species was assumed to be the rate-controlling step. The LHHW model provided a good fit to the experimental data and kinetic rate parameters were estimated.

**Keywords**: Liquid phase, Acetylene hydrogenation, selective solvent, ethylene production, kinetics

## 1. INTRODUCTION

Ethylene, the simplest of the olefins, is an important precursor and a primary building block in petrochemical industries, especially in the production of polyethylene. Recently, ethylene demand is increasing as an alternative source for fuel production by catalytic conversion to higher hydrocarbons as a part of intensifying the gas-to-liquid fuel (GTL) technology [1]. A conventional method of ethylene production is thermal cracking, which is accompanied by acetylene as a byproduct. Although acetylene can be absorbed/stripped from the gas mixture using a selective solvent, it is more beneficial to selectively hydrogenate acetylene to ethylene. While hydrogenation of acetylene in the gas phase, the following observations were made in the literature. The hydrogenation of acetylene using supported catalysts in the gas phase is an exothermic reaction, which can reach reactor temperatures of up to 430°C mostly leading to thermal runaway [2-5]. Additional cooling costs, in turn, increase the operational expenses as well as accounting the risk of failure.

During the hydrogenation of acetylene, acetylene molecules can dimerize to form butadiene ($C_{4+}$ compounds), further, oligomerize to form compounds commonly called as 'green oil.' Green oil poisons the surface of the catalyst requiring periodic catalyst regeneration [5-8]. Also, the acidity of the support (generally alumina) was considered as a significant cause for catalyst deactivation by increasing the oligomerization of the olefins

[9, 10]. The rate of green oil formation was mainly affected by $H_2$:$C_2H_2$ ratio and temperature [2, 3].

Using a liquid solvent eliminates the risk of a thermal runaway because it absorbs more heat with less temperature rise at the catalyst-liquid interface. Heat transfer can also be improved because of the higher thermal conductivity of the solvent than the gases. The liquid phase could potentially remove the green oil formed during the reaction, due to the presence of liquid flow in the system and its physical properties (less volatile and stable) thereby increasing the catalyst life. Moreover, the acetylene absorption process from ethylene streams can be integrated into a more economically beneficial and safer process for ethylene production. This process is promising as an alternate route for ethylene to fuel production [1, 11, 12]. Furthermore, abundant sources of acetylene from calcium carbide hydrolysis and partial oxidation of natural gas will enable acetylene as a more reliable source for ethylene production.

The high selective solubility of acetylene in comparison to ethylene in polar solvents like NMP, DMF (N, N-dimethylformamide), and acetone has been reported in the literature [4, 13-15]. The polar liquid solvent improves selectivity to ethylene over gas-phase hydrogenation because of the greater solubility of acetylene than ethylene [4, 14]. After the reaction, the product separation was more straightforward owing to the low solubility of ethylene and the high binding energy of acetylene on the active catalyst sites.

To develop a kinetics model and evaluate the kinetic parameters for the hydrogenation of acetylene in the liquid phase, the possible reactions and side reactions need to be understood. Table 1 summarizes the main reactions possible during the reaction. In literature, most of the gas phase studies available were in the presence of excess ethylene

as they were aimed at hydrogenating the feed from the cracker to reduce the acetylene content [16, 17]. Although the formation of ethylene is the primary and desired reaction, over hydrogenation leads to the formation of ethane and oligomers from acetylene. Additionally, the formation of ethane from acetylene hydrogenation is as equally possible as it is from ethylene [18], but few studies did not consider this in the reaction kinetics for its low significance due to their operating conditions [5, 17, 19, 20]. Different reaction pathways of butadiene formation from acetylene on the catalyst surface can be found elsewhere [6, 20-23].

Most of the kinetics models included the addition of Carbon monoxide (CO) term as CO was needed to control the kinetics mainly when the reactant mixture has ethylene to avoid ethylene hydrogenation to ethane. On the other hand, CO also reduces the sites on the catalyst surface for the adsorption of reactant molecules leading to catalytic poisoning [23, 24]. Adapting the kinetic models developed for gas-phase kinetics directly from the literature may have its limitations due to the nature of the studies. The solubility of gases in the liquid solvent at the operating conditions needs to be understood while evaluating the kinetic parameters, as they can significantly affect the conversion and selectivity.

In our study to assess the reactor performance of hydrogenation of acetylene in the liquid phase using a selective solvent over a commercial catalyst involving hydrodynamics, kinetics and packed bed reactor experiments to our knowledge only a few open works of literature were found to our knowledge [4, 14, 25, 26]. Although patented literature [27, 28] was available for the liquid phase hydrogenation using NMP as a selective solvent in packed bed reactors seldom focused on kinetic modeling, scale-up, and related studies.

Table 1. Reactions possible in acetylene hydrogenation

| **Reaction** | **Equation** |
|---|---|
| r1 | $C_2H_2 + H_2 \rightarrow C_2H_4$ |
| r2 | $C_2H_4 + H_2 \rightarrow C_2H_6$ |
| r3 | $C_2H_2 + 2H_2 \rightarrow C_2H_6$ |
| r4 | $2C_2H_2 + H_2 \rightarrow C_4H_6$ |
| r5 | $2C_2H_2 + 2H_2 \rightarrow C_4H_8$ |

This proposed study focuses on the kinetics in the liquid phase hydrogenation as only the gas phase kinetics have been investigated in the open literature, and no liquid phase kinetic studies were available. It was significant to understand both apparent and intrinsic kinetics, which can help in understanding the performance of the catalyst at different operating conditions, and facilitate during the scale-up of the process. The kinetics studies involved the hydrogenation of acetylene absorbed in a solvent acting as the liquid phase over a commercial gas-phase hydrogenation catalyst commonly used for gas-phase hydrogenation. Different parameters like temperature, catalyst loading, and operating pressure were investigated. In this work of liquid phase acetylene hydrogenation, CO was not used during the reaction. This study also focuses on developing an intrinsic kinetic model, which is commendable progress in this area of research using which can be analyzed and further implemented in a reactor scale model. These results will help in optimizing the operating conditions for fixed bed reactor experiments.

# 2. METHODOLOGY

## 2.1. MATERIALS

A commercial catalyst of 0.5 wt% Pd on alumina spheres (Alfa-Aesar) of 2-4 mm diameter was used. NMP (Sigma-Aldrich) (99% Purity) was the polar solvent. Purified acetylene, nitrogen, and hydrogen gas were used in the experiments.

## 2.2. PROCEDURE

The experimental setup was designed to operate in a batch, semi-batch, or continuous mode at pressures up to 2000 psi and temperature up to 500$^{o}$C. A 300 mL three-phase stirred tank reactor was used to run as both slurry and basket conditions. The gas feed was injected from the head from a high-pressure gas cylinder. The hollow shaft of the six-bladed turbine in the reactor was used to bubble the gas through the batch liquid feed. The impeller was driven by an overhead motor (at 100-2000 rpm). For the basket reactor configuration, the impeller blades rotated at the center while the basket was fixed. No cooling coil was attached for basket reactor studies. The liquid phase comprising of NMP and $C_2H_2$ was prepared and preloaded in the reactor as a batch. The materials in the vessel were heated to the required temperature before stirring, and a sample was collected to determine initial reactor conditions before the reaction. To initiate the reaction, $H_2$ gas was fed continuously into the reactor with agitation to ensure saturation and samples were collected at regular intervals. The effluent samples were analyzed using an on-line gas chromatograph (TRACE 1310) with a flame ionization detector. Pure reactants and products were used as internal standards. To study the intrinsic kinetics**,** experiments were

conducted using crushed and sieved catalysts ($d_p < 200\mu$) as a slurry at selected conditions to evaluate the intrinsic kinetics. A specific catalyst loading was used at an operating pressure of 250 psig. The temperatures were varied from 80-100$^oC$, and the data was used to estimate the intrinsic kinetic parameters.

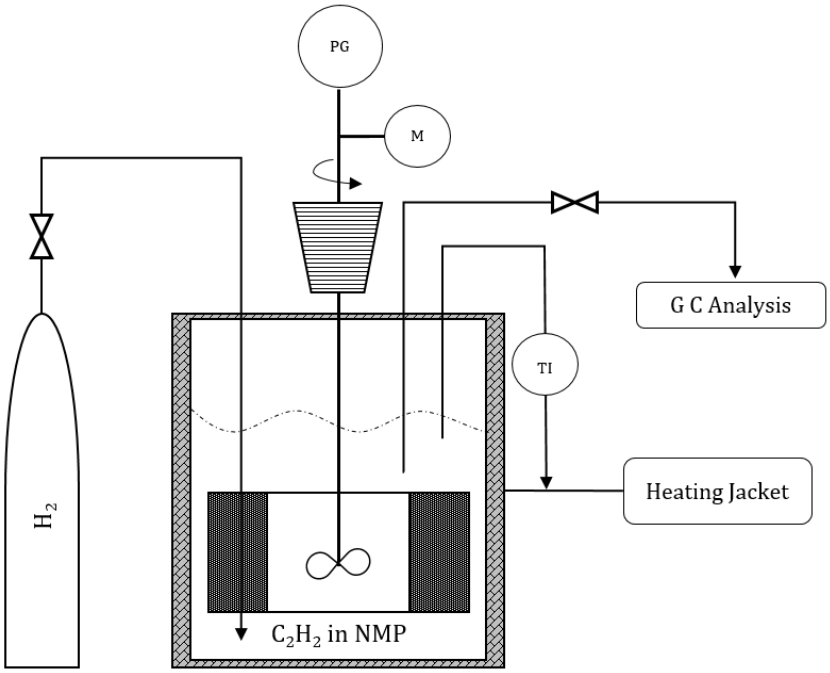


Figure 1. Experimental setup for kinetic study of liquid-phase hydrogenation of acetylene

## 2.3. LIQUID PHASE PREPARATION

A test to confirm the amount of acetylene dissolved in NMP was conducted at ambient conditions. Pure $C_2H_2$ was bubbled in a pre-weighed tared container with a known quantity of NMP. The solubility was 32 mL of gas/mL of NMP at room temperature and atmospheric pressure, which was in accordance with the literature [15, 31, 32]. The solubilities of ethylene and hydrogen were 3.1 mL of gas/mL of NMP and 0.5 mL of gas/mL of NMP respectively. These values are low in comparison with acetylene, which

is preferred for the study. This mixture of acetylene dissolved in NMP was prepared for the investigations at 1atm and 25$^{o}$C. The initial concentration of acetylene in NMP (3 wt%) was kept constant throughout the study. Conversion and species selectivity are defined as follows in Equations 1-4:

$$Acetylene\ conversion = \frac{C_2H_2(i) - C_2H_2(o)}{C_2H_2(i)} \quad (1)$$

$$S_{C2H4}, Ethylene\ selectivity = \frac{C_2H_4(o)}{C_2H_2(i) - C_2H_2(o)} \quad (2)$$

$$S_{C2H6}, Ethane\ selectivity = \frac{C_2H_6(o)}{C_2H_2(i) - C_2H_2(o)} \quad (3)$$

$$C_4^+\ selectivity = 2\frac{\sum C_4H_{10}(o) + \sum C_4H_8(o) + C_4H_6(o)}{C_2H_2(i) - C_2H_2(o)} \quad (4)$$

## 3. RESULTS AND DISCUSSIONS

The gas chromatograph was calibrated with pure $C_2H_2$, $C_2H_4$, $C_2H_6$, and $C_4$ gases. The samples were analyzed based on the formation of the gaseous products and consumption of $C_2H_2$ in the liquid. The catalyst was loaded in the basket appropriately and tested at different operating conditions to investigate the reaction. Initial tests were conducted at different impeller speeds to eliminate the effect of external mass transfer resistances. Ideal operating conditions (pressure (250 psig), 3g/L catalyst loading, and 3 wt%, $C_2H_2$ in NMP) were chosen for the basket experiments. At a stirring rate of above 600 rpm, the conversion of acetylene remained constant, and the rate did not change with further increase in the speed at different temperatures. It is safe to assume that, over 700

rpm, the tests are not limited by external mass transfer resistances. Once the green oil formation was observed in the liquid sample, the reaction was stopped.

The initial reaction mixture of acetylene absorbed in the NMP was heated to the desired temperature at the operating pressure; there was a loss of acetylene from the batch due to the desorption of acetylene, especially at temperatures above 100$^{o}$C. At 100$^{o}$C, traces of acetylene was observed in the gas sample and increased with an increase in temperature. This was due to the decrease in the solubility of acetylene in the NMP. To keep the starting conditions consistent, the operating reaction temperature ranges for this study were chosen in between 60-100$^{o}$C. The initial rates were estimated for each experiment at a constant time interval.

### 3.1. EFFECT OF CATALYST LOADING

The effect of catalyst loading at different operating temperatures at 250 psig pressure was investigated, as shown in Figures 2 and 3. From Figure 2, it was observed that the initial rate was linearly dependent on the catalyst loading at the temperatures investigated suggesting the gas-liquid mass transfer may be negligible under these conditions and the reaction in the kinetically controlled regime [31]. With an increase in the weight of the catalyst from 3 g/L to 6 g/L, no more than 10% increase in the overall acetylene conversion was observed (Figure 3). Although the initial rates were high at 100$^{o}$C at a catalyst loading of 6 g/L, to optimize the amount of catalyst used per volume of the solvent mixture with respect to cost, 3 g/L was used in estimating the intrinsic kinetic parameters.

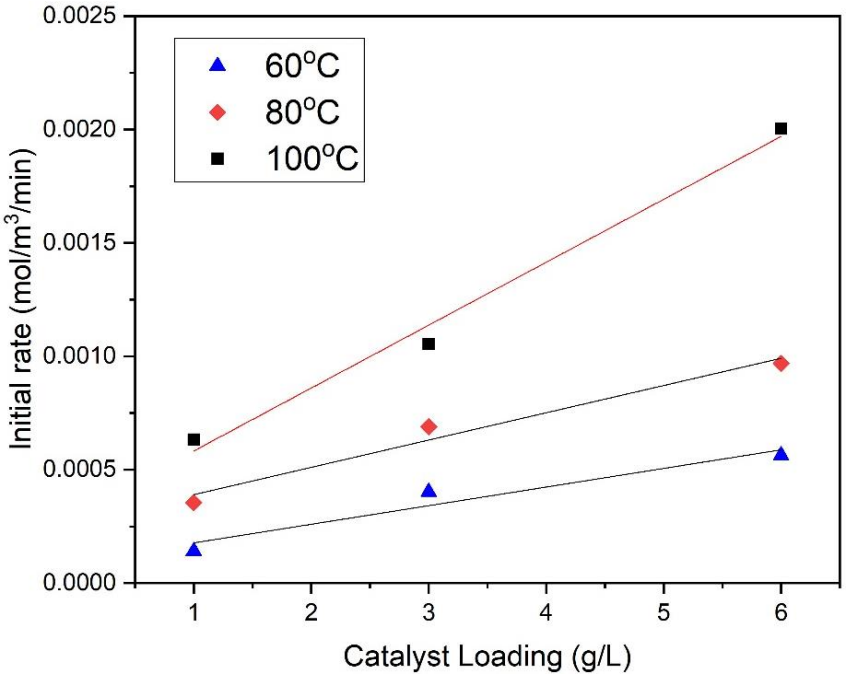


Figure 2. Effect of catalyst loading on the initial rates at different temperatures **(**P=250 psig)

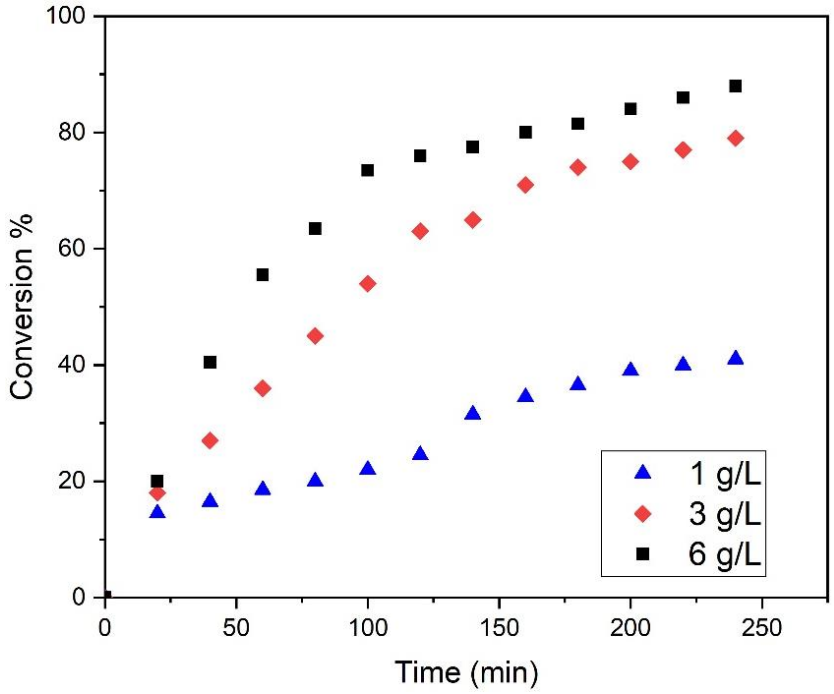


Figure 3. Effect of catalyst loading on the conversion of acetylene with respect to time (P=250 psig, T=80°C)

### 3.2. EFFECT OF TEMPERATURE

The overall conversion of acetylene to ethylene increased with an increase in temperature, thereby having a significant effect on the rate of reaction. The depletion of acetylene was found to be higher with an increase from 60-90$^{o}$C, as shown in Figure 4. It was observed at temperatures higher than 100$^{o}$C that acetylene was consumed completely, and the rate of reaction was faster in comparison with the lower temperatures.

Additionally, the formation of ethylene with high selectivity at these higher temperatures confirms that, with an increase in temperature both selectivity and conversion increase (Figures 4 and 5). This was also due to the fewer moles of ethylene available relative to acetylene for the reaction due to the decrease in solubility of ethylene at higher temperatures. The ethylene after formation is in the gas phase and does not dissolve in NMP to react with hydrogen on the catalyst surface.

At 60$^{o}$C, more intermediates were formed due to the over hydrogenation of the acetylene due to the increased acetylene solubility. It can also be understood that at lower temperatures, the low ethylene selectivity was due to higher solubility values of ethylene and acetylene in NMP. Overall, the reaction has to be fast (increase in temperature) and controlled; this way, the ethylene formed is still not available to form ethane, and the acetylene available on the catalyst surface does not increase the selectivity of undesired compounds. From Figure 5, the selectivity of ethylene was low due to the formation of other compounds in the reaction at lower temperatures.

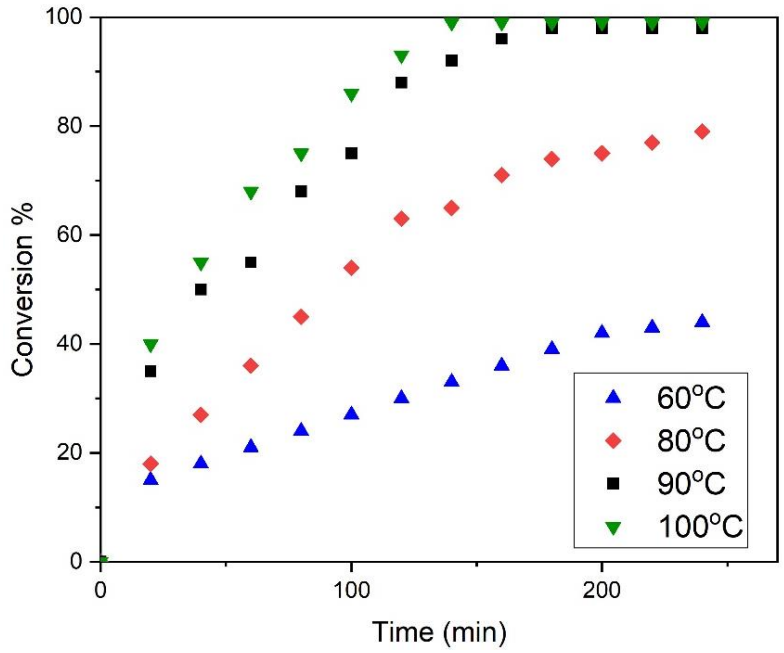


Figure 4. Effect of temperature on the conversion of acetylene with respect to time (Catalyst loading: 3g/L, P=250 psig)

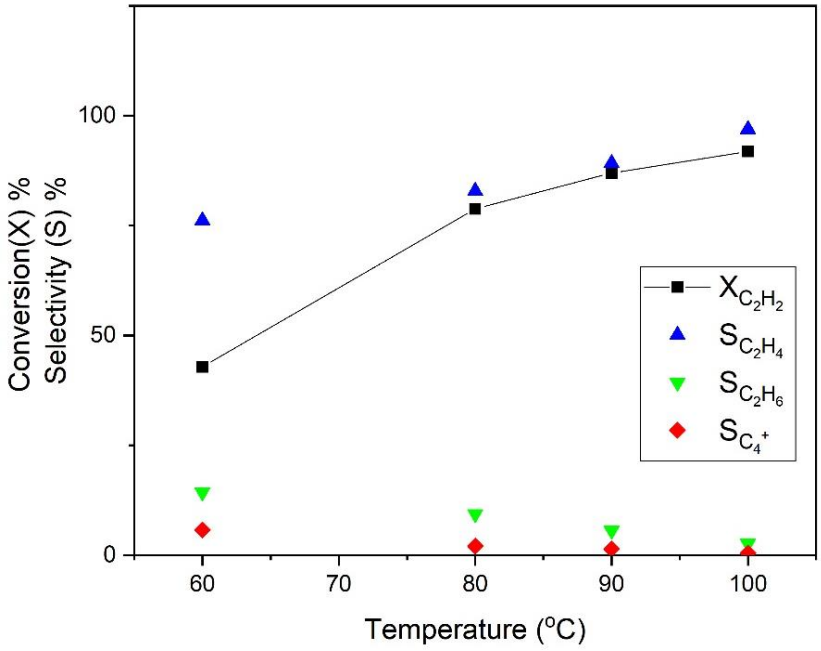


Figure 5. Effect of temperature on the conversion of acetylene and selectivities (Catalyst loading: 3g/L, P=250 psig)

### 3.3. EFFECT OF PRESSURE

The operating pressure was another parameter that affected the conversion and selectivity in the reaction. The effect of pressure was studied for two temperatures (80 and 100$^{o}$C), and it was observed that the conversion increased with an increase in pressure for the reaction (Figure 6). As mentioned earlier, after the initial interaction of hydrogen molecules with acetylene in the reactor, the hydrogen partial pressure was maintained. The solubility of hydrogen in the solvent increases with an increase in pressure leading to a higher rate of conversion [32]. This increases the hydrogen availability in the liquid phase for reaction with the acetylene molecules, which is less at low pressures. While conducting the experiments in a flow reactor system, operating at a high pressure will be beneficial.

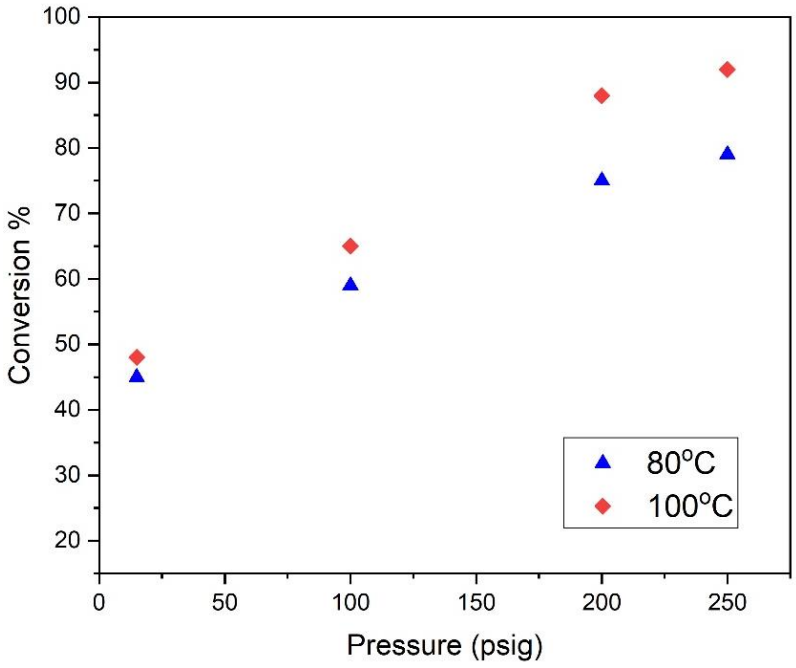


Figure 6. Effect of pressure on the conversion of acetylene (Catalyst loading: 3g/L)

## 3.4. INTRINSIC KINETIC MODELING

The intrinsic kinetics studies were carried out in conditions based on the operating conditions from the basket experiments with the catalyst as a slurry. The experiments were conducted at an operating pressure of 250 psig with a catalyst loading of 3 g/L at different temperatures. The power-law and LHHW models were used to obtain the estimates of the kinetic parameters, and the LHHW model equations were derived assuming the surface reaction was rate-limiting.

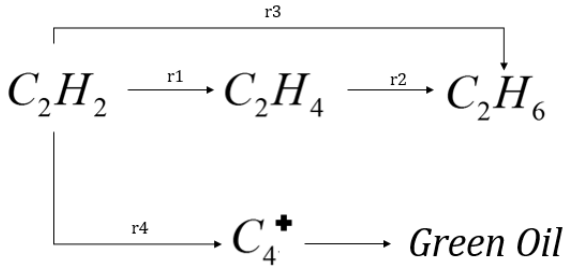


Figure 7. Acetylene Hydrogenation Network Model

**3.4.1. Power-Law Model.** The power-law model shown in Equation 5 was used to obtain the kinetic parameters.

$$r_{C2H2} = -k_{C2H2} * C_{C2H2}^{a} * C_{H2}^{b} \quad (5)$$

where *a* and *b* are reaction order corresponding to acetylene and hydrogen respectively.

It was always beneficial to fit the data using a power-law model mainly to understand and identify if the reaction is mass-transfer limited or operating in a kinetically controlled regime. Since it was difficult to estimate the amount of ethylene hydrogenating to form ethane, the power-law estimation was kept simple with only the disappearance of acetylene. The experimental data were fit to the power-law model equation, and the parameters were optimized by least-square curve fitting method. The power-law model

was fit for the intrinsic experimental conditions and the resulting power-law model equation (SQR = 4.4) was

$$r_{C2H2} = 8.11 * 10^{-4}\ [C_2H_2]^{1.13}[H_2]^{0.96} \quad (6)$$

The intrinsic activation energy was 63.66 ±19.1 kJ/mol from the slope of rate constants vs (1/T), indirectly confirming the absence of mass transfer resistances.

**3.4.2. Langmuir-Hinshelwood-Hougen-Watson Model.** The kinetic rate model equation was derived based on the Langmuir-Hinshelwood-Hougen-Watson mechanism with the formation of ethylene (surface reaction) as the rate-determining step. The experiments were conducted mainly to understand the effect of the operating parameters on the acetylene conversion and selectivity of ethylene. Since the selectivity to ethylene was very high (above 90%) at 80 and 100$^{o}$C, only reaction 1 was considered in the model for its significance. Moreover, it becomes intricate to describe if the formation of ethane was from ethylene or acetylene [17]. Equation 7 was simplified to keep the kinetics straight forward and not over or under predict the experimental data. The model was kept in terms of acetylene and hydrogen due to the high ethylene selectivity in the operating conditions. The kinetic rate model for hydrogenation of acetylene based on the assumptions and discussions was as below

$$-r_{C_2H_2} = \frac{k_1[C_2H_2][H_2]}{\left(1+K_{C_2H_2}[C_2H_2]+\sqrt{K_{H_2}[H_2]}\right)^3} \quad (7)$$

where the rate and adsorption equilibrium constants were estimated from Equations 8 and 9 respectively.

$$k = A\exp\left(-\frac{E_A}{RT}\right) => A * \exp[-\frac{E}{R}(\frac{1}{T}-\frac{1}{T_m})] \quad (8)$$

$$K = K_o \exp\left(-\frac{E_A}{RT}\right) => K_o * \exp[\ \frac{H}{R}(\frac{1}{T} - \frac{1}{T_m})\ ] \quad (9)$$

$$SQR = \sum_{i=1}^{N}(\frac{[C_i]_{exp} - [C_i]_{sim}}{[C_i]_{exp}})^2 \quad (10)$$

### 3.5. PARAMETER ESTIMATION

Complex heterogeneous models based on the reaction mechanism provide more information on the reaction kinetics. The initial estimates for the rate constants and the for adsorption equilibrium constants to solve the LHHW based heterogeneous rate equations were taken from the literature and trial and error. The rate equation was numerically solved based on the Runge-Kutta method and parameters were optimized using non-linear regression to minimize the least-squares by the Levenberg-Marquardt algorithm in MATLAB® solver.

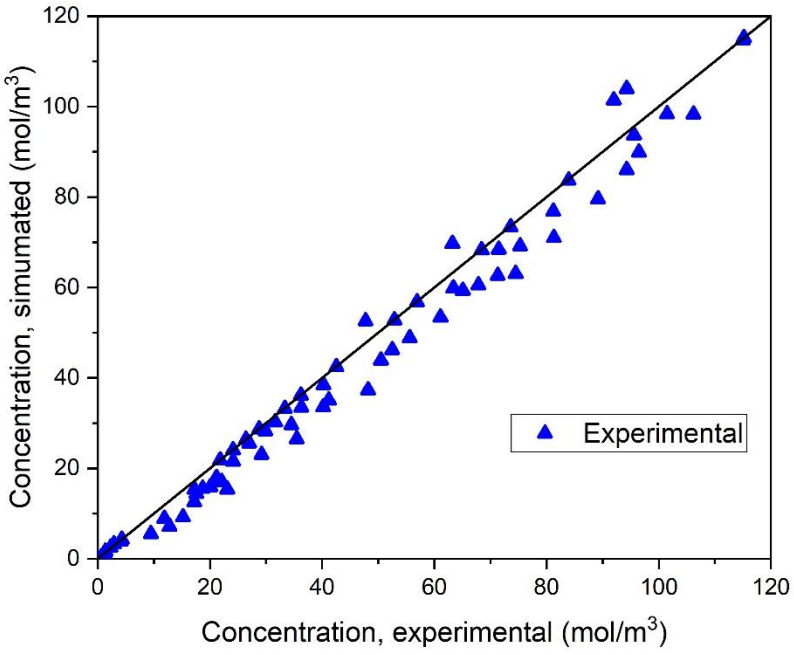


Figure 8. Parity plot of experimental and predicated concentration values

Table 2. Fitted rate parameters with their standard deviation for liquid-phase acetylene hydrogenation reaction at P=250 psig and slurry conditions (intrinsic kinetics)

| **Rate parameters** | **Values** |
|---|---|
| | |
| $k_1$ (mol/g.cat/min) | 1.18 ±0.0092 |
| $K_{C2H2}$ ($m^3$/mol) | 0.0108± 0.002 |
| $K_{H2}$ ($m^3$/mol) | 1.43 ± 0.412 |

The rate parameters were regressed to fit the experimental data at different temperatures, and the activation parameters were estimated from the rate constants using Equations 9 and 10. The concentration values calculated from the model equations were plotted against the experimental values. Figure 8 showed good agreement of the model, and experimental data with SQR was 1.92. Additionally, the reaction being temperature-sensitive and irreversible towards the formation of ethylene on the catalyst surface, the assumption of surface reaction limitation was valid in the operating conditions investigated [33].

## 4. CONCLUSIONS

The kinetics of the selective liquid-phase hydrogenation of acetylene using a selective solvent over a commercial catalyst for ethylene production was studied in a stirred tank reactor at constant initial acetylene concentration in NMP between 60-100$^o$C, the pressure of 15-250 psig and catalyst loading of 1-6 g/L. All the measurements were carried out in a kinetically controlled regime, neglecting inter- and intraparticle mass transfer resistances. Higher conversion and ethylene selectivity were observed at a pressure of 250

psig and temperature above 80$^{o}$C. The ideal catalyst loading of 3 g/L was identified to guide the packed bed reactor experiments. The parameters of the intrinsic kinetic model developed based on the LHHW mechanism were estimated by the regressive non-linear fitting. The model was able to predict the experimental data with the parameters giving realistic values to understand the reaction mechanism. The kinetics investigation provides an insight into the liquid-phase hydrogenation process as well as to identify the suitable operating conditions. This model will be used in predicting the reactor performance of lab-scale packed bed reactors and optimizing the liquid phase hydrogenation process towards scale-up.

## REFERENCES

1. Hall, K.R., A new gas to liquids (GTL) or gas to ethylene (GTE) technology. Catalysis Today, 2005. 106(1-4): p. 243-246.

2. Bos, A.N.R. and K.R. Westerterp, Mechanism and kinetics of the selective hydrogenation of ethyne and ethene. Chemical Engineering and Processing, 1993. 32: p. 1-7.

3. Edvinsson, R.K., A.M. Holmgren, and S. Irandoust, Liquid-Phase Hydrogenation of Acetylene in a Monolithic Catalyst Reactor. Industrial & engineering chemistry research, 1995. 34(1): p. 94-100.

4. Hou, R., T. Wang, and X. Lan, Enhanced Selectivity in the Hydrogenation of Acetylene due to the Addition of a Liquid Phase as a Selective Solvent. Industrial & Engineering Chemistry Research, 2013. 52(37): p. 13305-13312.

5. Sarkany, A., Weiss, A. H., Szilagyi, T., Sandor, P., & Guczi, L., Green oil poisoning of a Pd/Al203 acetylene hydrogenation catalyst. Applied Catalysis, 1984. 12: p. 373-379.

6. Borodziński, A. and G.C. Bond, Selective Hydrogenation of Ethyne in Ethene-Rich Streams on Palladium Catalysts. Part 1. Effect of Changes to the Catalyst During Reaction. Catalysis Reviews, 2006. 48(2): p. 91-144.

7. Asplund, S., Fornell, C., Holmgren, A., & Irandoust, S., Catalyst deactivation in liquid- and gas-phase hydrogenation of acetylene using a monolithic catalyst reactor. Catalysis Today, 1995. 24: p. 181-187.

8. Al-Ammar, A.S. and G. Webb, Hydrogenation of acetylene over supported metal catalysts. Part 2.—[14 C] tracer study of deactivation phenomena. Journal of the Chemical Society, Faraday Transactions 1: Physical Chemistry in Condensed Phases, 1978. 74: p. 657-664.

9. Wang, B. and G.F. Froment, Kinetic modeling and simulation of the selective hydrogenation of the C3-cut of a thermal cracking unit. Industrial & Engineering Chemistry Research, 2005. 44(26): p. 9860-9867.

10. Wehrli, J.T., Thomas, D. J., Wainwright, M. S., Trimm, D. L., & Cant, N. W., Reduced Foulant Formation During the Selective Hydrogenation of C2, C3, and C4 Acetylenes. Studies in Surface Science and Catalysis, 1991. 68: p. 203-210.

11. Anderson, R., J. Fincke, and C. Taylor, Conversion of natural gas to liquids via acetylene as an intermediate. Fuel, 2002. 81(7): p. 909-925.

12. Wood, D.A., C. Nwaoha, and B.F. Towler, Gas-to-liquids (GTL): A review of an industry offering several routes for monetizing natural gas. Journal of Natural Gas Science and Engineering, 2012. 9: p. 196-208.

13. Arpe, H.-J. and K. Weissermel, Industrial organic chemistry. Vol. 393. 2010: Wiley-VCH Weinheim.

14. Shitova, N. B., D. A. Shlyapin, T. N. Afonasenko, E. N. Kudrya, P. G. Tsyrul'nikov, and V. A. Likholobov, Liquid-phase hydrogenation of acetylene on the Pd/sibunit catalyst in the presence of carbon monoxide. Kinetics and Catalysis, 2011. 52(2): p. 251-257.

15. Lee, J.M., Palgunadi, J., Kim, J. H., Jung, S., Choi, Y. S., Cheong, M., & Kim, H. S., Selective removal of acetylenes from olefin mixtures through specific physicochemical interactions of ionic liquids with acetylenes. Physical Chemistry Chemical Physics, 2010. 12(8): p. 1812-1816.

16. Borodziński, A. and G.C. Bond, Selective Hydrogenation of Ethyne in Ethene Rich Streams on Palladium Catalysts, Part 2: Steady State Kinetics and Effects of Palladium Particle Size, Carbon Monoxide, and Promoters. Catalysis Reviews, 2008. 50: p. 379-469.

17. Bos, A.N.R., Botsma, E. S., Foeth, F., Sleyster, H. W. J., Westerterp, K. R., A kinetic study of the hydrogenation of ethyne and ethene on a commercial Pd/Al2O3 catalyst. Chemical Engineering and Processing, 1993. 32: p. 53-63.

18. Margitfalvi, J., L. Guczi, and A.H. Weiss, Reactions of acetylene during hydrogenation on Pd black catalyst. Journal of Catalysis, 1981. 72: p. 185-198.

19. Leviness, S., Nair, V., Weiss, A. H., Schay, Z., & Guczi, L., Acetylene hydrogenation selectivity control on PdCu/Al2O3 catalysts. Journal of Molecular Catalysis, 1984. 25: p. 131-140.

20. Borodziński, A. and A. Cybulski, The kinetic model of hydrogenation of acetylene–ethylene mixtures over palladium surface covered by carbonaceous deposits. Applied Catalysis A: General, 2000. 198: p. 51-66.

21. Yang, B., et al., Mechanistic Study of 1,3-Butadiene Formation in Acetylene Hydrogenation over the Pd-Based Catalysts Using Density Functional Calculations. The Journal of Physical Chemistry C, 2014. 118(3): p. 1560-1567.

22. Sárkány, A. and Z. Révay, Some features of acetylene and 1, 3-butadiene hydrogenation on Ag/SiO2 and Ag/TiO2 catalysts. Applied Catalysis A: General, 2003. 243(2): p. 347-355.

23. Borodziński, A. and G.C. Bond, Selective Hydrogenation of Ethyne in Ethene-Rich Streams on Palladium Catalysts, Part 2: Steady-State Kinetics and Effects of Palladium Particle Size, Carbon Monoxide, and Promoters. Catalysis Reviews, 2008. 50(3): p. 379-469.

24. Al-Ammar, A.S. and G. Webb, Hydrogenation of acetylene over supported metal catalysts. Part 3.—[14C] tracer studies of the effects of added ethylene and carbon monoxide on the reaction catalysed by silica-supported palladium, rhodium and iridium. Journal of the Chemical Society, Faraday Transactions 1: Physical Chemistry in Condensed Phases, 1979. 75: p. 1900-1911.

25. Huang, B., Wang, T., Lei, C., Chen, W., Zeng, G., & Maran, F, Highly efficient and selective catalytic hydrogenation of acetylene in N,N-dimethylformamide at room temperature. Journal of Catalysis, 2016. 339: p. 14-20.

26. Hou, R., X. Lan, and T. Wang, Selective hydrogenation of acetylene on $Pd/SiO_2$ in bulk liquid phase: A comparison with solid catalyst with ionic liquid layer (SCILL). Catalysis Today, 2015. 251: p. 47-52.

27. Johnson, M.M., Edward R. Peterson, and Sean C. Gattis, United States Patent No. 7,045,670. 2006.

28. Johnson, M., E. Peterson, and S. Gattis, Process for liquid phase hydrogenation. 2005, Google Patents.

29. Burr, B. and L. Lyddon. A comparison of physical solvents for acid gas removal. in 87th Annual Gas Processors Association Convention, Grapevine, TX, March. 2008.

30. Antonov, V. and A. Lapidus, Acetylene production. Khimiya, Moscow, 1970.

31. Chaudhari, R. V., Jaganathan, R., Kolhe, D. S., Emig, G., & Hofmann, H., Kinetic modelling of a complex consecutive reaction in a slurry reactor: hydrogenation of phenyl acetylene. Chemical engineering science, 1986. 41(12): p. 3073-3081.

32. Brunner, E., Solubility of Hydrogen in 10 Organic Solvents at 298.15, 323.15, and 373.15 K. Journal of chemical and Engineering Data, 1985. 30(3): p. 269-273.

33. Fogler, H.S., Elements of chemical reaction engineering. 1999.

# III. LIQUID PHASE ETHYLENE PRODUCTION BY HYDROGENATION OF ACETYLENE USING A SELECTIVE SOLVENT IN A FIXED BED REACTOR: EXPERIMENTS AND MODELING

Humayun Shariff and Muthanna H. Al-Dahhan

Department of Chemical and Biochemical Engineering, Missouri University of Science and Technology, Rolla, MO, 65409

## ABSTRACT

The performance of a packed bed reactor operating in downflow and upflow for hydrogenation of acetylene in the liquid phase using a selective solvent over a commercial catalyst was investigated. The effect of temperature, pressure, gas, and liquid velocities on the conversion and selectivity was studied. The operating conditions desired were the temperature of 80-100$^{o}$C at a low liquid hourly space velocity of 3 $hr^{-1}$, 0.08 m/s gas velocity operating at a pressure of 250 psig. Upflow mode of operation due to increased wetting of catalyst than the downflow performed better, while the ethylene selectivity above 90% in both modes at the selected operating conditions. The experimental data was validated using a reactor scale model accounting for pellet level effects in terms of overall effectiveness factor. The model also included intrinsic kinetics, catalyst wetting, liquid maldistribution, and transports. The model was able to predict the experimental data in good agreement.

**Keywords**: Liquid phase, Acetylene hydrogenation, selective solvent, ethylene production, packed bed reactors

# 1. INTRODUCTION

A cost-effective and safe method to produce liquid fuel efficiently from natural gas has always been a topic of research due to the increasing energy crisis. Ethylene production has been an important topic of research due to the increasing need for alternative fuel as well as to meet the rising polyethylene demand. Ethylene is a primary building block in the petrochemical industry as well as it has been used in manufacturing liquid fuel (higher hydrocarbons) by oligomerization [1]. This oligomerization process, commonly called Ethylene-to-liquids (ETL), is being considered as an alternative to the commonly used Fischer-Tropsch process for liquid fuel production. Also, due to the ever-growing demand for polyethylene across the globe projected at 100 million tons by 2018 [2], there are many ongoing types of research to increase the availability of ethylene. Acetylene, majorly produced directly from the partial oxidation of natural gas, partial combustion of methane, and calcium carbide-water reaction, can also be a potential feed to produce ethylene to meet the demand.

The ethylene stream from thermal cracking of naphtha has acetylene as the byproduct. This stream to be directly used for polyethylene production should contain less than 5ppm of acetylene as it acts as a catalytic poison to the polymerization catalyst. It has always been a challenge to selectively hydrogenate the acetylene to ethylene efficiently and safely, considering its high reactivity and exothermic nature during hydrogenation (Table 1). Moreover, acetylene hydrogenation to increase the ethylene yield has been an ongoing research area using different methodologies, types of catalysts, and approaches

[3-5]. The primary motivation for this study was to improve the existing gas-phase hydrogenation process to convert acetylene to ethylene.

Gas-phase catalytic hydrogenation of acetylene to ethylene is widely used in industries and by researchers using packed bed reactors (one or more reactors in series), but it has its drawbacks such as unsafe operation (high reaction of heat) and low selectivity and yield. Many types of catalysts have been tested for this process, and still, there is room for improvement, mainly due to the demand of the ethylene commodity. Additionally, undesired product formation (butane and higher hydrocarbons) due to ethylene hydrogenation was reported leading to early deactivation of the catalyst due to green oil formation (oligomerization). This not only affects the yield but also requires the purification of the product stream [3, 6]. Due to the green oil formation, there is a high cost for catalyst regeneration, and catalyst replacement may be necessary. To control the reaction heat, heat exchangers, or other modifications to the system are required to remove the reaction heat, which makes the process expensive and labor-intensive. Considering the shortcomings of gas-phase hydrogenation, improved heat transfer, and wetting of the reactants over the catalyst bed could be achieved by using a liquid medium in the reactor. This way, the process is safe by avoiding high exothermicity and more efficient by reducing the formation of green oil [3, 7-9].

Two studies reported the use of a solvent (liquid-phase) in the acetylene hydrogenation to ethylene where the liquid phase [8, 9]. The solvent was utilized in the reaction mainly to reduce the green oil formation on the catalyst as well as absorb the high heat generated during the reaction and not used as a selective solvent for acetylene.

Table 1. Major reactions in acetylene hydrogenation with heat of reaction

| **Equation** | **ΔH, kJ/mol @298K** |
|---|---|
| $C_2H_2 + H_2 \rightarrow C_2H_4$ | Acetylene = -174 |
| $C_2H_4 + H_2 \rightarrow C_2H_6$ | Ethene = -137 |
| $C_2H_2 + 2H_2 \rightarrow C_2H_6$ | Ethane = -311 |
| $2C_2H_2 + H_2 \rightarrow C_4H_6$ | Butadiene = -109 |

Edvinsson et al. (1995) used heptane as the liquid phase for selective hydrogenation in a monolithic reactor. It was inferred that the use of the liquid phase improved the catalyst stability by washing out the green oil form on the catalyst [8]. As an alternative of using the liquid medium only for heat transfer [8, 9], a solvent with high acetylene solubility compared to other gases in the reaction system can be used to absorb acetylene selectively. This liquid can be used as the fed to the reactor for hydrogenation [7, 12]. By this means, we can control the heat generated as well as improve the acetylene selectivity to ethylene. Additionally, selecting the ideal solvent and recycling, it is very vital considering the economics.

The hydrogenation of acetylene in the liquid phase using a selective solvent was investigated in a shaker-type flow reactor over a Pd/Sibunit supported catalyst in the presence of CO. NMP was used as the liquid phase. CO was used mainly to enhance the competitive adsorption between acetylene and ethylene and inhibiting over hydrogenation to ethane. Sibunit was used as the support to eliminate the acidic effects of other supports like alumina, which were proven to promote oligomerization. An increase in both selectivity to ethylene (90%) and acetylene conversion (over 96%) was observed while

using NMP as the solvent and CO addition [12]. Hou et al. [7] focused on improving the selectivity to ethylene without the addition of CO in a magnetically stirred semi-batch reactor using a 0.01% $Pd/SiO_2$ catalyst. The $C_2H_2$:$H_2$ molar ratio was 4-40, while a fixed volume of NMP was preloaded as a batch in the flask. The results deduced that at a reaction temperature of around 100$^oC$ with a low gas hourly space velocity and high $C_2H_2$:$H_2$ molar ratio yielded a high conversion of 96% with a selectivity to ethylene of 90%. By using selective solvent, the catalyst stability improved, and selectivity to ethylene increased with conversion in comparison with gas-phase hydrogenation reaction. This was mainly due to the low acetylene concentration in the liquid phase after hydrogenation and low solubility of ethylene in the solvent.

An ionic liquid, 1,3-dimethyl imidazolium methyl phosphite, was investigated to improve catalytic performance for selective hydrogenation of acetylene. However, there have been contrasting results on the presence of the ionic liquid layer over the solid catalysts, with respect to the improvement of the catalytic activity and selectivity to ethylene [13-16]. A comparative study on using NMP and the ionic liquids both in bulk as the liquid phase in the selective hydrogenation of acetylene concluded that using NMP helps to improve the catalyst stability and selectivity [13]. The physical properties of NMP like low viscosity contributed to increasing the G-L and L-S mass transfer rates, thereby controlling over hydrogenation to ethane and deactivation of the catalyst.

Patents on this type of process using a liquid phase to selectively absorb acetylene from a gas mixture and then selectively hydrogenating using a heterogeneous catalyst are available [17, 18]. Many solvents were compared, and NMP was the chosen solvent for their future research for its high acetylene solubility and ethylene selectivity. In this

integrated process of liquid-phase hydrogenation using a selective solvent, the reactant stream is acetylene-rich, which requires a lower volume of acetylene gas. This enables the use of smaller, safer, and therefore less expensive reactors.

Multiphase catalytic reactors have been used in various industries such as petroleum, hydrotreating, hydro-processing, hydrogenation, and various selective applications [19-21]. Our focus mainly is to study the selective hydrogenation of acetylene in the liquid phase using a selective solvent. Practically, this hydrogenation step should have acetylene in the liquid phase either by i) selectively separating acetylene from the cracking effluent using a selective polar solvent or ii) dissolving the acetylene produced from a bulk source (hydrolysis of calcium carbide or methane to acetylene by partial oxidation) in the solvent.

The selective solvent should have high acetylene selectivity relative to ethylene, hydrogen, and other gases. The thermal conductivity of the solvent should be stable without much change at higher temperatures and pressures. These major factors ensure high yield and improved heat transfer due to the better heat absorption across the bed than the gas phase, which is desired from the liquid phase hydrogenation of acetylene. N-methyl pyrrolidone, a polar solvent with a high boiling point (204$^{o}$C) and high solubility of acetylene (mL gas / mL solvent), was chosen as the selective solvent [10, 22]. This solvent is commonly used to absorb acetylene from the mixture of gases, mainly for its high selectivity towards acetylene [7, 11].

To conduct this liquid phase reaction over a catalyst bed in a continuous flow to assess the reactor performance, hydrodynamics and mass transfer needs to be understood. Moreover, to enable this study towards scale-up, optimizing the operating conditions (flow

rate, pressure, temperature), physical properties of reactor and catalyst, and flow mode (trickle or upflow) play a vital role.

It was very significant to understand the flow regime during the operation of packed bed reactors. In industries, the most commonly used flow mode in packed bed reactors is trickle flow (co-current downwards flow of reactants), while upflow (bubbly regime) is also being used based on the requirements of the multiphase system [19]. These modes were chosen mainly to enhance conversion, selectivity, and ease of operation. The major difference between these two modes is the wetting of the solid catalyst phase due to the liquid phase, which affects the liquid holdup, dispersion, and maldistribution, eventually the reaction process. Since the main reactant acetylene was absorbed in the NMP solvent, the moles of acetylene available in the liquid phase was dictated by the solubility of acetylene in the operating conditions. Moreover, it was very critical to have a controlled flow regime for the acetylene to be available to the active sites of the catalyst. More information on the acetylene hydrogenation reaction on the active sites of a Pd/Alumina catalyst are available elsewhere [3, 6, 23].

Palladium over Alumina supported catalysts has been used by many researchers, and industries have used for the acetylene hydrogenation [3, 5, 6, 24]. Process development and intensification point of view, in our work, a commercial Pd/Alumina catalyst was tested. This had its advantages and drawbacks while using them in a lab-scale reactor setup. The exact performance of the reactor is predicted when the same catalyst size is investigated in flow systems; on the other hand, the ratio of the reactor to particle diameter needs to be at least 20. This ratio was suggested to avoid wall effects, axial dispersion, and irregular wetting patterns in lab-scale studies. This helps during scale up as the scaled-

down system can be close to plug flow as in industrial scale [19, 25, 26]. Although, the $D_R$/Dp ratio was low as a commercial catalyst was used, packing the reactor with fines helps to maintain the plug flow conditions as in the commercial reactors maintaining the physical properties of the catalyst like porosity, size and shape thereby enabling scale-up. Many researchers studied the effect of packing the reactor bed with fines identifying the significance of bed dilution mainly to avoid deviation from plug flow [26-31].

In this continuing work to understand the liquid phase hydrogenation of acetylene using a selective solvent over a commercial catalyst, a packed bed reactor will be investigated to understand the reactor performance. Being simple reaction chemistry, each mole of hydrogen reacting with a mole of acetylene to form ethylene, the operating conditions (flowrates) needs to be consistent to enable scale-up and avoid over hydrogenation of undesired products. From the previous studies, the kinetic parameters, along with ideal operating conditions were identified, in addition to an estimate of liquid holdup and liquid dispersion for the chosen operating conditions from the residence time distribution studies. This experimental information, in addition to a reactor scale model, will be used to validate, optimize, and suggest conditions for further scaling of this process.

## 2. EXPERIMENTAL SETUP

### 2.1. MATERIALS

A commercial catalyst of 0.5 wt% Pd on alumina spheres (Alfa-Aesar) of 2-4 mm diameter was used. Silicon carbide (500μ) was used as the diluent in the catalyst bed. NMP

(Sigma-Aldrich, 99% purity) was used as the liquid phase. Purified acetylene, nitrogen, and hydrogen gas were used in the experiments.

## 2.2. EXPERIMENTAL PROCEDURE

The laboratory-scale experimental facility is shown in Figure 1. This unit was built to withstand high-pressure and high-temperatures for sensitive reactions. A blast shield was installed for safety to withstand any explosions due to any potential failure if any. The complete setup excluding gas cylinders and analytical instruments were placed in a walk-in hood. A stainless steel reactor, 1-inch internal diameter and 60cm long, was used to conduct the experiments. The reactor has a seven port distributor for even distribution of the gas-liquid mixture to avoid any maldistribution. The reactant mixture flow can be easily switched from downflow to upflow by means of a three-way valve. Five temperature ports were equipped on the side of the reactor for temperature measurements. The reactor was fixed to a stand for easy installation and removal inside the blast shield and heated using heating tape wrapped with insulation to maintain the operating temperature. All the other plumbing was ¼ inch stainless steel tubing rated to handle high pressure. The temperatures in the bed, inlet, and outlet were monitored by the thermocouples connected to the data acquisition board. The gas flow rates were maintained by Brooks Mass flow controllers and the liquid solvent with acetylene was pumped using an HPLC pump. A condenser was fixed at the reactor outlet to cool the effluent to the desired temperature before sending it to the gas-liquid separator. The gas-liquid separator was 1L in volume with a cooling jacket to ensure the products were at the desired output temperature for sampling. The gas sampling line was opened using a needle valve and the remaining gases were vented to the

lab hood. The liquid samples were manually taken using a needle valve at regular intervals from the bottom outlet of the gas-liquid separator. The remaining liquid from the gas-liquid separator was collected in a recycle tank. The pressure drop in the reactor was measured with a differential pressure transducer, and the system pressure was maintained using a backpressure regulator at the exit.

The catalyst was packed in the middle of the reactor for a length of 30cm with diluents and glass beads on the top and bottom as the inert zone. The bed was prewetted using the solvent overnight and drained before the start of every experiment. The liquid phase comprising of acetylene absorbed in the NMP was used as the reactant along with the hydrogen as the gas phase. The liquid phase of the reactant was prepared by bubbling $C_2H_2$ in a pre-weighed vessel with NMP to obtain the required concentration. The gas and liquid reactants were premixed in a static mixer and preheated to the operating temperature before they enter the reactor. Before the reaction, the reactor was preheated with nitrogen and pure solvent mixture to the desired operating conditions; then, the inlet stream was switched to hydrogen and the liquid phase. The reactor effluent mixture was cooled at the condenser at the reactor outlet and liquid samples were collected at the exit of the gas-liquid separator at regular intervals. The overhead gas in the gas-liquid separator was connected online directly to the TRACE gas chromatograph (GC) and analyzed by an FID. The consumption of acetylene and the formation of heavier compounds ($C_6$+) were calculated from the GC analysis of the liquid sample. Each experiment was carried out with fresh catalyst and the conversion values were measured at steady state.

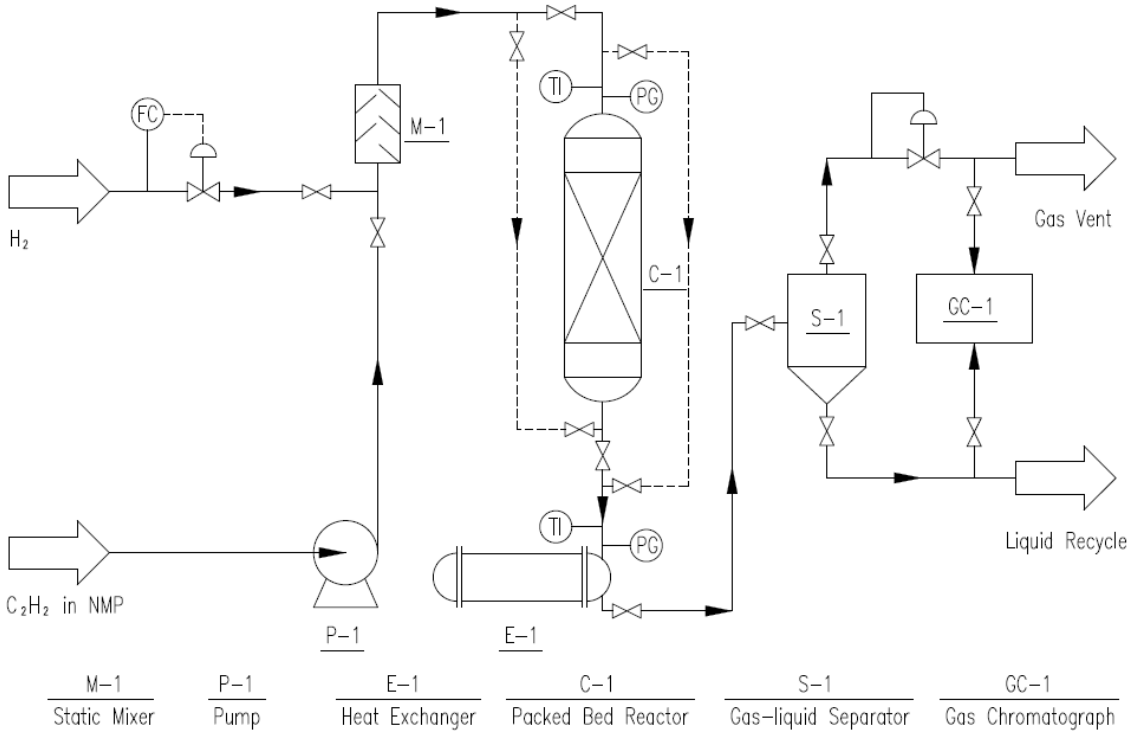


Figure 1. Experimental setup of a packed-bed reactor for cocurrent downflow and upflow modes of operation

## 3. RESULTS AND DISCUSSIONS

The operating conditions were based on the previous related work conduct to investigate the liquid phase hydrogenation of acetylene. The reactor was packed with the catalyst with dilution using fines to improve the liquid holdup during the reaction. From the residence time distribution studies, the dispersion and liquid holdup were estimated providing valuable information about the wetting phenomena in the system and the efficiency of diluting the bed.

Since the motivation was to demonstrate this process towards scaling up aided with kinetic study and reactor scale modeling, an appropriate scale-up parameter was required.

Liquid Hourly Space Velocity (LHSV), the ratio of superficial liquid velocity to the length of the reactor, was used to identify the scaled-down operating flowrates. Using LHSV was convenient and is valid when the bed voidage and catalyst bed length are constant since the rate of reaction depends on the catalyst loading available for the reaction to occur. Also, low liquid velocities in lab-scale studies correspond to the LHSVs in the industrial scale operating in trickle flow conditions and while comparing the trickle and upflow modes.

It was noted that the gas Reynold's number should be less than 350 to ensure the flow is in trickle regime [32-34]. The liquid Reynolds number based on the average particle size was maintained in the range of 5-20 and LHSV 3-12 $hr^{-1}$. The velocities were matched accordingly, this way, the operating conditions were not close to the spray flow regime, and mass transfer resistance was dependent on the liquid phase surrounding the catalyst. These conditions were chosen to ensure good catalyst wetting in a trickle flow regime [20, 21, 31]. The wetting efficiency values from correlation by Al-Dahhan and Dudukovic [35] were in the range of 0.6 to 0.75 at high pressure for the operating conditions. The solubility of acetylene decreased in NMP above 100$^{o}$C due to desorption. These conversion values were obtained considering consumption of acetylene, accounting for the selectivity during the reaction, and formation of green oil in the effluent.

At a higher gas velocity of 0.16 m/s, the residence time and dynamic liquid holdup values were less compared to lower velocities from our previous studies for this system. The concentration of oligomers ($C_6$+) was monitored in the liquid effluent of the gas-liquid separator for all experiments. At higher gas velocity, more oligomerization was observed, especially at higher LHSVs due to higher availability of the gas reactant per acetylene on the surface of the catalyst. The formation of green oil in both the flow modes was less than

7% based on the initial concentration of the liquid phase at all other operating conditions. The catalyst was subjected to Thermogravimetric analysis using TGA-Q50 Instrument under the air environment at a heating rate of 10°C/min to 1000$^{o}$C and not more than 12% of carbonaceous deposits were observed. As only select conditions were compared for both flow modes, this section will focus on trickle bed reactor performance followed by comparing both flow modes.

### 3.1. EFFECT OF GAS AND LIQUID VELOCITIES

As only select conditions were compared for both flow modes, this section will focus on trickle bed reactor performance followed by comparing both flow modes. The liquid velocities ranged from 0.0005 m/s to 0.02 m/s corresponding to LHSVs in the range of 3-12 $hr^{-1}$. The experiments were conducted at two different temperatures in trickle flow conditions for two gas velocities. From Figure 2, it was observed that the overall conversion values were high at low liquid and gas velocities and decreased with an increase in the velocities. The conversion was linearly decreasing with an increase in the LHSV at each gas velocity, not more than 15%, with an increase in the gas velocities at a specific LHSV and temperature. The conversion values were high at low LHSV, mainly due to the increased residence time and dynamic holdup of the liquid reactant in the reactor, thereby increasing the moles of acetylene available on the catalyst surface for hydrogenation. At low LHSVs, the wetting around the catalyst may not be high, which may improve the gas availability to the pores for the reaction. The liquid reactant will spread on the catalyst surface; the thickness will also be larger at higher LHSVs leading to an increase in gas-liquid (external) mass transfer resistances. This can also be attributed to the molar ratio of

$H_2/C_2H_2$. For instance, at 12 $hr^{-1}$ and gas velocity of 0.04m/s, the $H_2/C_2H_2$ molar ratio would be low leading to low conversion although the selectivity to ethylene was high.

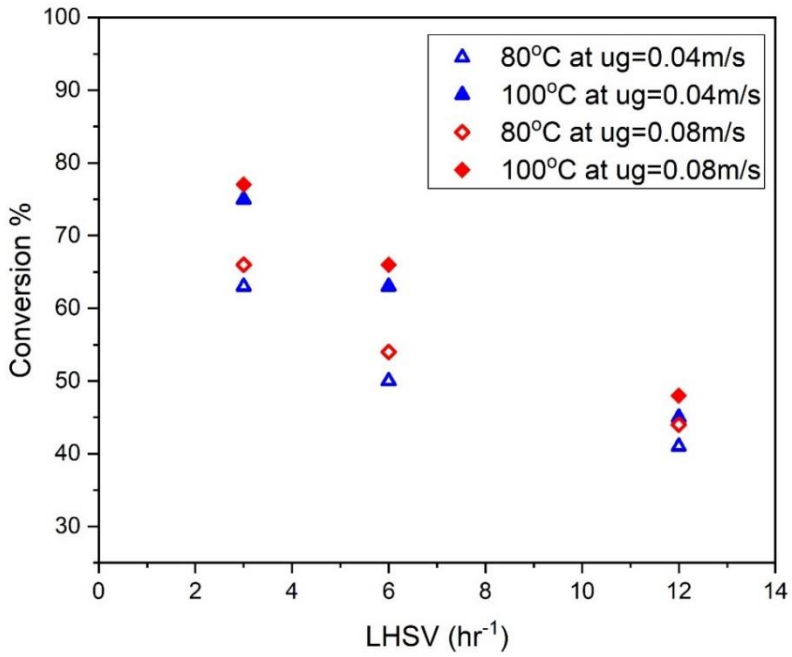


Figure 2. Effect of gas velocities on reactor performance in trickle flow at different temperatures and LHSVs (P=250 psig)

With an increase in gas flow rates at constant LHSV, although the residence time decreases, reducing the liquid holdup, the acetylene conversion increases due to the availability of the hydrogen for the reaction to happen. It has to be understood that although the entire process is in the liquid phase, ultimately, the reactants are gases with the reaction on the active site of the catalyst. The external diffusional resistances to the liquid film around the catalyst was diminished since the operating conditions were in the trickle flow regime with low liquid velocities [36]. Moreover, since the reaction rate was temperature-sensitive, the overall conversion increases with an increase in temperature.

### 3.2. EFFECT OF TEMPERATURE

The conversion of acetylene increased with an increase in temperature, and the increase was constant above 90°C. Although the selectivity of ethylene increased with temperature, the reaction rate increased, which may lead to the formation of undesired ethane, $C_4$, and oligomers affecting the reactor performance. From Figure 3, it was observed that the conversion increases with an increase in gas velocity, as mentioned in the above discussion. From Figure 4, it can be seen that the selectivity of $C_4$ compounds was very low, while the selectivity to ethane decreased with an increase in temperature. The conversion was low at 60oC, due to slower reaction rates at the operating conditions.

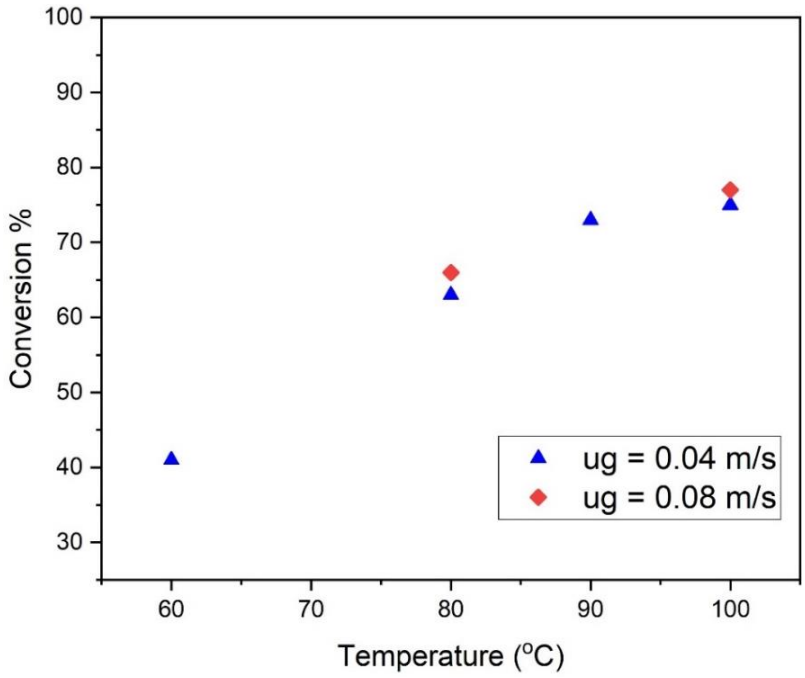


Figure 3. Effect of temperature on reactor performance in trickle flow (LHSV = $3hr^{-1}$, P=250 psig)

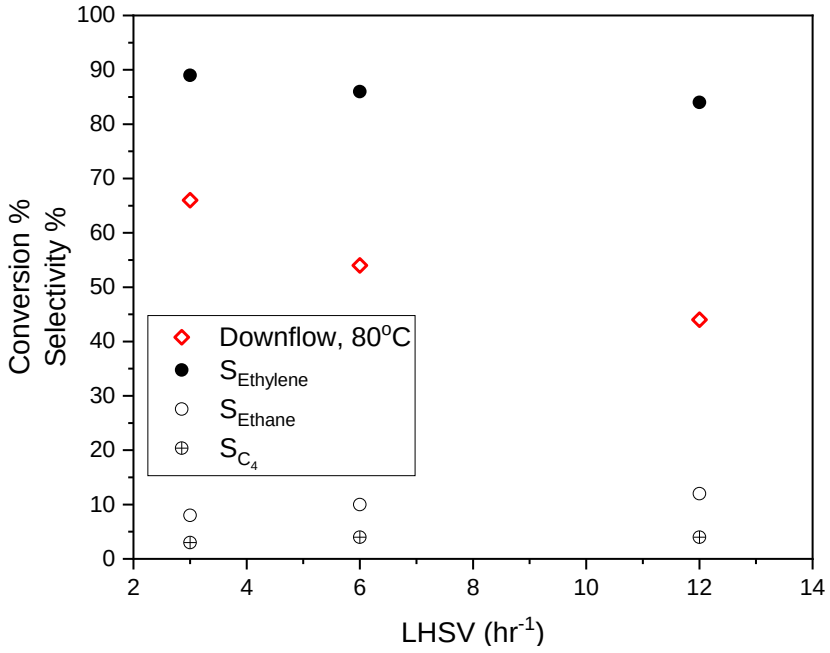


a

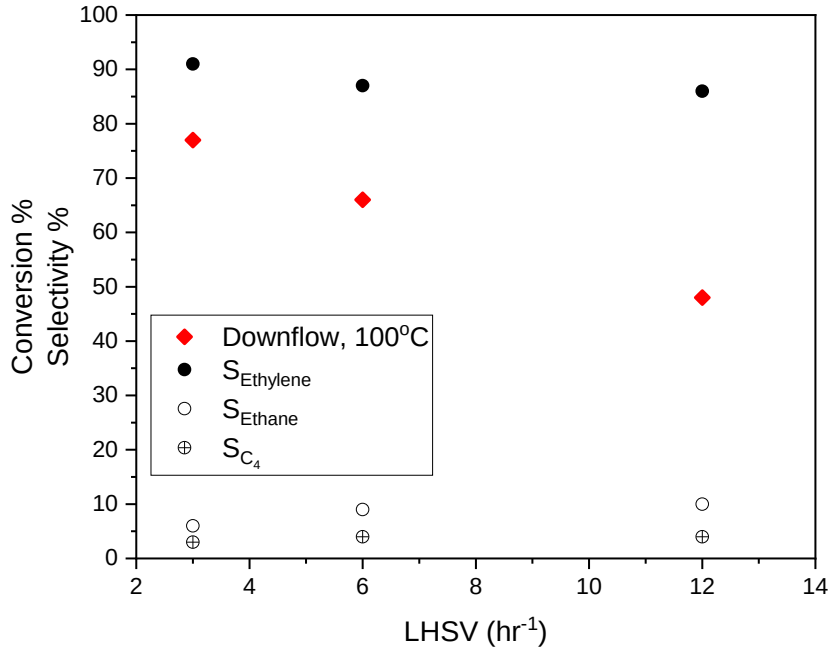


b

Figure 4. Conversion and Selectivity in trickle flow conditions (P=250 psig, $u_g$=0.08 m/s) a) 80°C; b) 100°C

At low LHSVs with a gas velocity of 0.08 m/s, the residence time increases along with the molar ratio. This flow condition at higher temperatures (80-100$^{o}$C) was ideal for better conversion, and ethylene selectivity as the effect of temperature improves the kinetics and hence the reaction rate.

### 3.3. EFFECT OF PRESSURE

The effect of pressure on the reactor performance was studied at 80 and 100$^{o}$C at a gas velocity of 0.08 m/s and LHSV of 3 $hr^{-1,}$ as shown in Figure 5. The effect of pressure was very evident as the conversion increased from 150 to 200 psig and no significant increase was observed from 200-250 psig. The main reason was the increase in solubility of the hydrogen gas in the solvent, benefiting the external mass transport of the gas while improving the concentration gradient at the surface of the catalyst. This improves the reaction on the active sites of the wetted catalyst, eventually improving the rate of reaction. The gas-liquid interfacial area improves along with the interphase mass transfer with an increase in pressure. Furthermore, at high-pressure conditions, the catalyst bed in trickle flow modes may decrease the liquid holdup but improves the wetting efficiency since the reactor bed was diluted, thereby improving the liquid spreading [19, 29, 37].

### 3.4. COMPARISON OF REACTOR PERFORMANCE OF PACKED BED REACTORS IN DOWNFLOW AND UPFLOW

Following the reactor performance studies in downflow mode, experiments were carried out in upflow mode at different temperatures and LHSVs. The catalyst bed and other physical properties were maintained as in the downflow mode.

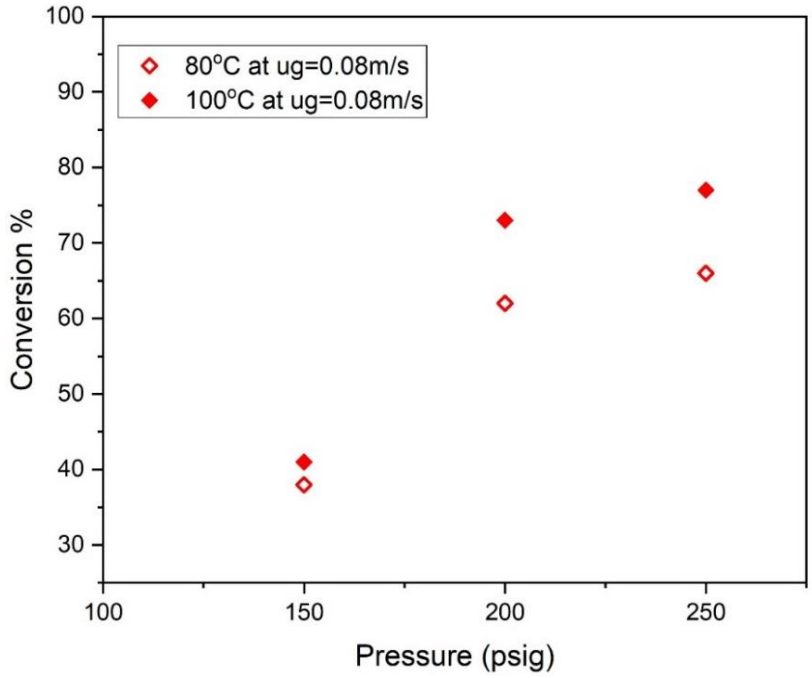


Figure 5. Effect of Pressure on reactor performance in trickle flow at different temperatures ($u_g$ = 0.08m/s; LHSV 3 $hr^{-1}$)

Generally, for liquid-limited conditions, the upflow mode of operation was preferred when the feed concentration was low and at high pressure [29, 30, 38]. From the trickle flow experiments, we found an increase in conversion with an increase in gas velocity; hence the comparative study was conducted at $u_g$=0.08 m/s at different temperatures and an operating pressure of 250 psig to understand the selectivity and conversion of the reaction. Moreover, the concentration of acetylene in NMP was the same for all studies, so our focus was to limit the formation of undesired products as well as have good temperature control in the process.

From Figures 6 and 7, the conversion and ethylene selectivity were comparable with the trickle flow conditions. The lower conversion at higher LHSVs in upflow was still due to the lower residence time of the reactants as in downflow conditions. The undesired

products formed were controlled, although a slight increase in ethane formation was observed in higher LHSVs as in trickle flow mode. This is likely due to the increased availability of acetylene molecules for the reaction leading to the formation of ethane.

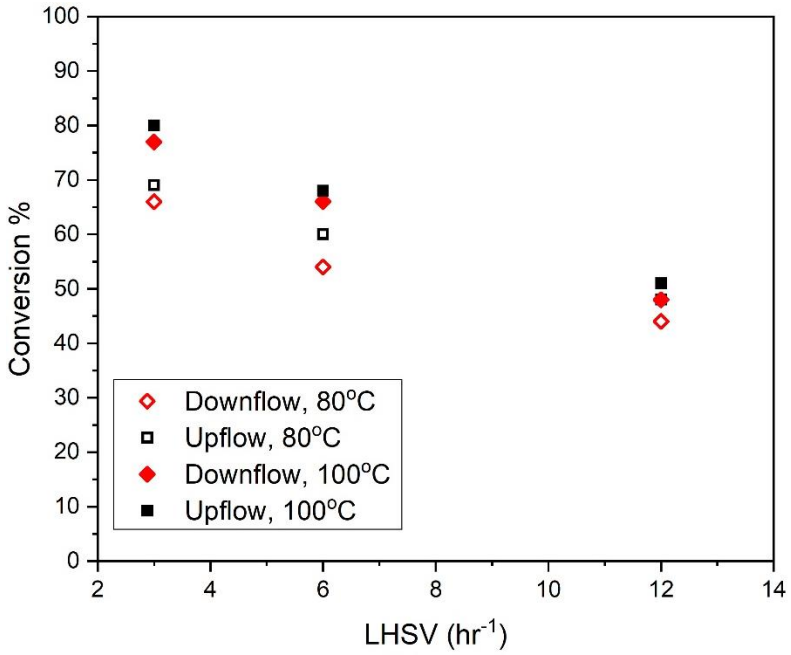


Figure 6. Reactor performance comparison for downflow and upflow (P=250 psig, $u_g$=0.08 m/s)

Figure 6 shows the comparable reactor performance of both flow modes. It can be seen that the upflow mode of operation had higher conversion than trickle mode despite the beds were diluted with fines confirming that the trickle bed reactor with dilution still does not provide complete wetting of the catalyst surface. This is consistent with what has been reported in the literature [30]. In general, although the wetting efficiency increases in upflow mode, the liquid film thickness surrounding the catalyst increases as well, leading to increased gas-liquid mass transfer resistance. This becomes important if the gas reactant

concentration in the liquid phase was not maintained high enough to be properly supplied to the catalyst with the other liquid reactant. Overall, the upflow mode due to the complete wetting of the catalyst and rate of the reaction being controlled by the liquid reactant, performed better than the downflow mode [29, 30, 37, 39].

### 3.5. REACTOR SCALE MODELING

The acetylene hydrogenation in the liquid phase using a selective solvent was simulated for a lab-scale trickle bed reactor. The reactor scale model, along with the correlations, was chosen based on the discussions mentioned by Shariff and Al-Dahhan [40]. By integrating the intrinsic kinetics (Equation 11 and 12) in the model along with the hydrodynamics for a lab-scale reactor, the reactor performance was predicted for scaled-down operating conditions. A sequential method of solving the reactor and pellet scale models integrated accounting for the variation in the local effectiveness factor was used [41]. The solution of Equation 6 and 7 were obtained using the local concentration from ADM as boundary conditions. The concentration values were accounted for in the local effectiveness factors for the dry, dry-wet, and wet regions. These values were integrated into Equation 8 along with wetting efficiencies to get the local effectiveness factor, which was integrated into the reactor scale model and solved at each axial collocation point and iterated until convergence. The same procedure was repeated for all the mesh across the reactor axis to obtain the local concentration at each point. This value was evaluated from the pellet scale equations. A more detailed explanation and correlations used in the model are available in the literature [40-42].

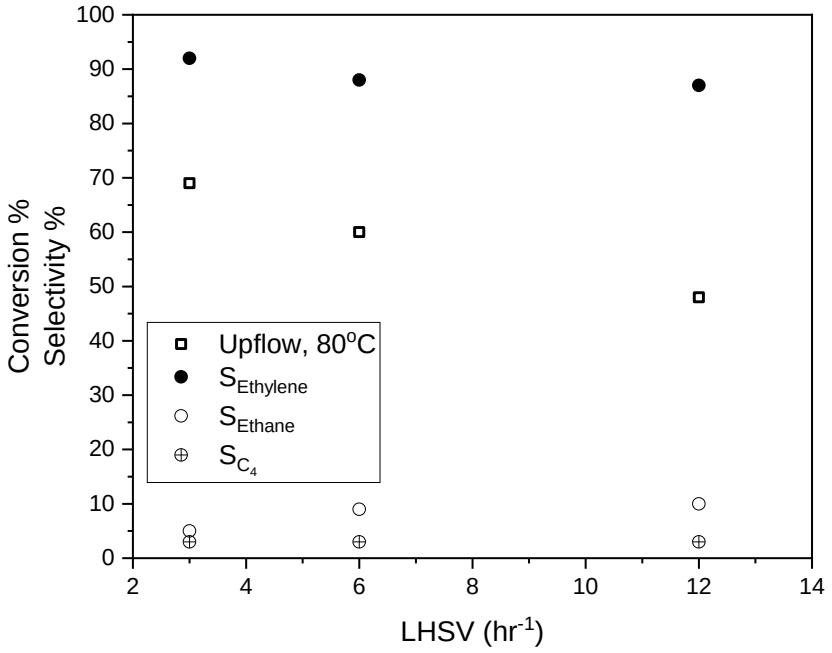


**a**

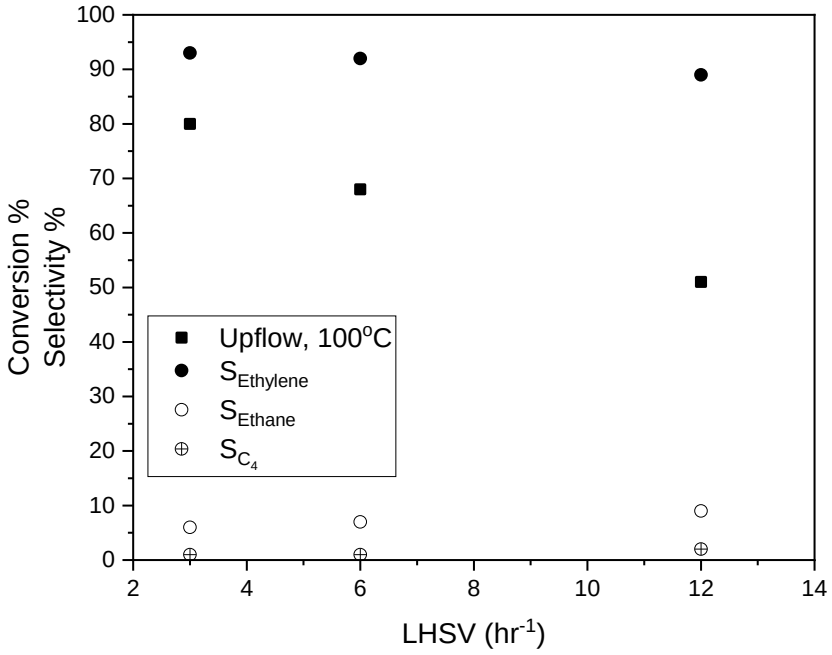


**b**

Figure 7. Conversion and Selectivity in upflow conditions (P=250 psig, $u_g$=0.08 m/s) a) 80°C; b) 100°C

The correlations for Peclet Number and liquid holdup (Equations 9 and 10) for the operating conditions for reactor bed with dilution and the intrinsic kinetic model (Equation 11) based on the Langmuir-Hinshelwood-Hougen-Watson mechanism were estimated in our previous work. The rate equations were validated at 80-100$^{o}$C in slurry conditions at a pressure of 250 psig. These equations will be used to assess the reactor performance using the model.

Reactor scale model equations (in the liquid phase)

A (Hydrogen) + B (Acetylene) → C (Ethylene)

Axial Dispersion Model (ADM) equations

$$\frac{D_{AL,A}}{u_L}\frac{d^2C_{A.L}}{dz^2} - \frac{dC_{A,L}}{dz} + \frac{1}{u_L}\left[(ka)_{GL}\left(C_{A,e} - C_{A,L}\right) - k_{LS,A}\, a_{LS}\left(C_{A,L} - C_{A,LS}\right)\right] = 0 \quad (1)$$

$$\frac{D_{AL,B}}{u_L}\frac{d^2C_{B.L}}{dz^2} - \frac{dC_{B,L}}{dz} + \frac{1}{u_L}\left[\vartheta_B k_{GS,A} a_{GS}\left(C_{A,e} - C_{A,GS}\right) - k_{LS,B}\, a_{LS}\left(C_{B,L} - C_{B,LS}\right)\right] = 0 \quad (2)$$

$$\frac{D_{AL,C}}{u_L}\frac{d^2C_{C.L}}{dz^2} - \frac{dC_{C,L}}{dz} - \frac{1}{u_L}\left[\, k_{LS,C}\, a_{LS}\left(C_{C,L} - C_{C,LS}\right)\right] = 0 \quad (3)$$

Mass Transport Equations at the pellet (i= A,B,C)

$$k_{LS,i}\, a_{LS}\left[C_{i,L} - C_{i,LS}\right] = \eta_o(1-\varepsilon_b)\eta_{CE}\, r_i\left(C_{i,LS}\right) \quad (4)$$

$$k_{GS,A} a_{GS}\left(C_{A,e} - C_{A,GS}\right) = \eta_o(1-\varepsilon_b)(1-\eta_{CE})\, r_A\left(C_{A,GS}\right) \quad (5)$$

Boundary Conditions

$$-\frac{D_{AL,i}}{u_{SL}}\frac{dC_{i,L}}{dz} = (C_{i,0} - C_{i,L}) \quad \text{at z = 0}$$

$$\frac{dC_{i,L}}{dz} = 0 \quad \text{at z = L}$$

Pellet Scale Model (PSM) Equations [39]

$$\frac{d^2C_i}{dx^2} - (1-\omega_x-\omega)^2 \left(\frac{V_s}{S_x}\right)^2 \frac{(-r_i)}{D_{ei}} = 0 \ ; 0< x< 1 \quad (6)$$

$$\frac{d^2C_i}{dy^2} - (1-\omega_x-\omega)^2 \left(\frac{V_s}{S_x}\right)^2 \frac{(-r_i)}{D_{ei}} = 0 \ ; 0< y< 1 \quad (7)$$

$i$ = A,B

Boundary conditions

$$\left.\frac{dC_A}{dy}\right|_{y=1} = (2-\omega)\, Bi_{LS,A}\left(C_{A,L} - C_A|_{y=1}\right)$$

$$\left.\frac{dC_B}{dy}\right|_{y=1} = (2-\omega)\, Bi_{LS,B}\left(C_{B,L} - C_B|_{y=1}\right)$$

$$\left.\frac{dC_A}{dx}\right|_{x=1} = \frac{1-\omega_x-\omega}{\omega+\left(\frac{1}{Bi_{GS,A}}\right)}\left(C_{A,L} - C_A|_{x=1}\right)$$

$$\left.\frac{dC_A}{dx}\right|_{x=0} = -\frac{1-\omega_x-\omega}{1-\omega_y}\left.\frac{dC_A}{dy}\right|_{y=0}$$

$$C_A|_{x=0} = C_A|_{y=0} - 2\left(\frac{V_s}{S_x}-1\right)\left.\frac{dC_A}{dy}\right|_{y=0}$$

$$C_B|_{x=1} = 0$$

$$C_B|_{x=0} = C_B|_{y=0} - \frac{2\left(\frac{V_s}{S_x}-1\right)+\omega_x+\omega_y}{1-\omega_y}\left.\frac{dC_B}{dy}\right|_{y=0}$$

$$\left.\frac{dC_B}{dx}\right|_{y=0} = 0$$

$$\left.\frac{dC_B}{dy}\right|_{x=0} = \frac{1-\omega_x-\omega}{1-\omega_y}\left.\frac{dC_B}{dy}\right|_{y=0}$$

where $i = \frac{kV_S}{D_e S_x}$, $C_i = \frac{C_{i,L}}{C_{Ae}}$

$$\eta_o = (1 - \eta_{CE})^2 \eta_{od} + 2\eta_{CE}(1 - \eta_{CE})\eta_{odw} + \eta_{CE}{}^2 \eta_{ow} \quad (8)$$

$$Pe_L = 2.74\, Re_L^{0.869} Ga_L^{-0.1456} \quad (9)$$

$$\varepsilon_L = \varepsilon_B\, (1.79\, Re_L^{0.198} Re_G^{-0.113}\,) \quad (10)$$

$$r_{C_2H_2} = \frac{k_1 [C_2H_2][H_2]}{\left(1 + K_{C_2H_2}[C_2H_2] + \sqrt{K_{H_2}[H_2]}\right)^3} \quad (11)$$

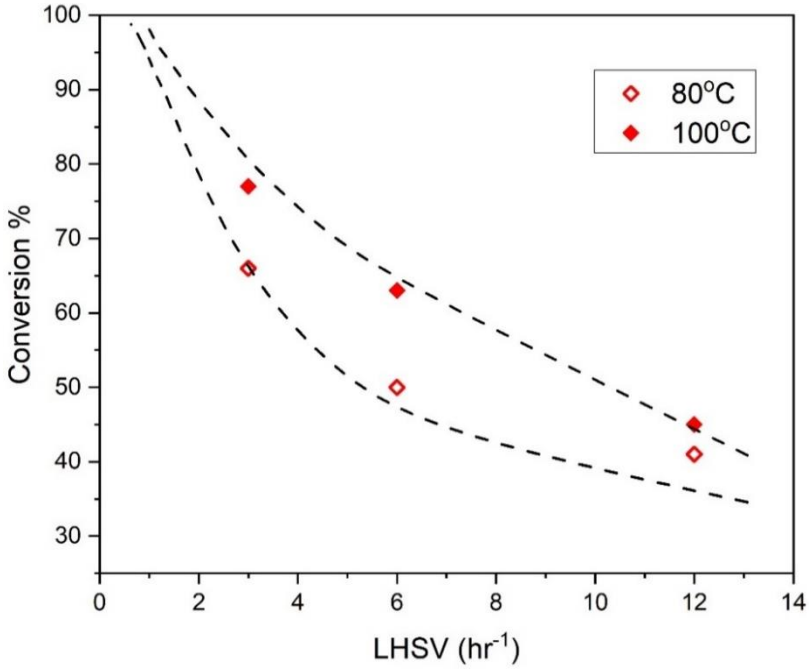


Figure 8. Reactor performance in trickle flow at different temperatures with reactor scale model validation (P=250 psig, $u_g$ = 0.08m/s)

The reactor scale model integrated with the pellet scale model had good agreement with the experimental data at different temperatures and LHSVs (Figure 8). This model

can be further used to simulate reactor performance for large-scale reactors with scaled-up experimental conditions, including the intrinsic kinetics of the reaction.

## 4. CONCLUSIONS

The hydrogenation of acetylene in the liquid phase using a selective solvent was studied in packed bed reactors in two flow modes of operation. A commercial 0.5 wt% Pd/Alumina spherical catalyst was used with the reactor bed diluted with fines. The operating conditions were controlled with low green oil formation during the reaction. The conditions to obtain high ethylene selectivity were 100$^{o}$C at LHSV 3hr$^{-1}$ and gas velocity of 0.08m/s at 250 psig. The reactor temperature and pressure significantly affected the conversion of acetylene. The upflow mode assuming fully wetted catalyst at the operating conditions performed better than the downflow. The effect of mass transfer, kinetics, and contacting efficiency, including the residence time, critically affect the performance of the reactor in the investigated operating conditions. Although the upflow mode performed better, the availability of acetylene molecule per hydrogen molecule on the catalyst surface should be controlled to avoid over-hydrogenation. Increased reactants availability in the liquid, the dissolved hydrogen concentration in the liquid supplied to the catalyst through the liquid film, may lead to the formation of undesired products. To consider this process towards scaling up, the intrinsic kinetics estimated for the liquid phase acetylene hydrogenation must be integrated into the reactor scale model. Since the catalyst bed was diluted, the kinetics and hydrodynamics were decoupled while operating in these flow

modes. A further investigation comparing these flow modes is recommended to extract proper scale-up parameters.

## REFERENCES


1. Hall, K.R., *A new gas to liquids (GTL) or gas to ethylene (GTE) technology.* Catalysis Today, 2005. **106**(1-4): p. 243-246.

2. *Global Demand For Polyethylene To Reach 99.6 Million Tons In 2018*, in *Pipeline and gas Journal*. 2014.

3. Borodziński, A. and G.C. Bond, *Selective Hydrogenation of Ethyne in Ethene-Rich Streams on Palladium Catalysts. Part 1. Effect of Changes to the Catalyst During Reaction.* Catalysis Reviews, 2006. **48**(2): p. 91-144.

4. Bos, A.N.R., et al., *A kinetic study of the hydrogenation of ethyne and ethene on a commercial Pd/Al2O3 catalyst.* Chemical Engineering and Processing, 1993. **32**: p. 53-63.

5. Pachulski, A., R. Schödel, and P. Claus, *Kinetics and reactor modeling of a Pd-Ag/Al2O3 catalyst during selective hydrogenation of ethyne.* Applied Catalysis A: General, 2012. **445-446**: p. 107-120.

6. Borodziński, A. and G.C. Bond, *Selective Hydrogenation of Ethyne in Ethene-Rich Streams on Palladium Catalysts, Part 2: Steady-State Kinetics and Effects of Palladium Particle Size, Carbon Monoxide, and Promoters.* Catalysis Reviews, 2008. **50**(3): p. 379-469.

7. Hou, R., T. Wang, and X. Lan, *Enhanced Selectivity in the Hydrogenation of Acetylene due to the Addition of a Liquid Phase as a Selective Solvent.* Industrial & Engineering Chemistry Research, 2013. **52**(37): p. 13305-13312.

8. Edvinsson, R.K., A.M. Holmgren, and S. Irandoust, *Liquid-Phase Hydrogenation of Acetylene in a Monolithic Catalyst Reactor.* Industrial & engineering chemistry research, 1995. **34**(1): p. 94-100.

9. Men'shchikov, V.A., Fal'kovich, Y. G., & Aerov, M. E., *Liquid-phase hydrogenation of acetylene in pyrolysis gas in presence of heterogeneous catalysts at atmospheric pressure.* J. Appl. Chem. USSR, 1983. **56**.

10. Shitova, N., et al., *Liquid-phase hydrogenation of acetylene on the Pd/sibunit catalyst in the presence of carbon monoxide.* Kinetics and Catalysis, 2011. **52**(2): p. 251-257.

11. Smirnova, N., et al., *EXAFS study of Pd/Ga2O3 model catalysts of selective liquid-phase hydrogenation of acetylene to ethylene.* Journal of Molecular Catalysis A: Chemical, 2012. **358**: p. 152-158.

12. Shitova, N.B., et al., *Liquid-phase hydrogenation of acetylene on the Pd/sibunit catalyst in the presence of carbon monoxide.* Kinetics and Catalysis, 2011. **52**(2): p. 251-257.

13. Hou, R., X. Lan, and T. Wang, *Selective hydrogenation of acetylene on Pd/SiO2 in bulk liquid phase: A comparison with solid catalyst with ionic liquid layer (SCILL).* Catalysis Today, 2015. **251**: p. 47-52.

14. Herrmann, T., et al., *High-performance supported catalysts with an ionic liquid layer for the selective hydrogenation of acetylene.* Chem Commun (Camb), 2011. **47**(45): p. 12310-2.

15. Lee, J.M., et al., *Selective removal of acetylenes from olefin mixtures through specific physicochemical interactions of ionic liquids with acetylenes.* Physical Chemistry Chemical Physics, 2010. **12**(8): p. 1812-1816.

16. Ruta, M., et al., *Pd nanoparticles in a supported ionic liquid phase: Highly stable catalysts for selective acetylene hydrogenation under continuous-flow conditions.* Journal of Physical Chemistry C, 2008. **112**: p. 17814-17819.

17. Johnson, M.M., Edward R. Peterson, and Sean C. Gattis, *United States Patent No. 7,045,670.* 2006.

18. Johnson, M., E. Peterson, and S. Gattis, *Process for liquid phase hydrogenation*. 2005, Google Patents.

19. Al-Dahhan, M.H., et al., *High-pressure trickle-bed reactors: a review.* Industrial & engineering chemistry research, 1997. **36**(8): p. 3292-3314.

20. Duduković, M.P., F. Larachi, and P.L. Mills, *Multiphase catalytic reactors: a perspective on current knowledge and future trends.* Catalysis reviews, 2002. **44**(1): p. 123-246.

21. Ranade, V.V., R. Chaudhari, and P.R. Gunjal, *Trickle bed reactors: Reactor engineering and applications*. 2011: Elsevier.

22. Harris, H. and J. Prausnitz, *Thermodynamics of solutions with physical and chemical interactions. solubility of acetylene in organic solvents.* Industrial & Engineering Chemistry Fundamentals, 1969. **8**(2): p. 180-188.

23. Borodziński, A. and A. Cybulski, *The kinetic model of hydrogenation of acetylene–ethylene mixtures over palladium surface covered by carbonaceous deposits.* Applied Catalysis A: General, 2000. **198**: p. 51-66.

24. Bos, A.N.R. and K.R. Westerterp, *Mechanism and kinetics of the selective hydrogenation of ethyne and ethene.* Chemical Engineering and Processing, 1993. **32**: p. 1-7.

25. Sie, S., *Scale effects in laboratory and pilot-plant reactors for trickle-flow processes.* Revue de l'Institut français du pétrole, 1991. **46**(4): p. 501-515.

26. Gierman, H., *Design of laboratory hydrotreating reactors: scaling down of trickle-flow reactors.* Applied Catalysis, 1988. **43**(2): p. 277-286.

27. Al-Dahhan, M.H. and M.P. Duduković, *Catalyst bed dilution for improving catalyst wetting in laboratory trickle-bed reactors.* AIChE journal, 1996. **42**(9): p. 2594-2606.

28. Al-Dahhan, M.H., Y. Wu, and M.P. Dudukovic, *Reproducible technique for packing laboratory-scale trickle-bed reactors with a mixture of catalyst and fines.* Industrial & engineering chemistry research, 1995. **34**(3): p. 741-747.

29. Guo, J. and M. Al-Dahhan, *Catalytic wet air oxidation of phenol in concurrent downflow and upflow packed-bed reactors over pillared clay catalyst.* Chemical Engineering Science, 2005. **60**(3): p. 735-746.

30. Wu, Y., et al., *Comparison of upflow and downflow two-phase flow packed-bed reactors with and without fines: experimental observations.* Industrial & engineering chemistry research, 1996. **35**(2): p. 397-405.

31. Sie, S. and R. Krishna, *Process development and scale up: III. Scale-up and scale-down of trickle bed processes.* Reviews in Chemical Engineering, 1998. **14**(3): p. 203-252.

32. Fukushima, S. and K. Kusaka, *Liquid-phase volumetric and mass-transfer coefficient, and boundary of hydrodynamic flow region in packed column with cocurrent downward flow.* Journal of Chemical Engineering of Japan, 1977. **10**(6): p. 468-474.

33. Fukushima, S. and K. Kusaka, *Boundary of hydrodynamic flow region and gas-phase mass-transfer coefficient in packed column with cocurrent downward flow.* Journal of Chemical Engineering of Japan, 1978. **11**(3): p. 241-244.

34. Fukushima, S. and K. Kusaka, *Gas–liquid mass transfer and hydrodynamic flow region in packed columns with cocurrent upward flow.* Journal of Chemical Engineering of Japan, 1979. **12**(4): p. 296-301.

35. Al-Dahhan, M.H. and M.P. Dudukovic, *Catalyst wetting efficiency in trickle-bed reactors at high pressure.* Chemical Engineering Science, 1995. **50**: p. 2377-2389.

36. Chaudhari, R.V., et al., *Hydrogenation of 1, 5, 9-cyclododecatriene in fixed-bed reactors: Down-vs. upflow modes.* AIChE journal, 2002. **48**(1): p. 110-125.

37. Al-Dahhan, M.H. and M.P. Duduković, *Catalyst wetting efficiency in trickle-bed reactors at high pressure.* Chemical Engineering Science, 1995. **50**(15): p. 2377-2389.

38. Khadilkar, M.R., et al., *Comparison of trickle-bed and upflow reactor performance at high pressure: Model predictions and experimental observations.* Chemical Engineering Science, 1996. **51**: p. 2139-2148.

39. Khadilkar, M.R., Wu, Y. X., Al-Dahhan, M. H., Duduković, M. P., & Colakyan, M., *Comparison of trickle-bed and upflow reactor performance at high pressure: Model predictions and experimental observations.* Chemical Engineering Science, 1996. **51**(10): p. 2139-2148.

40. Shariff, H. and M.H. Al-Dahhan, *Analyzing the impact of implementing different approaches of the approximation of the catalyst effectiveness factor on the prediction of the performance of trickle bed reactors.* Catalysis Today, 2019.

41. Guo, J. and M. Al-Dahhan, *A sequential approach to modeling catalytic reactions in packed-bed reactors.* Chemical engineering science, 2004. **59**(10): p. 2023-2037.

42. Beaudry, E., M. Duduković, and P. Mills, *Trickle-bed reactors: Liquid diffusional effects in a gas-limited reaction.* AIChE journal, 1987. **33**(9): p. 1435-1447.

# SECTION

# 2. CONCLUSIONS AND RECOMMENDATIONS

## 2.1. CONCLUSIONS

Liquid phase hydrogenation of acetylene using a selective solvent in packed bed reactors is a very good and safe alternative for the existing gas-phase hydrogenation process. Lab-scale optimization for this process was successfully demonstrated to obtain high ethylene selectivity at the investigated operating conditions. The research was to understand the hydrodynamics in the reactor scale and the kinetics at the pellet and pore levels to conduct lab-scale liquid phase hydrogenation experiments to optimize the reaction. The entire study was guided by modeling for kinetics, which was integrated into a reactor scale model to validate the packed bed reactor investigation. A laboratory-scale experimental unit was built with the appropriate design and materials to handle this sensitive reaction at the operating conditions. N-Methyl Pyrrolidone (NMP) was chosen as the selective solvent for the hydrogenation reaction over a commercial 0.5 wt% $Pd/Al_2O_3$ catalyst. Overall, the desired operating conditions were identified for the process with high ethylene selectivity, good heat removal, and less green oil formed on the catalyst surface. The assemblage of conclusions is mentioned below for each study conducted.

Paper I summarizes the results obtained by conducting residence time distribution (RTD) studies in a packed bed reactor potentially used in the reaction at scaled-down operating conditions. Diluting the bed with fines improved liquid holdup and reduced dispersion in the bed in comparison to undiluted bed. The Peclet Numbers evaluated from the axial dispersion coefficient increased with an increase in liquid velocities but were

insensitive to gas velocities. Packing the reactor with extrudates with no diluents had higher dispersion and lower holdup in comparison to the reactor with spherical catalysts with fines. The reactor packed with spherical catalysts and fines with thermowell had more dispersion than a reactor with the same packing without thermowell. Empirical correlations were proposed for liquid holdup and Peclet number (obtained from axial dispersion coefficient) for this system to be used during reactor scale modeling.

Paper II estimates the intrinsic kinetic parameters for the $Pd/Al_2O_3$ catalyst along with identifying the operating conditions in a stirred tank basket reactor at constant initial acetylene concentration. The conversion increased with an increase in temperature, pressure, and catalyst loading. At a temperature of 80-100$^oC$ at 250 psig with a catalyst loading of 3 g/L, the acetylene conversion and ethylene selectivity were high. The intrinsic kinetics experimental data with the catalyst as slurry was fitted to a kinetic model based on the LHHW mechanism to estimate the rate parameters. The kinetic model will be used along with the results from cold flow experiments in a reactor scale model to predict the reactor performance of lab-scale packed bed reactors and to optimize the number of experimental trials for liquid-phase hydrogenation process.

Paper III discusses the experimental observations of the liquid phase hydrogenation in a packed bed reactor in trickle flow and upflow models of operation. A commercial Pd/Alumina spherical catalyst was used with the reactor bed diluted with fines. The conditions to obtain high ethylene selectivity were 100$^oC$ at LHSV 3$hr^{-1}$ and gas velocity of 0.08m/s at high pressure of 250 psig. The upflow mode assuming fully wetted catalyst at the conditions performed better than the downflow. The reactor scale model was able to simulate the reactor performance in good agreement with the experimental data. This

model, along with the intrinsic kinetics and estimates of the hydrodynamic parameters, can be enabled towards scaling up the liquid phase acetylene hydrogenation. As the catalyst bed was diluted, the kinetics and hydrodynamics were decoupled while operating in these flow modes.

## 2.2. RECOMMENDATIONS

The following recommendations will help this work to be improved and understand the reaction to help during scaling up.

a) Defining and developing a suitable catalyst for this liquid phase acetylene hydrogenation. Performing intrinsic kinetic investigations to develop proper kinetic models. This model can be integrated into the developed multi-scale model to assess different modes of operating and design conditions.

b) Evaluating different types and shapes of catalyst to assess the reactor performance for the liquid phase acetylene hydrogenation. Bimetallic catalysts have been used recently in many studies, which will be a good choice to improve conversion and selectivity.

c) Integrating Residence time distribution investigations and with the measured kinetics to predict and evaluate the reactor performance.

d) Simulating the current experimental setup using computational fluid dynamics (CFD) tool and integrating kinetics to predict the reactor performance.

e) Conducting liquid phase hydrogenation experiments with acetylene-ethylene mixtures to mimic the actual industrial practice.

# APPENDIX A.

# ANALYZING THE IMPACT OF IMPLEMENTING DIFFERENT APPROACHES OF THE APPROXIMATION OF THE CATALYST EFFECTIVENESS FACTOR ON THE PREDICTION OF THE PERFORMANCE OF TRICKLE BED REACTORS

## ABSTRACT

A steady-state diffusion model comprising of diffusion and reaction in a catalyst pellet was used to study and understand the effect of the approximation of the catalyst effectiveness factor in the modeling of trickle bed reactors. The hydrogenation of alpha-methylstyrene was chosen as the case study reaction from literature for liquid-limited reaction conditions. The effectiveness factor values in this study were sensitive to reactor scale equations during the prediction of reactor performance. The approximation of accounting for the overall catalyst effectiveness factor in the reactor scale model equations from different models and solving the reactor scale model equations by different modeling approaches was assessed. It was observed that evaluating the overall effectiveness factor from pellet scale model equations and integrating the parameter in the reactor scale axial dispersion model at every local axial collocation point to simulate the reactor performance showed better agreement to the experimental data. This approach evaluates the effectiveness factor locally with the variation of the reactant concentration at different axial points across the reactor rather than using one value for the entire reactor. The approach of using a single effectiveness factor for the whole bed and using the effectiveness factor approximated as a fitted polynomial to the reactant concentrations did not properly predict the reactor performance.

# 1. INTRODUCTION

Trickle bed reactors (TBR) are one of the most widely used three phase catalytic systems (gas-solid-liquid) in petroleum industries such as hydrodesulfurization, hydrotreating of heavy oil fractions, hydrodenitrogenation, hydrodemetallization, and other hydrogenation processes. To predict/understand the performance of the TBRs various factors need to be accounted, to mention incomplete catalyst wetting, liquid maldistribution, interphase mass transfer and intraparticle diffusion (Figure 1)[1, 2]. Although, uneven irrigation, at lower liquid flow rates, are observed, leading to partial wetting of the catalyst and potential maldistribution in TBRs, their usage for three-phase catalytic reactions is inevitable. Hence, incorporating this physical information during the development of a reactor-scale model used for performance assessment, design and scale-up becomes critical.

Reactor scale modeling aiding the reactor design, operating conditions and optimization from lab scale to industrial scale not only needs the hydrodynamics information like holdup, wetting efficiency and pressure drop, but also the understanding of the internal diffusion of the reactants within the pores of the catalyst pellets. A precise mathematical modeling for packed bed catalytic reactors was near impossible due to complex interactions between the phases and the convenient assumptions made to solve the mathematical expressions. The heterogeneous models are widely used and have proven to have better accuracy than the homo- and pseudo-homogeneous models [2-4]. These models generally implement the simple plug flow model, axial dispersion model including

dispersion or model the reactor as a tank in series (stack of cells) and their combinations for liquid phase and gas phase, respectively [2, 5-11].

The reactor scale model is represented by mass and heat balance equations which can be rewritten in different ways based on the assumptions. The parameters like dispersion coefficient, mass transfer coefficients, and others are needed, which can be estimated by correlations chosen based on the operating conditions that are available in the literature. The mass transport equations account for the reaction kinetics, catalyst properties like effectiveness factor, porosity and wetting efficiency. Integrating the complexities of the kinetics including catalyst deactivation along with the changes in the hydrodynamics across the reactor axis is vital. Hence, accounting for the catalyst effectiveness factor as a simple theoretical concept is beneficial during the modeling. The concept of using the effectiveness factor minimizes the equations used in solving for the diffusion and reactions in the fluid and catalyst pellets [3, 12]. Otherwise, the model may require more equations (gradients) accounting for the diffusion and intraparticle transport effects by integrating particle scale modeling and reactor scale modeling. The effectiveness factor of the catalyst must be estimated from the experiments or the available data of the system and not from the data in the open literature. The effectiveness factor is a function of the concentrations for a particular catalyst used that accounts for the structure of the pores of the catalyst pellet. It quantifies the resistance for the intraparticle diffusion of the reactants in the porous catalyst [13-15]. Moreover, the concentrations of the reactants vary across the reactor bed height locally and hence the catalyst effectiveness factor is expected to vary as well.

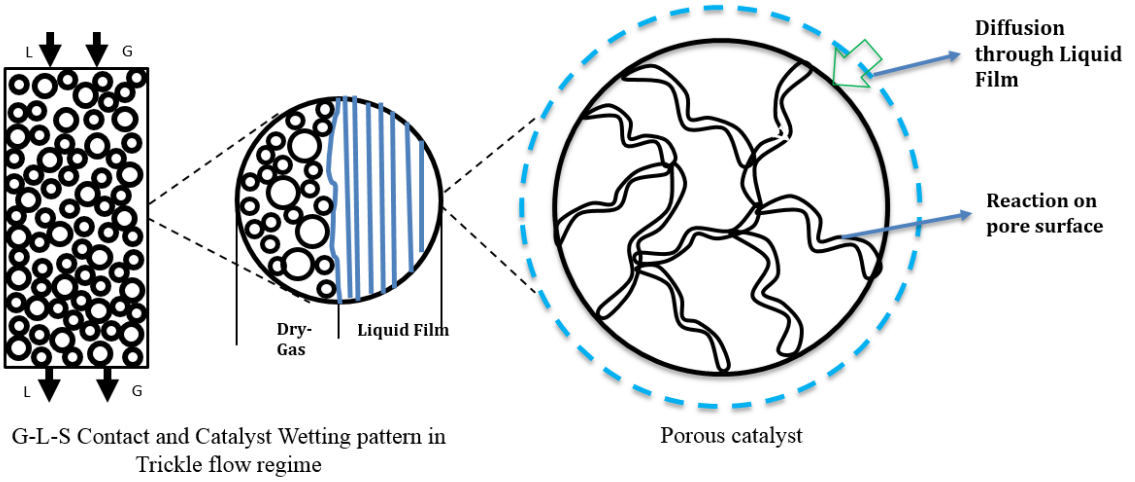


Figure A.1. Catalyst wetting pattern in trickle flow regime

A simple way of defining the effectiveness factor from experimental data has been by estimating the ratio of the apparent reaction rate to the intrinsic kinetics in the absence of external mass-transfer resistances. In this case, one value of the effectiveness factor for the whole reactor bed has been used ignoring its dependency on the species concentration. The concept of using the effectiveness factor is not needed or does not need to be accounted for while using apparent kinetics in the mass transport equations in the reactor scale model. This way of using the apparent kinetics is mainly applied when there is no information available for the effectiveness factor and intrinsic kinetics [7]. On the other hand, this way of inferring the kinetics (apparent) for the whole bed may not be complete as it does not account for the catalyst wetting and the changes in concentration. Especially for non-linear kinetics, apparent kinetics approximation cannot be applicable to support the experimental work [6, 8].

In trickle bed reactors, the downflow of the reactants (gas and liquid) may not completely encompass the catalyst particle, especially at low liquid flow rates [16-18]

resulting in conflicting or non-uniform concentrations on the surface due to gas and liquid coverage. Hence, accounting the effectiveness factor is very significant due to its dependency on the concentration and wetting efficiency. Due to this condition, the conventional method of calculating the effectiveness factor as mentioned above is not adequate due to the presence of irregular contact between the catalyst particles and varying reactants' concentrations [19, 20]. To explain this non-uniform wetting, the effectiveness factor has been approximated for trickle bed reactors using various equations and parameters based on the bulk reactant concentrations [9, 11, 21].

Aris [22] and Bischoff [13] first represented the effectiveness factor as a function of the Thiele modulus (Φ) which included the pellet geometry and intrinsic surface reaction kinetics. Thiele modulus, Φ has also been used in the calculation of the effectiveness factor since Φ can be written as a function of wetting efficiency for different geometries [13, 17, 20, 23-25]. Bischoff's generalized approximation of the $\eta$ is the commonly used form as shown below in Equation 1 [9]. However, this form didn't account for the wetting efficiency.

$\eta = \left(\frac{\tanh \Phi}{\Phi}\right)$ ; in the case of a slab geometry (1-1)

$\eta = \frac{1}{\Phi}\left(\cot 3\Phi - \frac{1}{3\Phi}\right)$ ; in the case of a spherical geometry (1-2)

where $\Phi = \frac{V_S}{S_x}\sqrt{\frac{k}{D_{eff}}}$

Dudukovic (1977) mentioned that catalyst wetting efficiency ($\eta_{CE}$) and the effectiveness factors are always coupled in TBRs. This is mainly due to the effect of incomplete liquid contacting at particle scale thereby affecting the effectiveness factor of the pellet. Hence, the effectiveness factor of the catalyst pellets in a TBR ($\eta_{TB}$) was

expressed as a function of Thiele Modulus (Φ), incomplete external wetting ($\eta_{CE}$), and fractional pore fill-up ($\eta_i$, internal partial wetting) as shown in Equation 2 [23].

$$\eta_{TB} = \eta_i \frac{\tanh(\frac{\eta_i}{\eta_{CE}}\Phi)}{(\frac{\eta_i}{\eta_{CE}}\Phi)} = \eta_{CE} \frac{\tanh(\frac{\eta_i}{\eta_{CE}}\Phi)}{\Phi} \quad (2\text{-}1)$$

If the reaction is very fast, then the Thiele modulus is very large or when the ratio $(\frac{\eta_i}{\eta_{CE}}) \cong 1$, Equation 2 reduces to Equation 2a [4, 26].

$$\eta_{TB} = \eta_{CE}\,\eta \quad (2\text{-}2)$$

Another expression for the overall effectiveness factor was proposed based on Biot number (*Bi*) and Aris' version of Thiele modulus ($\Phi_T$) for different geometries (slab, cylinder, and sphere) [27]. The shape factor ($\vartheta$) was assumed as 0, 1 and 2, respectively for the mentioned geometries which are used in the equation below. This expression was widely used in different studies as it accounts for the mass transfer effects by implementing the *Bi* for both dry and wet areas of the catalyst.

$$\eta_{TB} = \frac{\eta_{CE}}{\left(\frac{{\Phi_T}^2}{Bi_w}+\frac{\Phi_T}{tanh\Phi_T}\right)} + \frac{(1-\eta_{CE})}{\left(\frac{\Phi^2}{Bi_d}+\frac{\Phi_T}{tanh\Phi_T}\right)}\text{; Where } \Phi_T = \frac{\Phi}{\vartheta+1} \quad (3)$$

Ramachandran and Smith [17] proposed their version to determine the effectiveness factor for a slab geometry based on bulk concentrations as a function of Sherwood number (Sh) and Φ. The explicit equations were derived for both gas and liquid limiting conditions. This work was further substantiated by Tan and Smith [20] where the weighted average models were reported for the slab, spherical and cubical shaped geometry.

Table A.1. Evolution of the overall effectiveness factors (weighted) for different geometries

| Author | Equation | Geometry | Notes |
|---|---|---|---|
| Herskowitz, Carbonell, and Smith, 1979 [28] | $\eta_o = \frac{R}{k\, C_{eq}}$ | Cubic | Where $C_{eq}$ is determined by solving differential equations for the Cartesian coordinates for the cubical model considering values of $\eta_{CE}$ from 1/6,2/6 to 1. |
| Ramachandran and Smith, 1979 [17] | $\eta_o = \eta_{CE}\,\eta_L + (1 - \eta_{CE})\eta_G$ | Slab | $\eta_L, \eta_G$ are functions of Thiele modulus |
| Mills and Dudukovic, 1980 [29] | $\eta_o = \eta_{CE}\,\eta_T + \varepsilon(1 - \eta_{CE})\eta_T$ | Slab, cylindrical, Spherical | $\eta_T$ – Modified Thiele Modulus |
| Tan and Smith, 1980 [20]* | $\eta_o = \eta_{CE}\,\eta_L + (1 - \eta_{CE})\eta_G$ | Slab, cubical, Spherical | Equations and the Thiele modulus varied according to the geometry |
| Goto, Lakota, and Levec, 1980 [30] | $\eta_o = \eta_{CE}\, C_{s,w}\eta_L + (1 - \eta_{CE})C_{s,a}\eta_G$ | Spherical | nth order kinetics, a separate equation for both liquid, and gas limited reactions |
| Martinez, Barreto, and Lemcoff, 1980 [31]* | $\eta^A = \frac{2-\gamma}{2}\,\eta^I + \frac{\gamma}{2}\,\eta^{II}$ | Slab | Expressions for $\eta^I$ and $\eta^{II}$ are mentioned in the work |
| Sakornwimon, Wirat, and Sylvester, 1982 [32]* | $\eta_{TBL} = \eta_{CE}\,\eta_L + (1 - \eta_{CE})\eta_G$ | Slab | Expression for $\eta_L$ and $\eta_G$ for different limiting reactant conditions were mentioned. |
| Beaudry, Dudukovic , and Mills, 1987 [33]* | $\eta_o = (1 - \eta_{CE})^2\eta_{od} + 2\eta_{CE}(1 - \eta_{CE})\eta_{odw} + \eta_{CE}{}^2\eta_{ow}$ | Slab | Radial mixing is indicated by the equation. Analytical expressions for $\eta_{od}$, $\eta_{ow}$, *and* $\eta_{odw}$ were mentioned |

Table A.1. Evolution of the overall effectiveness factors (weighted) for different geometries (cont.)

| | | | |
|---|---|---|---|
| Rajashekharam, Jaganathan, and Chaudhari, 1998 [34] (based on Tan and Smith (1980)) | $\eta_c = \eta_{CE,D}\,\eta_D + \eta_{CE,S}\eta_S + (1 - \eta_{CE,D} - \eta_{CE,S})\eta_G$ | Spherical | Effectiveness factor was represented as dynamic, stagnant and dry (gas) zones (the overall rate of hydrogenation is first-order with respect to hydrogen ) |

* based on Ramachandran and Smith (1979)

## 1.1. DEVELOPMENT OF THE OVERALL EFFECTIVENESS FACTOR CONCEPT

The concept of approximating overall effectiveness factor ($\boldsymbol{\eta_o}$) as a weight averaged function of wetting efficiency and particle effectiveness factor was determined for various geometries in the literature although the value of $\eta_o$ has not been integrated into the reactor scale model or did not mention the fact the $\eta_o$ value changes across the reactor axis [6, 8, 17, 18, 20, 21, 24, 28, 34]. This way of calculating the overall effectiveness factors was mainly to achieve appropriate solutions for the resulting geometries. Various equations are summarized in Table A.1 to evaluate the overall effectiveness factor for a partially wetted catalyst pellet. The different approaches incorporated to identify the value of $\eta_o$ for the cases when the limiting reactant is in the gas phase with complete and partial internal wetting and in the liquid phase with complete internal wetting are mentioned. According to Lemcoff [19], the approximation approach by Ramachandran and Smith [17] yielded more suitable values for the catalyst effectiveness factor and further various works

followed their method to calculate the pellet effectiveness factor during reactor modeling [19]. Experimental studies on understanding the effectiveness factor parameter were conducted by various researchers [17-19, 23, 30, 35, 36]. Gas and liquid phase reactions were conducted and the results were substantiated by their heterogeneous models using different approaches to evaluate the $\eta_o$ [7, 8, 20, 37]. A comprehensive review of both calculated $\eta_o$ and its experimental validation is available elsewhere [2, 4, 19, 28].

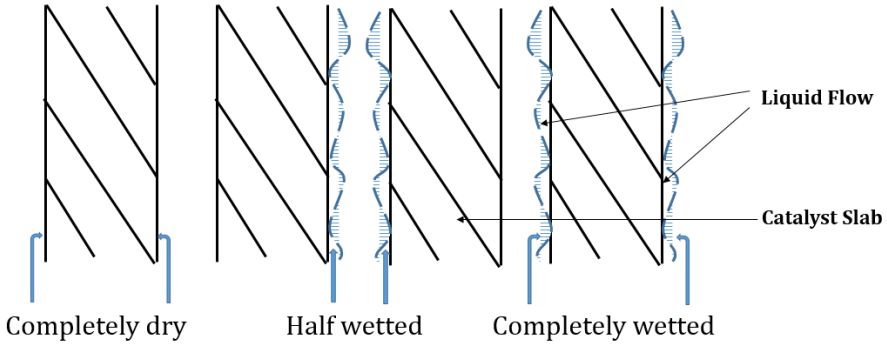


Figure A.2. Overall effectiveness factor as a weighted average of the wetting efficiency

To appropriately weigh $\eta_o$, fractions of the wetting efficiency ($\eta_{CE}$) was included in the $\eta_o$ equation depending on the geometry. [17, 20, 33]. A slab geometry was used in the mathematical calculations of the effectiveness factor at pellet scale for its simplicity although spherical, cylindrical, and cubical geometries are available elsewhere [23, 29, 34, 38, 39]. A comprehensive equation for the overall effectiveness factor for a slab geometry accounting for dry, completely wet and partially wet contacts can be written as

$$\eta_o = (1 - \eta_{CE})^2 \eta_{od} + 2\eta_{CE}(1 - \eta_{CE})\eta_{odw} + \eta_{CE}{}^2 \eta_{ow} \quad (4)$$

where $\eta_o$ is the weighted average of the dry, completely wet and partially wet effectiveness factors ($\eta_{od}$, $\eta_{ow}$, and $\eta_{odw}$) of the catalyst pellet. This value of $\eta_o$ was used to evaluate the

reactor performance by accounting for the pellet scale effects in the reactor scale model equations. The effectiveness factors $\eta_{od}$ , $\eta_{ow}$ and $\eta_{odw}$ were represented as a function of the reactant concentration, and the analytical solutions were available. Generally, for slab geometries with completely dry, half-wetted, and completely wetted pellets as shown in Figure 2, the values of the contacting efficiencies are 0.0, 0.5 and 1 respectively [33].

Using one value of overall effectiveness factor for the whole bed may not be realistic as the value changes due to the reactor's performance and concentration variation. The catalyst wetting, the local concentration of the reactants, operating conditions, catalyst deactivation, pressure drop, and related factors play a major role in changing the overall effectiveness factor axially. Many models do not mention or implement this condition resulting in a simplified and approximated solution. Although computational models are available elsewhere or can be developed, they are time-consuming and need information like kinetics, geometry, mass transfer data and much more. They may also need the expertise to develop user-defined functions to solve the model for convergence. Recent selected models and approaches to predict TBRs performance are summarized in Table A.2 although there are many models for trickle bed reactors available in the open literature.

Khadilkar et al. [8] employed a heterogeneous plug flow model [5] and a pellet scale model [21] to compare and validate their experimental observations for liquid-limited reactions (high pressure). It was observed that the reactor scale model needed an overall effectiveness factor $\eta_o$ to include the pellet level effects. In the model, the intrinsic kinetics was determined from the slurry experimental data and used while solving the pellet scale model equations. The pellet effectiveness factor was determined by solving the pellet scale equations at select bulk concentrations in accordance to the experimental observations and

then used as a fitting parameter to solve the reactor scale equations for all spacetimes. Although this concept is numerically easy to solve and to predict the performance, using the pellet effectiveness factor from selected bulk reactant concentrations at a specific space-time cannot indicate the exact representation in the reactor at different operating conditions. Moreover, using a polynomial to represent the trend and magnitude of the effectiveness factor varying with the change in local concentration along the bed height may not exactly represent the intra-pellet mass transfer resistance and the wetting efficiency around the pellet. In fact, the value of the local effectiveness factor varies axially due to the change in the reactant concentrations in the catalyst surface. This confirmed the need to implement the local effectiveness factor obtained from the pellet scale equations at all operating conditions and every axial point to predict the reactor performance precisely.

Later, Guo and Al-Dahhan [6] developed the sequential approach for evaluating the $\eta_o$ at every axial location inside the bed. The local effectiveness factor was evaluated based on Beaudry et al. [21] at each axial collocation point and updated in the reactor scale equations to simulate the reactor performance. This approach will be further discussed in this work. Following these works, researchers used the method of extracting the $\eta_o$ from the pellet scale equations and implementing the value in reactor scale model equations. This proved to be very beneficial as well as effective while predicting the reactor performance for their experimental studies.

Since many models are available in the literature, a simple starting point is needed to easily relate the model to the experimental observations before approximating the effectiveness factor. Furthermore, it is necessary to decide if the employed model needs to include axial dispersion effects.

Table A.2. Selected models in the literature for the prediction of TBRs performance

| Author/reference | Reaction | Model conditions | Remarks |
|---|---|---|---|
| Rajashekharam et al. (1998) [34] | Hydrogenation of 2,4-dinitrotoluene/TBR | Non-isothermal, plug flow, partial wetting, stagnant liquid | L-H kinetics Temperature rise, hysteresis behavior well predicted |
| Jiang et al. (1998) [40] | Hydrogenation of a-nitromethyl-2-furan methanol/TBR | Isothermal, plug flow, partial wetting Reactor scale plug flow model for a network of reactions | L-H kinetics Reactor scale plug flow model for the network of reactions |
| Tukac and Hanika (1998) [41] | Oxidation of substituted phenols/TBR | Isothermal, plug flow | Linear kinetics |
| Herrmann and Emig (1998) [42] | Hydrogenation of maleic anhydride/UFR | Isothermal, axial dispersion, full wetting | L-H kinetics |
| Chaudhari et al. (2002) [43] | Hydrogenation of 1,5,9-cyclododecatriene/TBR and UFR | Non-isothermal, plug flow, partial wetting, stagnant liquid | L-H kinetics |
| Dietz, Julcour, and Delmas (2003) [44] | Hydrogenation of 1,5,9-cyclododecatriene/TBR | Non-isothermal heterogeneous model, partial wetting effect | Eley-Rideal kinetics |
| Avraam and Vasalos (2003) [45] | Catalytic hydroprocessing of oil feedstock | Non-isothermal, homogeneous plug flow axial dispersion model | L-H kinetics |
| Guo and Al-Dahhan (2004) [6] | Hydrogenation of a-methyl styrene and phenol oxidation/TBR and UFR | Axial dispersion model | L-H kinetics |

Table A.2. Selected models in the literature for the prediction of TBRs performance (cont.)

| | | | |
|---|---|---|---|
| Guo and Al-Dahhan (2005) [46] | Catalytic wet air oxidation/TBR and UFR | Axial dispersion model for liquid phase coupled with the cell stack model for gas phase | L-H kinetics |
| Suwanprasop et al. (2005) [47] | Wet air oxidation of phenol | Non-isothermal, plug flow model, partial wetting effect | Power law kinetics |
| Guo et al. (2008) [48] | Hydrotreating of benzene/TBR | Non-isothermal, one-dimensional and two-dimensional cell network models, radial liquid maldistribution, partial wetting effect | L-H kinetics |
| Roininen et al. (2009)[49] | Hydrogenation of benzene/TBR | Non-isothermal heterogeneous three-phase model, Maxwell-Stefan mass transfer model, and effective diffusivity model | L-H kinetics |
| Wu et al. (2009) [50] | Catalytic oxidation of phenol/TBR | Isothermal, axial dispersion model, plug flow model | L-H kinetics |
| Magoo et al 2013 [51] | Fischer-Tropsch reaction | Dynamic axial dispersion model with effectiveness factor in terms of Thiele modulus | nth-order kinetics |

Table A.2. Selected models in the literature for the prediction of TBRs performance (cont.)

| | | | |
|---|---|---|---|
| Kilpio et al. 2014 [52] | Synthesis of Hydrogen Peroxide | Dynamic axial dispersion model and the single particle model | L-H kinetics |
| Durante et al. (2014) [53] | Hydrogenation of sugar | Dynamic axial dispersion model including deactivation | L-H kinetics with effectiveness factor in terms of Thiele modulus |
| Ghouri et al. (2015) [54] | Fischer-Tropsch reaction | Pseudo-homogeneous one-dimensional Plug Flow model and particle diffusion model for spherical geometry | Fully mixed assumption with effectiveness factor in terms of Thiele modulus |

This way we can estimate the performance of the reactor even before the experiments are conducted using the initial conditions which gives a better understanding of the system. Also, the various approaches discussed in this work helps to model different phases in the trickle bed reactor using the available operating conditions and properties.

Studies on scaled-down TBRs are unavoidable due to their existence in industries. The paper focuses on demonstrating that using a single value of effectiveness factor all over the reactor length can erroneously lead to improper estimation of the reactor performance for industrial applications. Accordingly, the objective of this study is to assess the effect of different approaches to understand the implementation of the effectiveness

factor on the performance prediction of the TBRs and defining their shortcomings. Moreover, the proposed approaches are transformative to any multiphase reactions involving complex kinetics and can be extended to benefit all the processes used in trickle bed reactors with porous catalysts. A comparative study was conducted using models which include plug flow model (PFM) and axial dispersion model (ADM) equations to evaluate the necessity of using axial dispersion coefficient. This study helps in understanding the need for an overall effectiveness factor or its local estimation and the significance while modeling the reactor.

## 2. GENERAL MODEL

The heterogeneous model used in this study is formulated to estimate the conversion of the reactants in the liquid phase from the reactant concentrations (both liquid and gas). A simple reaction is given below (Equation 5) for which the modeling approaches are analyzed.

$$A_{(g)} + \boldsymbol{\nu}_B B_{(l)} \rightarrow C \text{ (Products)} \quad (5)$$

The focus of this work is based on the models mentioned in Table 3, and the governing model equations are mentioned later in the section. For simplicity, we have chosen to use one-dimensional model while this work can be extended to two- and three-dimensional for liquid-limited reactions. These models cover most of the common assumptions employed while modeling a reactor and follow similar kinetics. This work can be further extended to study the sensitivity of the reactor performance with respect to parameters. In the dimensionless form, with using appropriate variables like liquid hourly

space velocity (LHSV), Peclet Number and more this model can be used a good tool for scale-up for liquid-limited reactions. Usually, the hydrogenation reactions are exothermic that can generate temperature gradients along the catalyst bed. This does influence the effectiveness factor as the local temperatures in the inter- and intra-pellet are different. This model can be expanded by including energy balance equations which comprise the local temperature effects to obtain the local rate of reaction. However, for the hydrogenation of alpha-methyl styrene in the literature the temperature gradients have not been measured or addressed. Therefore, in this work, we consider it as isothermal operation and hence energy balance equations have not been included.

The reactor scale equations in the model are represented by ordinary differential equations (ODE) with Danckwerts' boundary conditions. All the mass balance equations were developed for the reactants in the liquid phase assuming no significant effects of the gas phase at a constant partial pressure of the reacting gas. The mass transfer resistances are accounted in an equation which includes the interphase resistances between the liquid, gas and solid catalyst phases [5, 6, 55]. The reaction kinetics accounts for the intraparticle mass transfer of the reactants in the catalyst pellet. The correlations for the internal and external diffusion in the model in terms of gas-liquid, liquid-solid and gas-solid mass transfer coefficients are mentioned in the Appendix of this article which were chosen based on the reactor operating conditions. The mass transport equations in the model were expressed reflecting the driving force (concentration gradient) required for the reactants to diffuse through the liquid film and the catalyst pellet. The plug flow model assumptions were adopted as proposed by El-Hisnawi et al. [5] and Khadilkar et al. [8]. The ADM equations were developed based on the assumptions made by Guo and Al-Dahhan [6].

Table A.3. Models used in this study

| **Authors** | **Model description** | **Experimental system** | **Remarks** |
|---|---|---|---|
| El-Hisnawi et al. (1982) [5] | Plug flow of each phase, effect of contacting efficiency, Rate enhancement, gas limited conditions | α-methylstyrene hydrogenation | Doesn't account for the pellet effectiveness factor determined from Thiele Modulus or a fitting parameter. Gas-limited reaction |
| Beaudry et al. (1987) [21] | Pellet Scale diffusion effects with multiple wetting conditions for a gas-limiting reaction for reaction order <= 1 | α-methylstyrene hydrogenation | Overall effectiveness factor based on weighted average of wetting efficiency and effectiveness of pellet based on wetting. Solved for conversion using a plug flow equation, gas-limited reaction |
| Khadilkar et al. (1996) [55] | Reactor scale (El-Hisnawi) and pellet scale (Beaudry) models with pressure dependent intrinsic kinetics for both gas and liquid limited reaction conditions | α-methylstyrene hydrogenation | Performance at both gas and liquid-limited extremes predicted with pellet effectiveness factor as a fitting polynomial using the model by Beaudry. Gas and liquid limited reaction |
| Guo and Al-Dahhan (2004) [6] | Axial dispersion model integrated with Pellet scale model accounting for non-linear reaction kinetics expression and different types of pellet–liquid wetting contact | α-methylstyrene hydrogenation and wet oxidation of phenol | Effect of sequential modeling to predict local effectiveness factor to the corresponding local liquid reactant concentration. Effectiveness factor from Pellet scale model of Beaudry. liquid limited reaction |

Table A.4. Different approaches to assess the approximation of the effectiveness factor

| **Approach** | **Reactor scale model** | | **Pellet Scale model** (Beaudry et al. 1987) | Notes |
|---|---|---|---|---|
| | Liquid Phase | Gas Phase | | |
| OEM | ADM/PFM | PFM | Yes | Used simple reactor scale equations to solve |
| PNM | PFM | PFM | Yes, but not sequentially | Used a polynomial for effectiveness factor |
| SQM | ADM/PFM | ADM/PFM | Yes | Solved sequentially with an initial assumption of effectiveness factor |

The axial dispersion coefficient, $D_{ax}$ parameter, accounts for the diffusion of the reactants axially across the reactor. This parameter used in the ADM equations was calculated from the correlation of Cassanello et al. [56]. The pellet scale model (PSM) assumptions were according to Beaudry et al. [21]. The possible pellet concentration profiles are shown in Figure 3. These form the boundary conditions to solve the pellet scale equations and have to be identified before calculating the overall effectiveness factor. Pellet scale equations estimated the local overall effectiveness factor as a function of partial wetting in a catalyst pellet assuming an infinite slab geometry. The equations for the completely dry, half-wet and wet effectiveness factors, $\eta_{od}, \eta_{odw}$ and $\eta_w$ mentioned in Beaudry et al. [21] are a function of the catalyst concentrations, which in turn were obtained by solving the PSM equations. Analytical solutions for these reaction-diffusion equations were available at low pressure (gas-limited conditions) [21] while at high pressure (liquid-limited conditions) the mass balance equations were solved numerically. The equilibrium

concentration was calculated using the solubility data of hydrogen in alpha-methyl styrene in terms of Henry's constant.

The performance of the trickle bed reactor was estimated by PFM and ADM equations and compared for different approaches employed to evaluate the catalyst effectiveness factor in this work. The approaches are one effectiveness factor model (OEM) for using one value of effectiveness factor for the whole bed, fitted polynomial model (PNM) for using fitted polynomial that relates the effectiveness factor with the reactant concentrations, and sequential approach model (SQM) that estimates the effectiveness factor using pellet scale model along the bed height when the reactant concentration varies locally. All of the approaches incorporate the effectiveness factors in different ways thereby accounting for all the transport effects, reaction kinetics, and hydrodynamics in the reactor system. The model equations were solved based on the Runge-Kutta numerical method using MATLAB software with *bvp5c* and *ode45* routines. A more detailed explanation of these approaches and their methodology are provided in the next section.

## 3. NUMERICAL SOLUTIONS OF THE REACTOR SCALE MODEL

This section will discuss the various approaches in approximating the effectiveness factor and the methodology to solve the differential equations. Table A.4 summarizes the different approaches and corresponding model equations used to predict the reaction performance.

Reactor scale model equations (in the liquid phase) $i$ = A,B

Axial Dispersion Model (ADM) equations (Guo and Al-Dahhan [6])

$$\frac{D_{AL,A}}{u_L}\ \frac{d^2C_{A.L}}{dz^2} - \frac{dC_{A,L}}{dz} + \frac{1}{u_L}\left[(ka)_{GL}\left(C_{A,e} - C_{A,L}\right) - \ k_{LS,A}\ a_{LS}\left(C_{A,L} - \ C_{A,LS}\right)\right] = 0 \quad (6\text{-}1)$$

$$\frac{D_{AL,B}}{u_L}\ \frac{d^2C_{B.L}}{dz^2} - \frac{dC_{B,L}}{dz} + \frac{1}{u_L}\left[\vartheta_B k_{GS,A} a_{GS}(C_{A,e} - C_{A,GS}) - \ k_{LS,B}\ a_{LS}\left(C_{B,L} - \ C_{B,LS}\right)\right] = 0 \quad (6\text{-}2)$$

$$\frac{D_{AL,C}}{u_L}\ \frac{d^2C_{C.L}}{dz^2} - \frac{dC_{C,L}}{dz} - \frac{1}{u_L}\left[\ k_{LS,C}\ a_{LS}\left(C_{C,L} - \ C_{C,LS}\right)\right] = 0 \quad (6\text{-}3)$$

Mass Transport Equations at the pellet (i= A,B,C)

$$k_{LS,i}\ a_{LS}\left[C_{i,L} - \ C_{i,LS}\right] = \eta_o(1{-}\varepsilon_b)\eta_{CE}\ r_i\left(C_{i,LS}\right) \quad (6\text{-}4)$$

$$k_{GS,A}a_{GS}\left(C_{A,e} - C_{A,GS}\right) = \eta_o(1{-}\varepsilon_b)(1 - \eta_{CE})\ r_A\left(C_{A,GS}\right) \quad (6\text{-}5)$$

Boundary Conditions

$$-\frac{D_{AL,i}}{u_{SL}}\ \frac{dC_{i,L}}{dz} = (C_{i,0} - C_{i,L}) \quad \text{at z = 0}$$

$$\frac{dC_{i,L}}{dz} = 0 \quad \text{at z = L}$$

Plug Flow Model (PFM) equations [8]

$$-\frac{dC_{A,L}}{dz} + \frac{1}{u_{SL}}\left[(ka)_{GL}\left(C_{A,e} - C_{A,L}\right) - \ k_{LS,A}\ a_{LS}\left(C_{A,L} - \ C_{A,LS}\right)\right] = 0 \quad (6\text{-}6)$$

$$-\frac{dC_{B,L}}{dz} + \frac{1}{u_{SL}}\left[\vartheta_B k_{GS,A} a_{GS}(C_{A,e} - C_{A,GS}) - \ k_{LS,B}\ a_{LS}\left(C_{B,L} - \ C_{B,LS}\right)\right] = 0 \quad (6\text{-}7)$$

$$-\frac{dC_{C,L}}{dz} - \frac{1}{u_{SL}}\left[\ k_{LS,C}\ a_{LS}\left(C_{C,L} - \ C_{C,LS}\right)\right] = 0$$

Boundary Conditions

$$C_{A,L}(z)\big|_{z=0} = 0$$

$$C_B(z)|_{z=0} = C_{B,initial}$$

Pellet Scale Model (PSM) Equations (Beaudry at al. [21])

$$\frac{d^2C_i}{dx^2} - (1-\omega_x-\omega)^2 \left(\frac{V_s}{S_x}\right)^2 \frac{(-r_i)}{D_{ei}} = 0 \ ; 0< x< 1 \quad (6\text{-}8)$$

$$\frac{d^2C_i}{dy^2} - (1-\omega_x-\omega)^2 \left(\frac{V_s}{S_x}\right)^2 \frac{(-r_i)}{D_{ei}} = 0 \ ; 0< y< 1 \quad (6\text{-}9)$$

Boundary conditions (were written based on the possible reactant profiles as shown in Figure 3 based on x and y where x=1 is completely dry and y=1 is completely wet)

$$\left.\frac{dC_A}{dy}\right|_{y=1} = (2-\omega)\, Bi_{LS,A}\left(C_{A,L} - C_A|_{y=1}\right)$$

$$\left.\frac{dC_B}{dy}\right|_{y=1} = (2-\omega)\, Bi_{LS,B}\left(C_{B,L} - C_B|_{y=1}\right)$$

$$\left.\frac{dC_A}{dx}\right|_{x=1} = \frac{1-\omega_x-\omega}{\omega+\left(\frac{1}{Bi_{GS,A}}\right)}\left(C_{A,L} - C_A|_{x=1}\right)$$

$$\left.\frac{dC_A}{dx}\right|_{x=0} = -\frac{1-\omega_x-\omega}{1-\omega_y}\left.\frac{dC_A}{dy}\right|_{y=0}$$

$$C_A|_{x=0} = C_A|_{y=0} - 2\left(\frac{V_s}{S_x}-1\right)\left.\frac{dC_A}{dy}\right|_{y=0}$$

$$C_B|_{x=1} = 0$$

$$C_B|_{x=0} = C_B|_{y=0} - \frac{2\left(\frac{V_s}{S_x}-1\right)+\omega_x+\omega_y}{1-\omega_y}\left.\frac{dC_B}{dy}\right|_{y=0}$$

$$\left.\frac{dC_B}{dx}\right|_{y=0} = 0$$

$$\left.\frac{dC_B}{dy}\right|_{x=0} = \frac{1-\omega_x-\omega}{1-\omega_y}\left.\frac{dC_B}{dy}\right|_{y=0}$$

Where $i = \frac{kV_S}{D_e S_x}$, $C_i = \frac{C_{i,L}}{C_{Ae}}$

$$\eta_o = (1 - \eta_{CE})^2 \eta_{od} + 2\eta_{CE}(1 - \eta_{CE})\eta_{odw} + \eta_{CE}{}^2 \eta_{ow}$$

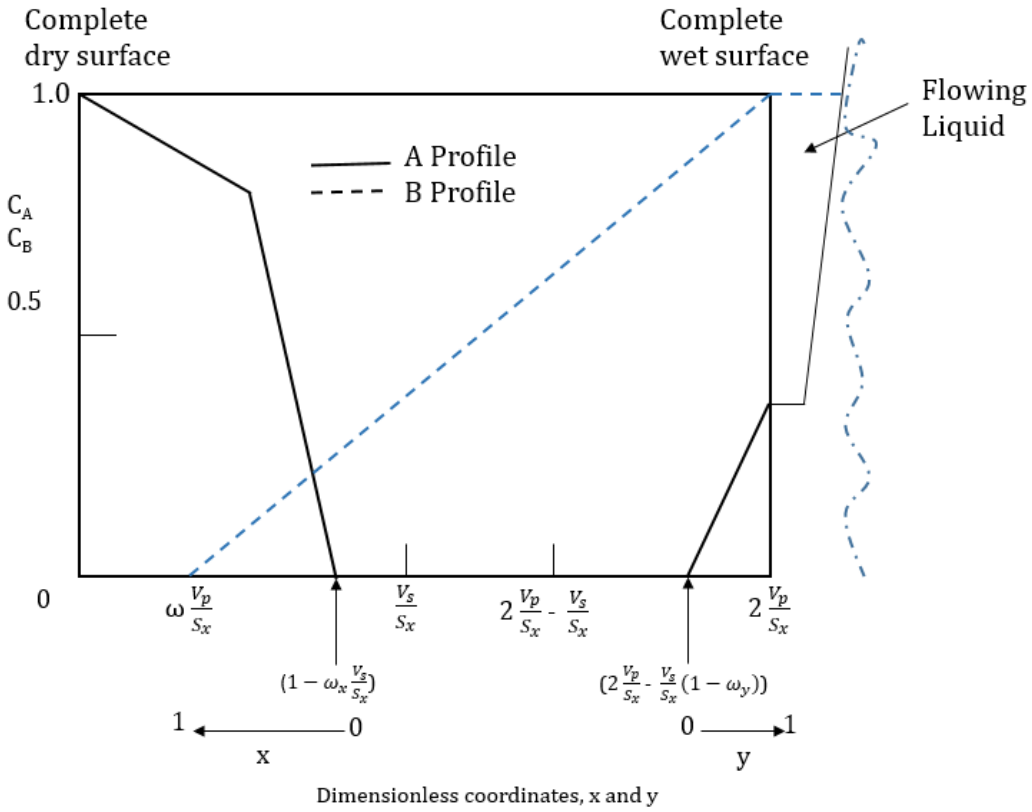


Figure A.3. Predicted Concentration profiles across the catalyst pellet for a slab geometry (A-Gas, B-Liquid); x - coordinate in the external shell to completely dry surface or plane where B is depleted; y - coordinate in the external shell to actively wetted surface

## 3.1. APPROACHES FOR USING THE CATALYST EFFECTIVENESS FACTOR IN REACTOR SCALE MODEL

**3.1.1. One Effectiveness Factor Model (OEM) Approach.** An approximately fixed value for the overall effectiveness factor representing the whole bed was evaluated to solve the reactor scale model equations mentioned above. This value can be obtained

from the literature or batch slurry experiments. Moreover, different correlations mentioned in Table A.5 from the literature were used in this approach to compare the reactor performance predictions. Also, a single value for the effectiveness factor ($\eta_o$) evaluated from the pellet scale equations was used in the reactor scale models during the assessment.

**3.1.2. Fitted Polynomial Model (PNM) Approach.** In this approach of approximating the local overall catalyst effectiveness factor, the pellet scale model equations were solved for selected bulk liquid concentrations as the boundary conditions. A polynomial was fitted for the $\eta_o$ as a function of the selected bulk concentrations at the catalyst surface ranging in the experimental operating conditions. This polynomial was used in the transport equations while solving the PFM equations to estimate overall effectiveness factor at each spacetime with the variation of the local reactant concentrations to predict the reactor performance.

If intrinsic kinetics data were available, then the apparent kinetics will be identified using the single value of the overall effectiveness factor multiplied by the intrinsic kinetics. A value near to unity reflects that the reaction rate is not affected by the internal transport resistances at any operating conditions.The limitation of this assumption is that the internal transport largely influences the measured reaction rate and this approach may be suitable to predict the reaction systems which have not yet been experimentally investigated.

**3.1.3. Sequential Approach Model (SQM) Approach.** The sequential approach represents the combination of ADM and PSM to predict reactor performance [6]. A initial assumption for the overall effectiveness factor ($\eta_o$) was taken, and the reactor scale equations were solved to obtain a concentration profile aiding to identify the local concentrations at different axial points.

Table A.5. Different correlations for estimating the overall catalyst effectiveness factor

| Model | Equations | Reference and Remarks |
|---|---|---|
| M1 | $\eta_o = \eta_{CE} \frac{\tanh(\frac{\Phi}{\eta_{CE}})}{\Phi}$ | Duduković [23] - kinetics involved Function of Thiele Modulus, wetting efficiency and Fractional fill up |
| M2 | $\eta_o = \frac{\eta_{CE}}{(\frac{{\Phi_T}^2}{Bi_w} + \frac{\Phi_T}{tanh\Phi_T})} + \frac{(1-\eta_{CE})}{(\frac{{\Phi_T}^2}{Bi_d} + \frac{\Phi_T}{tanh\Phi_T})}$ | Mills [27] - Modified Thiele Modulus with Biot number accounting for mass transfer in dry and wet regions of the pellet |
| M3 | $\eta_o = \frac{\frac{\eta_{CE}}{\Phi_T}\tanh(\frac{\Phi_T}{\eta_{CE}})}{(1 + \frac{\Phi_T}{Bi_w}\tanh(\frac{\Phi_T}{\eta_{CE}}))}$ | Ramachandran and Smith [17] |

The reactor axis is then divided into a specific number of axial collocation points (Figure A.4**)** where the local concentration at each of these points is known from the concentration profile obtained earlier by solving the reactor scale model. The PSM is solved sequentially with the reactor scale model to estimate the $\eta_o$ at that location based on the local reactant concentration obtained from the reactor scale model. These local concentration values become the boundary conditions for the PSM which is solved to obtain a catalyst level concentration profile using which we can calculate the overall effectiveness factor ($\eta_o$) from Equation 4 for that specific axial collocation [21]. This way we will have different $\eta_o$ values at different axial positions and these values of $\eta_o$ are now used to solve the reactor scale model (ADM and PFM) equations mentioned earlier at each of the axial collocation points to obtain the local bulk concentrations using which the PSM model is solved again to obtain the updated local $\eta_o$ values.

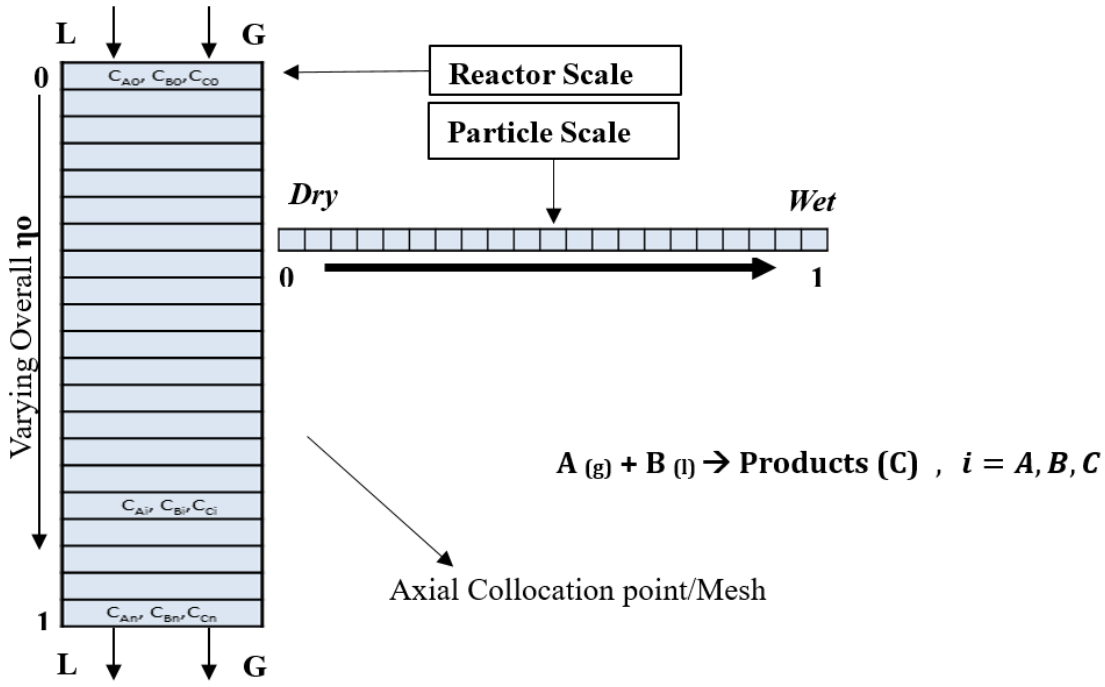


Figure A.4. Mesh structure for SQM approach at the reactor and pellet scale modeling

The iterations are repeated where the local $\eta_o$ and local concentration values are updated after each step until the values of the $\eta_o$ converge for each mesh from which the final local concentration values are extracted. This means that the equations are solved for each mesh until they converge and then the calculations move forward to the next mesh. This way the local concentration is obtained at each mesh. The iteration loop continues for convergence to occur at every mesh. These local concentration values are further used to determine the reactor performance in terms of conversion. The flowsheet explaining this sequential approach is shown in Figure A.5.

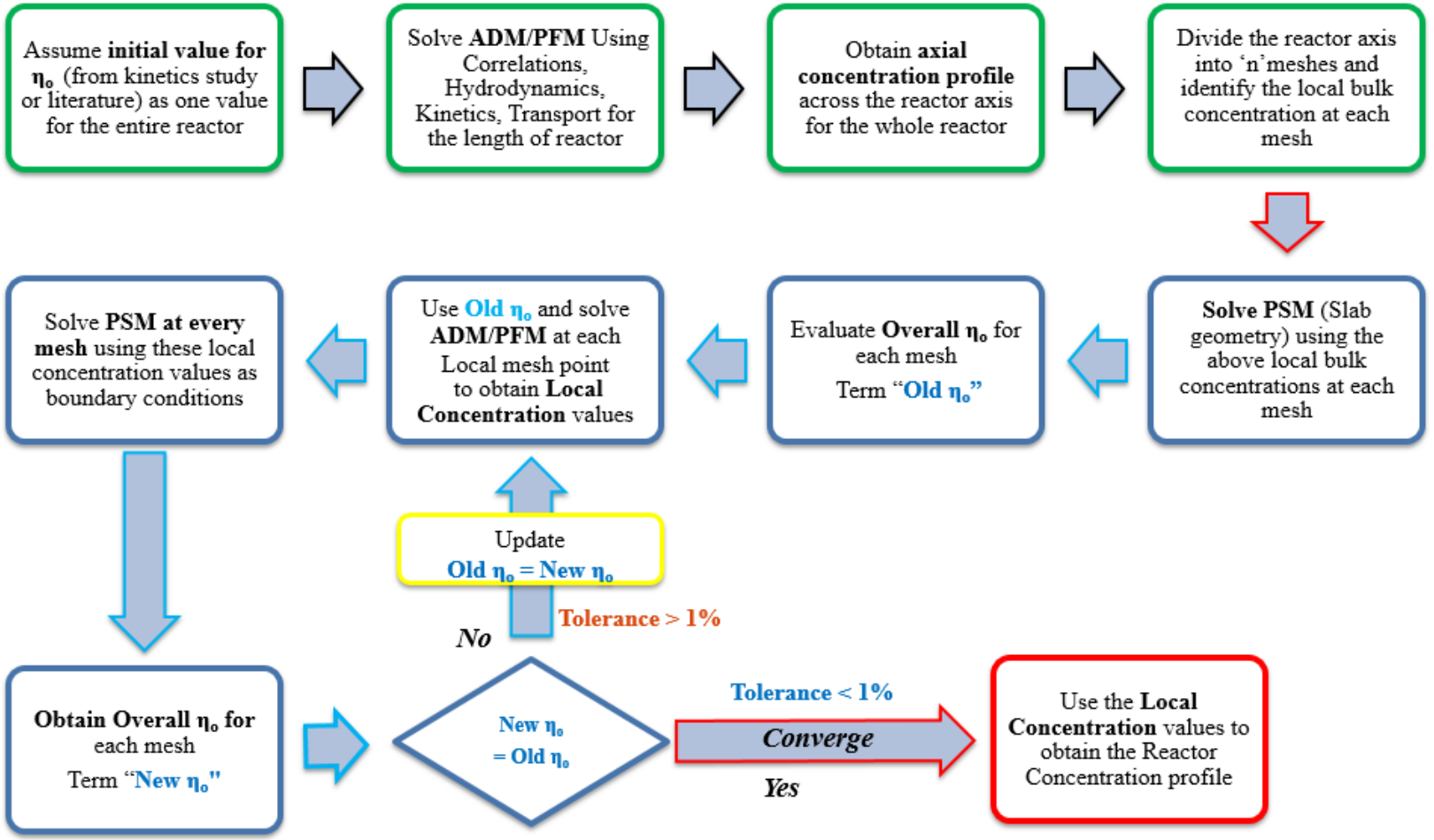


Figure A.5. Flowsheet for the sequential approach for multiscale modeling (SQM)

Table A.6. Operating conditions and properties used in the model for Hydrogenation of α-methylstyrene [8, 57]

a. Reactor and catalyst properties

| | |
|---|---|
| Total length (cm) | 50 |
| Catalyst bed length (cm) | 27.5 |
| Reactor Diameter (cm) | 2.2 |
| Active metal | 2.5% Pd |
| Catalyst support | Alumina |
| Catalyst size (1/16 inch) (cm) | 0.15875 |
| Packing shape | Cylinder |
| Packing dimensions (cm) | 0.13 x0.56 |
| Bed porosity $\varepsilon_B$ | 0.36 |
| Surface area ($m^2/g$) | 184 |
| Total pore volume ($cm^3/g$) | 0.481 |
| Pellet density FP ($g/cm^3$) | 1.222 |
| True pellet density $\rho_t$ ($g/cm^3$) | 2.965 |
| Pellet porosity $\varepsilon_p$ | 0.5878 |

b. Range of Operating Conditions for Steady-State Experiments

| | |
|---|---|
| Temperature | 25°C |
| Pressure | 30-200 psig |
| Concentration of alpha-methylstyrene | 3.1-7.8 % (v/v) (230-600 $mol/m^3$) |
| Superficial gas velocity (mass velocity) | 3.8-14.4 cm/s ($3.3e^{-3}$-$12.8e^{-3}$ $kg/m^2s$) |
| Superficial liquid velocity (mass velocity) | 0.09-0.5 cm/s (0.63-3.85 $kg/m^2s$) |

Table A.6.: Operating conditions and properties used in the model for Hydrogenation of α-methylstyrene [8, 57] (cont.)

c. Kinetic rate constants from slurry experiments

| Pressure (psig) | $k_{vs}$ ($m^3$ liquid/$m^3$ cat/s*($m^3$/mol) ($m^{-1}$) | $K_1$ ($m^3$/mol) | $K_2$ ($m^3$/mol) | β |
|---|---|---|---|---|
| 200 | 0.022 | $2.73*10^{-2}$ | $2.1*10^{-2}$ | 2 |

## 4. RESULTS AND DISCUSSIONS

To assess the effect of implementing different approaches of approximating the catalyst effectiveness factor and using it in the reactor scale modeling, the hydrogenation of α-methylstyrene (AMS) was chosen as the test reaction. Various studies used this test reaction for different performance studies of TBRs [5, 6, 8, 21]. The rate and operating parameters and reaction conditions used in the model are summarized in Table 6. In this work, the liquid-limited reaction kinetics (Langmuir–Hinshelwood form as shown in Equation 7) of the hydrogenation of AMS was employed to predict the reactor performance using all the approaches mentioned in this work. This rate equation is based on the work done by Khadilkar et al. [55]. This rate equation has been implemented in the model equations and approaches mentioned in the previous sections.

$$rate = \frac{k_{vs} C_A C_B}{(1 + K_1 C_B + K_2 C_C)^{\beta}} \tag{7}$$

The performance of the reactor was predicted using the effectiveness factor evaluated from the different approximation approaches and compared with the experimental observations of the hydrogenation of AMS. The initial analysis was to check

of the sensitivity of the overall conversion in respect with the effectiveness factor on for the reactor using simple plug flow model equations to assess the predictions. The sensitivity of the effectiveness factors employed in the reactor scale model needs to be understood and justified. Since our focus was on the overall effectiveness factor, we conducted a sensitivity analysis only on this parameter and fixing all other parameters that affect the performance. The correlations used to evaluate the other parameters were kept the same throughout the study. The PFM equations incorporated the interphase mass transfer equations to account for the gas-liquid, gas-solid and liquid-solid transports for nonlinear kinetics. Figure 6 explains that with an increase in the effectiveness factor the conversion increases which can be attributed to the less resistance to the intraparticle diffusion of the liquid reactants. As the internal mass transport of the reactants through the pellet influence the conversion, identifying the effectiveness factor from a pellet scale model or another valid methodology is significant to predict the reactor performance properly.

Figure A.7 compares the reactor performance predictions of the PFM equations using the single value of overall effectiveness factor for the entire reactor. The value of the $\eta_o$ was calculated by solving the PSM for the entire reactor using the inlet concentration as the boundary conditions ($PSM_{IC}$) and the models M1, M2, and M3 mentioned in Table A.5. It can be noticed that evaluating the $\eta_o$ from the pellet scale equations ($PSM_{IC}$) and from M1, M2, and M3 were close to each other although the effectiveness factor calculated from PSM gave a slightly better prediction of the reactor performance in comparison to the other models. The value of $\eta_o$ from pellet scale equations, $PSM_{IC}$ was used in ADM model equations to understand the influence of the dispersion parameter (Figure 8).

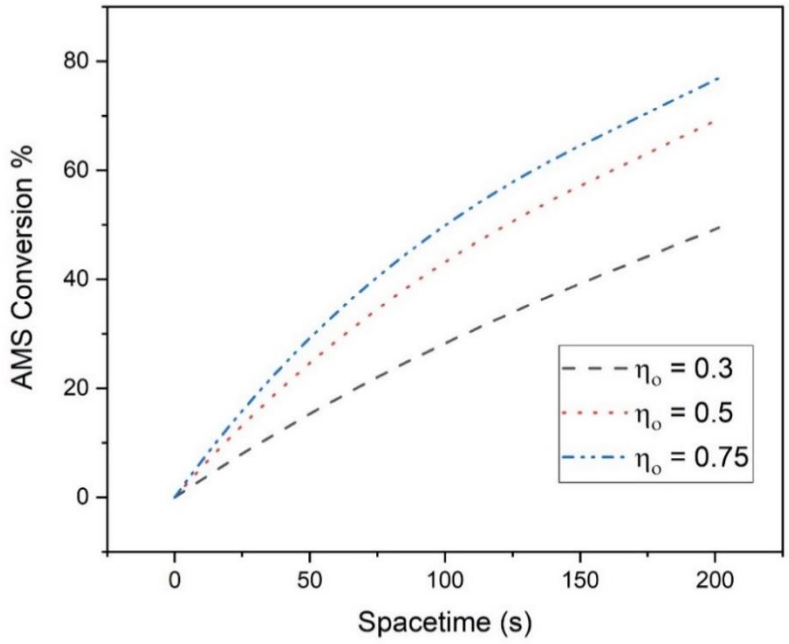


Figure A.6. Sensitivity of the overall conversion in respect with the effectiveness factor for the predictions of the PFM equations for hydrogenation of AMS using single effectiveness factor for the whole bed. (ug=0.038ms$^{-1}$, P=200 psig, $C_{AMS}$=230 mol m$^{-3}$)

The Peclet number estimated from the correlation [56] for the operating conditions was found to be in the range of 0.75-2. It is evident that the axial dispersion model was able to predict the experimental data better than the plug flow model (Figure A.8). Also, it is crucial to model the liquid phase when it comes to liquid-limited conditions especially at higher spacetimes as in this work. Although, the axial dispersion plays a vital role in predicting the reactor performance, evaluating the parameter from the correlations may have its drawbacks. PFM is simpler but doesn't account for the dispersion effects which is prominent in packed bed reactors especially in trickle flow. We can still match the models with the experimental data when more information is provided. This comparison signifies the need to include the $D_{ax}$ in the model equations. On the other hand, it is important to identify a better approach to incorporate the $\eta_o$ due its varying nature across the reactor.

For the PNM approach, the $\eta_o$ was evaluated fitted polynomial where the $\eta_o$ is a function of the surface concentration of the liquid reactants from the pellet scale equations. Although, this model uses $\eta_o$ as a parameter, this approach is useful when few experiments are conducted, or less computational capabilities are available. From the Figure A.9, it was observed the prediction using PFM equations were similar to the OEM approach due to nature of the polynomial fitting and the effectiveness factor values didn't show much change at different conditions. Moreover, this approach has the disadvantage of accounting the error caused due to fitting while using different bulk reactant concentration values and space-times. This approach of estimating the $\eta_o$ was mainly to highlight the fact that this approach may not predict the reactor performance due to its limitations.

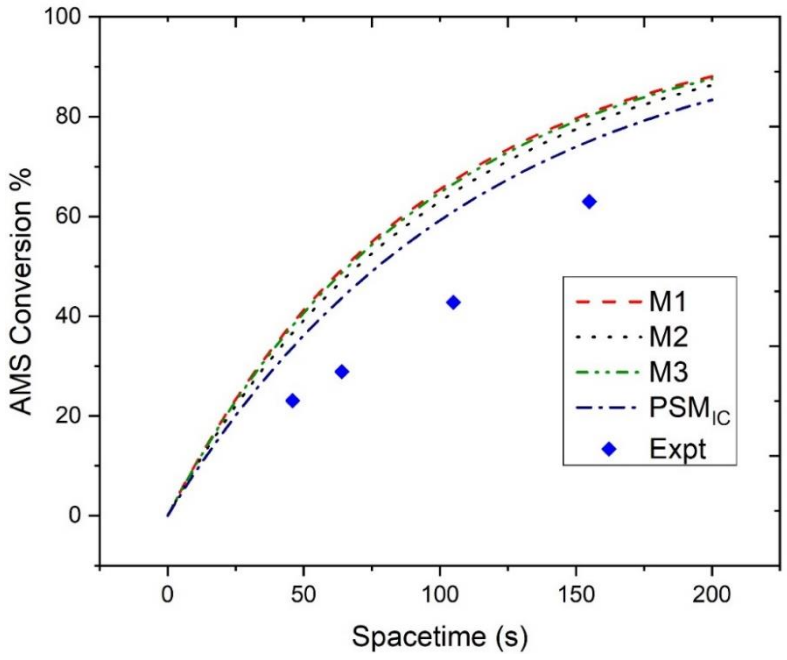


Figure A.7. Prediction of the reactor performance using PFM equations for hydrogenation of AMS with single effectiveness factor for the whole bed from M1, M2 and M3 and Pellet scale model, $PSM_{IC}$ (ug=0.038ms$^{-1}$, P=200 psig, $C_{AMS}$=230 mol m$^{-3}$)

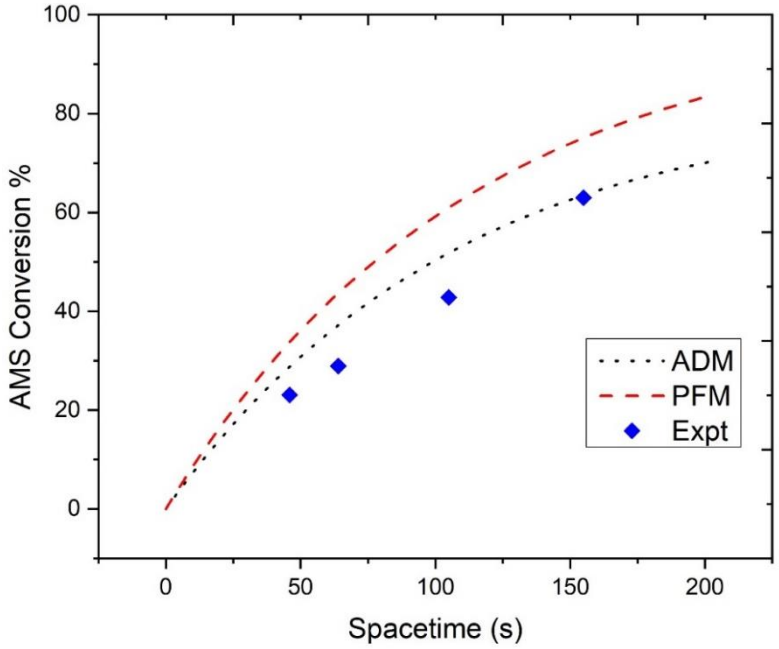


Figure A.8. Comparison of the reactor performance predictions of ADM and PFM equations using the single value of effectiveness factor from Pellet scale model, ($PSM_{IC}$) using hydrogenation of AMS. (ug=0.038ms$^{-1}$, P=200 psig, $C_{AMS}$=230 mol m$^{-3}$)

At this point, we can understand that the OEM approach using the $\eta_o$ values from the PSM is a better approach than the M1, M2 and M3. As stated earlier, the change in local concentration gradient affects the local effectiveness factor, it is vital to estimate the local $\eta_o$ values and integrate into the reactor scale model in order to avoid under-estimation or over-estimation of the design/performance of the reactor. Furthermore, understanding the influence of axial dispersion in the reactor system becomes significant too.

The SQM approach is solved using ADM and PFM model equations and it is compared to the OEM approach. From the Figure A.10, it can be understood that the SQM approach has the best fit than the other approaches. This should be mainly due to the two main reasons: a) accounting of the dispersion parameter while solving the equations making the approach more realistic; b) including the variation in the $\eta_o$ at every axial

collocation point. This approach of predicting the reactor performance is useful as we can assume the initial $\eta_o$ values to get a better fit to the experimental data.

This sequential approach accounts for the variation for the $\eta_o$ with concentration thereby incorporating the approximation of the overall effectiveness factor properly during modeling. The SQM approach of solving the model equations is very efficient in predicting the reactor performance in TBRs. This approach proves to be a good starting point during modeling of reactor packed with porous catalysts for any process to understand the significance of implementing $\eta_o$ properly during reactor performance prediction.

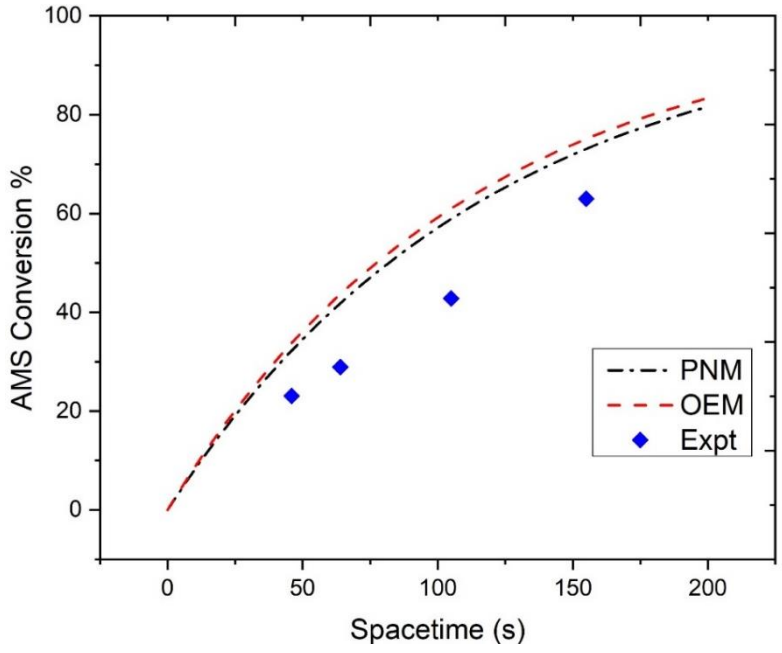


Figure A.9. Prediction of the reactor performance using PFM equations for hydrogenation of AMS with the overall effectiveness factor from PNM and OEM approach. (ug=0.038ms$^{-1}$, P=200 psig, $C_{AMS}$=230 mol m$^{-3}$)

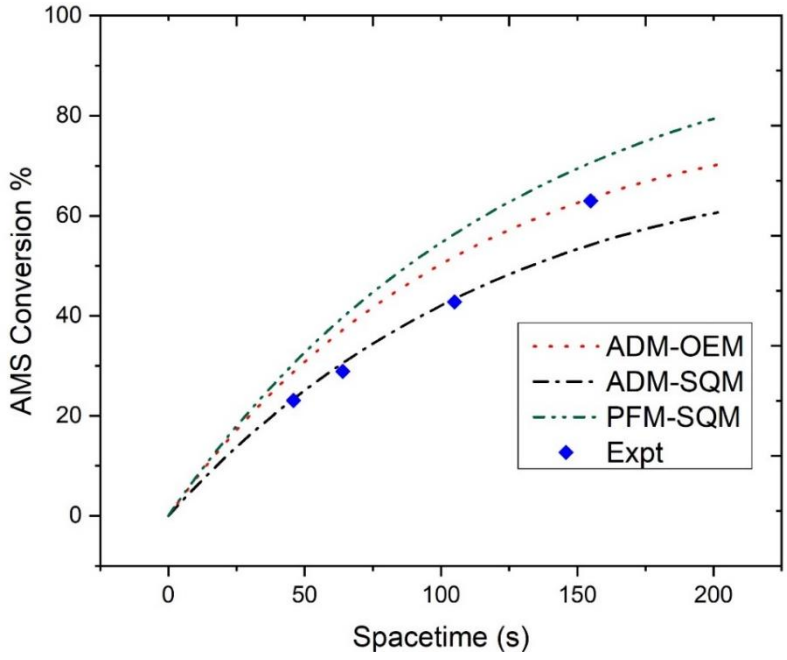


Figure A.10. Prediction of the reactor performance for hydrogenation of AMS using SQM and OEM approach with ADM and PFM equations (ug=0.038ms$^{-1}$, P=200 psig, $C_{AMS}$=230 mol m$^{-3}$)

The interfacial areas required for interphase transport (gas-liquid, liquid-solid, and gas-solid) are evaluated using the following correlations.

$$a_{GL} = 3.9x10^{-4}(1-\frac{\varepsilon_L}{\varepsilon_B})(\frac{S_X}{V_p})\,\mathrm{Re}_L^{0.4}(\frac{d_P}{D_R})^{-2} \tag{8}$$

$$a_{LS} = (1-\varepsilon_B)(\frac{S_X}{V_p})\eta_{CE} \tag{9}$$

$$a_{GS} = (1-\varepsilon_B)(\frac{S_X}{V_p})(1-\eta_{CE}) \tag{10}$$

$$(\Delta P)_{GL} = 3\,u_G^2\rho_G\,\frac{1-\varepsilon_b}{d_p\varepsilon_b}\,exp(8-1.12\,log\,Z-0.0769\;(log\,Z)^2+0.0152(log\,Z)^3 \tag{11}$$

(Holub model)

$$Z = \frac{Re_G^{1.167}}{Re_L^{0.767}} \quad (12)$$

$[\frac{\left(\frac{\Delta P}{Z}\right)}{\rho_L g}]$ - dimensionless pressure drop (the ratio of the pressure drop to the gravitational forces)

The molecular diffusivity $D_m$ (mutual diffusion coefficient of solute at very low concentrations in the solvent, $cm^2/s$ ) was evaluated from the correlation of Wilke and Chang (1955).

$$D_m = \frac{\left[7.4\ X\ 10^{-8}(\varphi_j M_j)^{\frac{1}{2}} T\right]}{(\mu_B\ V_A^{0.6})} \quad (13)$$

$V_A$- molal volume of solute at normal boiling point, cc/gmol (or) molar volume of solute A at its normal boiling temperature, $cm^2$ /mol

$\mu_B$ – viscosity of solvent B in cP

j – each species in the mixture

$M_j$ - molecular weight, g/mol

$\varphi_j$ -association parameter, the effective molecular weight of the solvent with respect to the diffusion process (obtained from Wilke and Chang (1955)

x=2.6 for water; x=1 for non-associated solvents.

The effective diffusivity, $D_e$ ,was derived from the equation with ε and τ represent porosity and tortuosity factor

$$D_e = \frac{\varepsilon}{\tau} D_m \quad (14)$$

Table.A.7. Correlations involved in the model (Downflow (Trickle flow))

| | | |
|---|---|---|
| Wetting efficiency | $\eta_{CE} = 1.617\ Re_L^{0.146}\ Ga_L^{-0.0711} \leq 1$<br>$\eta_{CE} = 1.104 Re_L^{0.33} \left[ \frac{1 + \left[ \frac{\left(\frac{\Delta P}{Z}\right)}{\rho_L g} \right]}{Ga_L} \right]^{1/9}$ | El-Hisnawi et al. (1982)<br>Al-Dahhan and Dudukovic (1995) at high pressure |
| Liquid –solid interface mass transfer coefficient | $k_{LS,A} = 4.25 * \frac{D_m \varepsilon_p}{d_p\ \eta_{CE}}\ Re_L^{0.48}\ Sc_L^{0.33}$ | Tan and Smith (1980) |
| Gas –solid interface mass transfer coefficient | $k_{GS,A} = 0.4548 \frac{u_g}{\varepsilon} Re_G^{-0.4069}\ Sc_G^{-0.667}$<br>$Sc_G = \frac{\mu}{\rho D_{m,G}}$ | Dwivedi and Upadhyah (1977) |
| Gas-liquid mass transfer coefficient, $(ka)_{GL}$ | $(ka)_{GL,A} = 2\ \frac{D_{mA}\left(1 - \frac{\varepsilon_L}{\varepsilon_B}\right)}{d_p^2}\ (\frac{S_x\, Re'_G}{d_p d_R})^{0.2}\ Re'^{0.73}_L Sc_L^{0.5}$<br>$Re_G = \frac{d_p u_G\, \rho}{\mu}$ | Fukushima and Kusaka (1977, a) |
| Liquid Hold up | $\varepsilon_L = \varepsilon_B \left[ 1 - 1.8 \left( \frac{S_x}{d_p^2} \right)^{0.075} Re'^{-0.15}_L Re'^{0.06}_G \left( \frac{d_p}{d_R} \right)^{0.3} \right]$<br>$\varepsilon_L = \varepsilon_B\ (1.8\ Re_L^{0.03} Re_G^{-0.28}\ )$ | Fukushima and Kusaka (1977) |
| Axial Dispersion Coefficient | $Pe_L^P = 2.3\ Re_L^{0.33}\ Ga_L^{-0.19}$<br>$Ga_L = \frac{g\ d_p^3 \varepsilon_B^2}{\nu_A (1 - \varepsilon_B^2)}$ | Cassanello et al. (1992) |

The gas-liquid equilibrium concentration was calculated from the following equation

$$H_i = \frac{C_{i,G}}{C_{i,L}}\Big|_{G-L\ interface} = \frac{C_{G,bulk}}{C_{i,e}} \quad (15)$$

Where $H_i$ is the Henry's constant which gives the solubility of hydrogen in alpha-methylstyrene; $C_{G,bulk}$ is the $H_2$ concentration which can be related to the vapor pressure.

## 5. CONCLUDING REMARKS

The sequential modeling model (SQM) approach incorporating the overall effectiveness factor from the pellet scale equations and integrating the value in reactor scale model equations with axial dispersion appropriately predicts the reactor performance for hydrogenation of AMS accounting for the inter- and intra-particle effects. The SQM approach does not involve any fitting or approximating the values of the effectiveness factor. The PNM approach of approximating the overall effectiveness factor as a fitted polynomial doesn't appropriately predict the reactor performance in comparison to the SQM due to the fitting errors. Moreover, using a single effectiveness factor for the whole bed calculated from the pellet scale equations and incorporating in reactor scale model with axial dispersion gave a good prediction of the reactor performance still it doesn't account for the change in the reactant concentrations axially which impact the local catalyst effectiveness factor. The implementation of different approaches and modeling information in this work to approximate the overall effectiveness factor while solving the reactor scale model provided will help researchers to understand the effect of approximating the catalyst effectiveness factor and improve the usage of pellet scale

equations while modeling their reactor system. These models and approaches will be useful in predicting the reactor performance and analyzing the desirable conditions to a degree of confidence even before conducting experiments. Moreover, this will help in reducing any errors caused during the design of the reactor and during scale-up.

## REFERENCES


1. Al-Dahhan, M.H., et al., *High-pressure trickle-bed reactors: A review.* Industrial & Engineering Chemistry Research, 1997. **36**(8): p. 3292-3314.

2. Ranade, V.V., R.V. Chaudhari, and P.R. Gunjal, *Trickle Bed Reactors: Reactor Engineering & Applications.* Trickle Bed Reactors: Reactor Engineering & Applications, 2011: p. 1-274.

3. Szukiewicz, M., Kaczmarski, K., & Petrus, R., *Modelling of fixed-bed reactor: two models of industrial reactor for selective hydrogenation of acetylene.* Chemical engineering science, 1998. **53**(1): p. 149-155.

4. Ancheyta, J., *Modeling and simulation of catalytic reactors for petroleum refining*. 2011: John Wiley & Sons.

5. El-Hisnawi, A.A., Duduković, M. P., & Mills, P. L. , *Trickle-Bed Reactors: Dynamic Tracer Tests, Reaction Studies, and Modeling of Reactor Performance.* Am. Chem. Soc. Symp. Ser, 1982. **196**: p. 421.

6. Guo, J. and M. Al-Dahhan, *A sequential approach to modeling catalytic reactions in packed-bed reactors.* Chemical Engineering Science, 2004. **59**(10): p. 2023-2037.

7. Guo, J. and M. Al-Dahhan, *Modeling catalytic trickle-bed and upflow packed-bed reactors for wet air oxidation of phenol with phase change.* Industrial & engineering chemistry research, 2005. **44**(17): p. 6634-6642.

8. Khadilkar, M.R., et al., *Comparison of trickle-bed and upflow reactor performance at high pressure: Model predictions and experimental observations.* Chemical Engineering Science, 1996. **51**(10): p. 2139-2148.

9. Ramachandran, P.A. and R.V. Chaudhari, *Three-phase catalytic reactors*. Vol. 2. 1983: Gordon & Breach Science Pub.

10. Ramachandran, P. and J. Smith, *Mixing-cell method for design of trickle-bed reactors.* The Chemical Engineering Journal, 1979. **17**(2): p. 91-99.

11. Fogler, H.S., *Elements of chemical reaction engineering*. 1999.

12. Szukiewicz, M.K., *New Approximate Model for Diffusion and Reaction in a porous catalyst.* AIChE Journal, 2000. **46**(3): p. 661-665.

13. Bischoff, K.B., *Effectiveness Factor for General Reaction Rate Forms.* AIChE Journal, 1965. **11**(2): p. 351-355.

14. Fletcher, T.H., J.H. Hong, and W.C. Hecker, *Predicting the effectiveness factor for mth order Langmuir rate equations in spherical coordinates.* Abstracts of Papers of the American Chemical Society, 1999. **218**: p. U641-U641.

15. Mears, D.E., *Tests for Transport Limitations in Experimental Catalytic Reactors.* Industrial & Engineering Chemistry Process Design and Development, 1971. **10**: p. 541-547.

16. Satterfield, C.N., *Trickle-bed reactors.* AIChE Journal, 1975. **21**(2): p. 209-228.

17. Ramachandran, P.A. and J.M. Smith, *Effectiveness factors in trickle-bed reactors.* AIChE Journal, 1979. **25**(3): p. 538-542.

18. Herskowitz, M., Carbonell, R. G., & Smith, J. M., *Effectiveness factors and mass transfer in trickle-bed reactors.* AIChE Journal, 1979. **25**(2): p. 272-283.

19. Lemcoff, N.O., Cukierman, A. L., & Martinez, O. M. , *Effectiveness factor of partially wetted catalyst particles: evaluation and application to the modeling of trickle bed reactors.* Catalysis Reviews Science and Engineering, 1988. **30**(3): p. 393-456.

20. Tan, C.S. and J.M. Smith, *Catalyst particle effectiveness with unsymmetrical boundary conditions.* Chemical Engineering Science, 1980. **35**(7): p. 1601-1609.

21. Beaudry, E.G., M.P. Duduković, and P.L. Mills, *Trickle-bed reactors: Liquid diffusional effects in a gas-limited reaction.* AIChE journal 1987. **33**(9): p. 1435-1447.

22. Aris, R., *On shape factors for irregular particles—I: The steady state problem. Diffusion and reaction.* Chemical Engineering Science, 1957. **6**(6): p. 262-268.

23. Duduković, M.P., *Catalyst effectiveness factor and contacting efficiency in trickle-bed reactors.* AIChE Journal, 1977. **23**(6): p. 940-944.

24. Goto, S., A. Lakota, and J. Levec, *Effectiveness factors of nth order kinetics in trickle-bed reactors.* Chemical Engineering Science, 1981. **36**(1): p. 157-162.

25. Haynes, H.W., *An explicit approximation for the effectiveness factor in porous heterogeneous catalysts.* Chemical Engineering Science, 1986. **41**(2): p. 412-415.

26. Mears, D.E., *The role of liquid holdup and effective wetting in the performance of trickle-bed reactors.* Chemical Reaction Engineering II ,ACS Monograph Series, 1974. **133**: p. 218.

27. Mills, P.L., & Duduković, M. P., *A dual-series solution for the effectiveness factor of partially wetted catalysts in trickle-bed reactors.* Industrial & Engineering Chemistry Fundamentals, 1979. **18**(2): p. 139-149.

28. Herskowitz, M., & Smith, J. M., *Trickle-bed reactors: A review.* AIChE Journal, 1983. **29**(1): p. 1-18.

29. Mills, P.L., & Duduković, M. P., *Analysis of catalyst effectiveness in trickle-bed reactors processing volatile or nonvolatile reactants.* Chemical Engineering Science, 1980. **35**(11): p. 2267-2279.

30. Goto, S., Lakota, A., & Levec, J., *Effectiveness factors of nth order kinetics in trickle-bed reactors.* Chemical Engineering Science, 1981. **36**(1): p. 157-162.

31. Martinez, O.M., Barreto, G. F., & Lemcoff, N. O. , *Effectiveness factor of a catalyst pellet in a trickle bed reactor: limiting reactant in the gas phase.* Chemical Engineering Science, 1981. **36**(5): p. 901-907.

32. Sakornwimon, W., and Nicholas D. Sylvester, *Effectiveness Factors for Partially Wetted Catalysts in Trickle-Bed Reactors.* Industrial & Engineering Chemistry Process Design and Development, 1982. **21**(1): p. 16-25.

33. Beaudry, E.G., Duduković, M. P., & Mills, P. L. , *Trickle-bed reactors: Liquid diffusional effects in a gas-limited reaction.* AIChE journal 1987. **33**(9): p. 1435-1447.

34. Rajashekharam, M.V., Jaganathan, R., & Chaudhari, R. V., *A trickle-bed reactor model for hydrogenation of 2, 4 dinitrotoluene: experimental verification.* Chemical Engineering Science, 1998. **53**(4): p. 787-805.

35. Tan, C.S., & Smith, J. M. , *Catalyst particle effectiveness with unsymmetrical boundary conditions.* Chemical Engineering Science, 1980. **35**(7): p. 1601-1609.

36. Dudukovic, M.P., Kuzeljevic, Ž. V., & Combest, D. P., *Three-Phase Trickle-Bed Reactors*, in *Ullmann's Encyclopedia of Industrial Chemistry*. 2008.

37. Julcour, C., Jaganathan, R., Chaudhari, R. V., Wilhelm, A. M., & Delmas, H., *Selective hydrogenation of 1, 5, 9-cyclododecatriene in up-and down-flow fixed-bed reactors: experimental observations and modeling.* Chemical Engineering Science, 2001. **56**(2): p. 557-564.

38. Knudsen, C.W., Roberts, G. W., & Satterfield, C. N., *Effect of geometry on catalyst effectiveness factor. Langmuir-Hinshelwood kinetics.* Industrial & Engineering Chemistry Fundamentals, 1966. **5**(3): p. 325-326.

39. Mills, P.L., Erk, H. F., Evans, J., & Duduković, M. P. , *Some comments on models for evaluation of catalyst effectiveness factors in trickle-bed reactors.* Chemical Engineering Science, 1981. **36**(5): p. 947-950.

40. Jiang, Y., et al., *Two-phase flow distribution in 2D trickle-bed reactors.* Chemical Engineering Science, 1999. **54**(13-14): p. 2409-2419.

41. Tukac, V. and J. Hanika, *Catalytic oxidation of substituted phenols in a trickle bed reactor.* Collection of Czechoslovak Chemical Communications, 1997. **62**(6): p. 866-874.

42. Herrmann, U. and G. Emig, *Liquid phase hydrogenation of maleic anhydride to 1, 4-butanediol in a packed bubble column reactor.* Industrial & engineering chemistry research, 1998. **37**(3): p. 759-769.

43. Chaudhari, R.V., et al., *Hydrogenation of 1, 5, 9-cyclododecatriene in fixed-bed reactors: Down-vs. upflow modes.* AIChE journal, 2002. **48**(1): p. 110-125.

44. Dietz, A., et al., *Selective hydrogenation in trickle-bed reactor: experimental and modelling including partial wetting.* Catalysis today, 2003. **79**: p. 293-305.

45. Avraam, D.G. and I.A. Vasalos, *HdPro: a mathematical model of trickle-bed reactors for the catalytic hydroprocessing of oil feedstocks.* Catalysis Today, 2003. **79**: p. 275-283.

46. Guo, J., & Al-Dahhan, M. , *Modeling catalytic trickle-bed and upflow packed-bed reactors for wet air oxidation of phenol with phase change.* Industrial & engineering chemistry research, 2005. **44**(17): p. 6634-6642.

47. Suwanprasop, S., et al., *Scale-up and modeling of fixed-bed reactors for catalytic phenol oxidation over adsorptive active carbon.* Industrial & engineering chemistry research, 2005. **44**(25): p. 9513-9523.

48. Guo, J., Y. Jiang, and M.H. Al-Dahhan, *Modeling of trickle-bed reactors with exothermic reactions using cell network approach.* Chemical Engineering Science, 2008. **63**(3): p. 751-764.

49. Roininen, J. and V. Alopaeus, *The moment method for one-dimensional dynamic reactor models with axial dispersion.* Computers & Chemical Engineering, 2011. **35**(3): p. 423-433.

50. Wu, Q., et al., *Modeling of a pilot-scale trickle bed reactor for the catalytic oxidation of phenol.* Separation and Purification Technology, 2009. **67**(2): p. 158-165.

51. Magoo, A.K., A. Mittal, and S. Roy, *Modeling Packed Bed Fischer–Tropsch Reactors with Phase Evolution.* Indian Chemical Engineer, 2013. **55**(1): p. 29-37.

52. Kilpiö, T., et al., *Modeling of Direct Synthesis of Hydrogen Peroxide in a Packed-Bed Reactor.* Industrial & Engineering Chemistry Research, 2012. **51**(41): p. 13366-13378.

53. Durante, D., et al., *Modeling and simulation of a small-scale trickle bed reactor for sugar hydrogenation.* Computers & Chemical Engineering, 2014. **66**: p. 22-35.

54. Ghouri, M.M., et al., *Multi-scale modeling of fixed-bed Fischer Tropsch reactor.* Computers & Chemical Engineering, 2016. **91**: p. 38-48.

55. Khadilkar, M.R., Wu, Y. X., Al-Dahhan, M. H., Duduković, M. P., & Colakyan, M., *Comparison of trickle-bed and upflow reactor performance at high pressure: Model predictions and experimental observations.* Chemical Engineering Science, 1996. **51**(10): p. 2139-2148.

56. Cassanello, M.C., O.M. Martinez, and A.L. Cukierman, *Effect of the Liquid Axial-Dispersion on the Behavior of Fixed-Bed 3-Phase Reactors*. Chemical Engineering Science, 1992. **47**(13-14): p. 3331-3338.

57. Wu, Y., et al., *Comparison of upflow and downflow two-phase flow packed-bed reactors with and without fines: experimental observations*. Industrial & engineering chemistry research, 1996. **35**(2): p. 397-405.

# APPENDIX B.

# CATALYST REGENERATION TESTS

The catalyst after subjecting to thermal treatment at 10°C/min to 1000 °C was tested for liquid phase hydrogenation of acetylene reaction. It was observed that eh regenerated catalyst showed good conversion with about 75% at low LHSVs. Although the conversion was significantly low at higher liquid velocities, the catalyst was efficient. More detailed study in this area which accounts for deactivation is recommended.

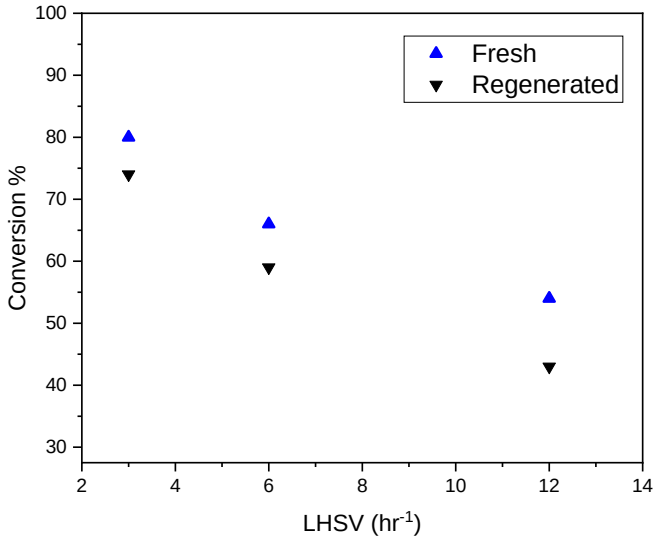


Figure B.1.Reactor performance in trickle flow using fresh and regenerated catalyst (P=250 psig, T=100°C, $u_g$=0.08 m/s)

# APPENDIX C.

# EXPERIMENTAL SETUP


Figure C.1. High Pressure High Temperature Experimental facility with explosion shield

Figure C.2. Reactors (From left) Thermowell reactor,1inch ID,60 cm long , Thermowell 1.4cm OD, 54cm long;  reactor with distributor 1inch ID, 60 cm long; gas-liquid distributor

Figure C.3. Mini Basket Reactor - 300mL volume with Basket and Slurry compatibility, Maximum T-500$^{o}$C and P-2000 psig

Figure C.4. Experimental setup used for Residence Time Distribution experiments using Liquid Tracer

# BIBLIOGRAPHY


1. Alshammari, A., Kalevaru, V. N., Bagabas, A., & Martin, A., *Production of Ethylene and its Commercial Importance in the Global Market*, in *Petrochemical Catalyst Materials, Processes, and Emerging Technologies*. 2016, IGI Global. p. 82-115.

2. True, W.R., *Global ethylene capacity poised for major expansion.* Oil & gas journal, 2013. **111**(7): p. 90-95.

3. Cavani, F., N. Ballarini, and A. Cericola, *Oxidative dehydrogenation of ethane and propane: How far from commercial implementation?* Catalysis Today, 2007. **127**(1-4): p. 113-131.

4. Bos, A.N.R. and K.R. Westerterp, *Mechanism and kinetics of the selective hydrogenation of ethyne and ethene.* Chemical Engineering and Processing, 1993. **32**: p. 1-7.

5. Edvinsson, R.K., A.M. Holmgren, and S. Irandoust, *Liquid-Phase Hydrogenation of Acetylene in a Monolithic Catalyst Reactor.* Industrial & engineering chemistry research, 1995. **34**(1): p. 94-100.

6. Men'shchikov, V.A., Fal'kovich, Y. G., & Aerov, M. E., *Liquid-phase hydrogenation of acetylene in pyrolysis gas in presence of heterogeneous catalysts at atmospheric pressure.* J. Appl. Chem. USSR, 1983. **56**.

7. Bos, A.N.R., Hof, E., Kuper, W., Westerterp, K. R., *The behaviour of a single catalyst pellet for the selective hydrogenation of ethyne in ethene.* Chemical engineering science, 1993. **48**(11): p. 1959-1969.

8. Asplund, S., Fornell, C., Holmgren, A., & Irandoust, S., *Catalyst deactivation in liquid- and gas-phase hydrogenation of acetylene using a monolithic catalyst reactor*. Catalysis Today, 1995. **24**: p. 181-187.

9. Godínez, C., a.L. Cabanes, and G. Víllora, *Experimental Study of the Selective Hydrogenation of Steam Cracking C 2 Cut. Front End and Tail End Variants.* Chemical Engineering Communications, 1998. **164**: p. 225-247.

10. Borodziński, A. and G.C. Bond, *Selective Hydrogenation of Ethyne in Ethene-Rich Streams on Palladium Catalysts. Part 1. Effect of Changes to the Catalyst During Reaction.* Catalysis Reviews, 2006. **48**(2): p. 91-144.

11. Leviness, S., Nair, V., Weiss, A. H., Schay, Z., & Guczi, L., *Acetylene hydrogenation selectivity control on PdCu/Al2O3 catalysts.* Journal of Molecular Catalysis, 1984. **25**: p. 131-140.

12. Sarkany, A., Weiss, A. H., Szilagyi, T., Sandor, P., Guczi, L. , *Green oil poisoning of a Pd/Al203 acetylene hydrogenation catalyst.* Applied Catalysis, 1984. **12**: p. 373-379.

13. Park, Y.H., & Price, G. L., *Deuterium tracer study on the effect of carbon monoxide on the selective hydrogenation of acetylene over palladium/aluminA.* Industrial & Engineering Chemistry Research, 1991. **30**: p. 1693-1699.

14. Westerterp, Roel, René Bos, Ruud Wijngaarden, Wout Kusters, and Albert Martens, *Selective hydrogenation of acetylene in an ethylene stream in an adiabatic reactor*. Chemical engineering & technology, 2002. **25**(5): p. 529-539.

15. McGown, William T., Charles Kemball, David A. Whan, and Michael S. Scurrell, *Hydrogenation of acetylene in excess ethylene on an alumina supported palladium catalyst in a static system.* Journal of the Chemical Society, Faraday Transactions 1: Physical Chemistry in Condensed Phases, 1977. **73**: p. 632-647.

16. Al-Ammar, A.S. and G. Webb, *Hydrogenation of acetylene over supported metal catalysts. Part 3.—[14C]tracer studies of the effects of added ethylene and carbon monoxide on the reaction catalysed by silica-supported palladium, rhodium and iridium.* Journal of the Chemical Society, Faraday Transactions 1: Physical Chemistry in Condensed Phases, 1979. **75**: p. 1900-1911.

17. Sarkany, A., L. Guczi, and A.H. Weiss, *On the aging phenomenon in palladium catalysed acetylene hydrogenation.* Applied catalysis, 1984. **10**(3): p. 369-388.

18. Cider, L., & Schoon, N. H., *Competition between ethyne, ethene and carbon monoxide for the active sites during hydrogenation at transient conditions over supported metal catalysts.* Applied Catalysis, 1991. **68**: p. 191-205.

19. Borodziński, A. and G.C. Bond, *Selective Hydrogenation of Ethyne in Ethene-Rich Streams on Palladium Catalysts, Part 2: Steady-State Kinetics and Effects of Palladium Particle Size, Carbon Monoxide, and Promoters.* Catalysis Reviews, 2008. **50**(3): p. 379-469.

20. Bos, A.N.R., Botsma, E. S., Foeth, F., Sleyster, H. W. J., Westerterp, K. R., *A kinetic study of the hydrogenation of ethyne and ethene on a commercial Pd/Al2O3 catalyst.* Chemical Engineering and Processing, 1993. **32**: p. 53-63.

21. Bond, G.C., *Catalysis by Metals.* 1962.

22. Bond, G.C., *The hydrogenation of acetylene III. The Reaction of Acetylene with Hydrogen Catalyzed by Alumina-Supported Rhodium and Iridium.* Journal of Catalysis, 1966. **6**: p. 397-410.

23. Bond, G.C., *The hydrogenation of acetylene: V. The reaction of acetylene with hydrogen and deuterium catalyzed by alumina-supported ruthenium and osmium.* Journal of Catalysis, 1966. **6**: p. 397-410.

24. Bond, G.C. and P.B. Wells, *The hydrogenation of acetylene: IV. The reaction of acetylene with deuterium catalyzed by alumina-supported rhodium, palladium, iridium, and platinum.* Journal of Catalysis, 1966. **6**: p. 397-410.

25. Bond, G.C., Dowden, D. A., Mackenzie, N., *The selective hydrogenation of acetylene*, in *Transactions of the Faraday Society*. 1958. p. 1537.

26. Bond, G.C. and P.B. Wells, *The hydrogenation of acetylene I. The Reaction of Acetylene with Hydrogen Catalyzed by Alumina-Supported Platinum.* Catalysis, 1965. **4**: p. 211-219.

27. Bond, G.C. and P.B. Wells, *The Mechanism of the Hydrogenation of Unsaturated Hydrocarbons on Transition Metal Catalysts.* Advances in Catalysis, 1965. **15**: p. 91-226.

28. Bond, G.C. and P.B. Wells, *The hydrogenation of acetylene: II. The reaction of acetylene with hydrogen catalyzed by alumina-supported palladium.* Journal of Catalysis, 1966. **5**(1): p. 65-73.

29. Borodziński, A. and A. Cybulski, *The kinetic model of hydrogenation of acetylene–ethylene mixtures over palladium surface covered by carbonaceous deposits.* Applied Catalysis A: General, 2000. **198**: p. 51-66.

30. Borodziński, A., *Hydrogenation of acetylene–ethylene mixtures on a commercial palladium catalyst.* Catalysis letters, 1999. **63**(1-2): p. 35-42.

31. Men'shchikov, V., Y.G. Fal'kovich, and M. Aerov, *Hydrogenation kinetics of acetylene on a palladium catalyst in the presence of ethylene.* Kinet. Catal.(USSR)(Engl. Transl.);(United States), 1975. **16**(6).

32. Pachulski, A., R. Schödel, and P. Claus, *Performance and regeneration studies of Pd–Ag/Al2O3 catalysts for the selective hydrogenation of acetylene.* Applied Catalysis A: General, 2011. **400**(1-2): p. 14-24.

33. Pachulski, A., R. Schödel, and P. Claus, *Kinetics and reactor modeling of a Pd-Ag/Al2O3 catalyst during selective hydrogenation of ethyne.* Applied Catalysis A: General, 2012. **445-446**: p. 107-120.

34. Zhang, Q., Li, J., Liu, X., & Zhu, Q, *Synergetic effect of Pd and Ag dispersed on Al2O3 in the selective hydrogenation of acetylene.* Applied Catalysis A: General, 2000. **197**: p. 221-228.

35. Zhang, Y., Diao, W., Williams, C. T., & Monnier, J. R., *Selective hydrogenation of acetylene in excess ethylene using Ag- and Au-Pd/SiO2 bimetallic catalysts prepared by electroless deposition.* Applied Catalysis A: General, 2014. **469**: p. 419-426.

36. Guczi, L. and Z. Schay, *Role of bimetallic catalysts in catalytic hydrogenation and hydrogenolysis*, in *Studies in Surface Science and Catalysis*. 1986, Elsevier. p. 313-335.

37. Wang, B. and G.F. Froment, *Kinetic Modeling and Simulation of the Selective Hydrogenation of the C 3 -Cut of a Thermal Cracking Unit.* Ind. Eng. Chem. Res., 2005. **44**: p. 9860-9867.

38. Lee, D.K., *Green-oil formation and selectivity change in selective hydrogenation on titania-supported and unsupported palladium catalyst for acetylene removal from ethylene-rich stream.* Korean Journal of Chemical Engineering, 1990. **7**(3): p. 233-235.

39. Moses, J. M., Weiss, A. H., Matusek, K., & Guczi, L., *The effect of catalyst treatment on the selective hydrogenation of acetylene over palladium/alumina.* Journal of Catalysis, 1984. **86**: p. 417-426.

40. Wehrli, J.T., Thomas, D. J., Wainwright, M. S., Trimm, D. L., & Cant, N. W., *Reduced Foulant Formation During the Selective Hydrogenation of C2, C3, and C4 Acetylenes.pdf.* Studies in Surface Science and Catalysis, 1991. **68**: p. 203-210.

41. Al-Ammar, A.S. and G. Webb, *Hydrogenation of acetylene over supported metal catalysts. Part 2.—[14 C] tracer study of deactivation phenomena.* Journal of the Chemical Society, Faraday Transactions 1: Physical Chemistry in Condensed Phases, 1978. **74**: p. 657-664.

42. Lee, J. M., Palgunadi, J., Kim, J. H., Jung, S., Choi, Y. S., Cheong, M., & Kim, H. S., *Selective removal of acetylenes from olefin mixtures through specific physicochemical interactions of ionic liquids with acetylenes.* Physical Chemistry Chemical Physics, 2010. **12**(8): p. 1812-1816.

43. Hou, R., T. Wang, and X. Lan, *Enhanced Selectivity in the Hydrogenation of Acetylene due to the Addition of a Liquid Phase as a Selective Solvent.* Industrial & Engineering Chemistry Research, 2013. **52**(37): p. 13305-13312.

44. Shitova, N. B., D. A. Shlyapin, T. N. Afonasenko, E. N. Kudrya, P. G. Tsyrul'nikov, and V. A. Likholobov, *Liquid-phase hydrogenation of acetylene on the Pd/sibunit catalyst in the presence of carbon monoxide.* Kinetics and Catalysis, 2011. **52**: p. 251-257.

45. Johnson, M., E. Peterson, and S. Gattis, *Process for liquid phase hydrogenation*. 2005, Google Patents.

46. Johnson, M.M., Edward R. Peterson, and Sean C. Gattis, *United States Patent No. 7,045,670.* 2006.

47. Gattis, S.C., E.R. Peterson, and M.M. Johnson, *The ÉCLAIRS process for converting natural gas to hydrocarbon liquids*. 2004, Dallas, TX: Synfuels International.

48. Hou, R.J., X.C. Lan, and T.F. Wang, *Selective hydrogenation of acetylene on Pd/SiO2 in bulk liquid phase: A comparison with solid catalyst with ionic liquid layer (SCILL).* Catalysis Today, 2015. **251**: p. 47-52.

49. Afonasenko, T. N., Smirnova, N. S., Temerev, V. L., Leont'eva, N. N., Gulyaeva, T. I., & Tsyrul'nikov,P.G., *Pd/Ga2O3–Al2O3 catalysts for the selective liquid-phase hydrogenation of acetylene to ethylene*. Kinetics and Catalysis, 2016. **57**(4), 490-496.

50. Huang, B., Wang, T., Lei, C., Chen, W., Zeng, G., & Maran, F, *Highly efficient and selective catalytic hydrogenation of acetylene in N, N-dimethylformamide at room temperature.* Journal of catalysis, 2016. **339**: p. 14-20.

51. Al-Dahhan, M. H., Larachi, F., Dudukovic, M. P., & Laurent, A., *High-pressure trickle-bed reactors: a review.* Industrial & engineering chemistry research, 1997. **36**(8): p. 3292-3314.

52. Duduković, M.P., F. Larachi, and P.L. Mills, *Multiphase catalytic reactors: a perspective on current knowledge and future trends.* Catalysis reviews, 2002. **44**(1): p. 123-246.

53. Ranade, V.V., R. Chaudhari, and P.R. Gunjal, *Trickle bed reactors: Reactor engineering and applications*. 2011: Elsevier.

54. Sie, S., *Scale effects in laboratory and pilot-plant reactors for trickle-flow processes.* Revue de l'Institut français du pétrole, 1991. **46**(4): p. 501-515.

55. Gierman, H., *Design of laboratory hydrotreating reactors: scaling down of trickle-flow reactors.* Applied Catalysis, 1988. **43**(2): p. 277-286.

56. Al-Dahhan, M.H. and M.P. Duduković, *Catalyst bed dilution for improving catalyst wetting in laboratory trickle-bed reactors.* AIChE journal, 1996. **42**(9): p. 2594-2606.

57. Al-Dahhan, M.H., Y. Wu, and M.P. Dudukovic, *Reproducible technique for packing laboratory-scale trickle-bed reactors with a mixture of catalyst and fines.* Industrial & engineering chemistry research, 1995. **34**(3): p. 741-747.

58. Guo, J. and M. Al-Dahhan, *Catalytic wet air oxidation of phenol in concurrent downflow and upflow packed-bed reactors over pillared clay catalyst.* Chemical Engineering Science, 2005. **60**(3): p. 735-746.

59. Wu, Y., Khadilkar, M.R., Al-Dahhan, M.H. and Duduković, M.P., *Comparison of upflow and downflow two-phase flow packed-bed reactors with and without fines: experimental observations.* Industrial & engineering chemistry research, 1996. **35**(2): p. 397-405.

60. Sie, S. and R. Krishna, *Process development and scale up: III. Scale-up and scale-down of trickle bed processes.* Reviews in Chemical Engineering, 1998. **14**(3): p. 203-252.

61. Hall, K.R., A new gas to liquids (GTL) or gas to ethylene (GTE) technology. Catalysis Today, 2005. **106**(1-4): p. 243-246

62. Global Demand For Polyethylene To Reach 99.6 Million Tons In 2018, in Pipeline and gas Journal. 2014.

63. Harris, H. and J. Prausnitz, *Thermodynamics of solutions with physical and chemical interactions. solubility of acetylene in organic solvents.* Industrial & Engineering Chemistry Fundamentals, 1969. **8**(2): p. 180-188.

64. Smirnova, N. S., Shlyapin, D. A., Mironenko, O. O., Anoshkina, E. A., Temerev, V. L., Shitova, N. B. & Tsyrul'nikov, P. G., *EXAFS study of Pd/Ga2O3 model catalysts of selective liquid-phase hydrogenation of acetylene to ethylene.* Journal of Molecular Catalysis A: Chemical, 2012. **358**: p. 152-158.

# VITA

Humayun Shariff was born in Chennai, India. He obtained his Bachelor of Technology degree in Chemical Engineering with distinction from Anna University, India. During his undergraduate studies, his research training at the Central Leather Research Institute (CLRI), India focused on biodiesel production. This research interest encouraged him to pursue a master's degree. He received admission to the master of science program in the Chemical and Biochemical Engineering Department at Missouri University of Science and Technology, where his research was co-advised by Dr. Paul Nam and Dr. Muthanna Al-Dahhan. He received his Master of Science in Chemical Engineering from Missouri S&T in December 2010. Humayun was determined to continue his education further. In 2015, he was accepted to the Ph.D. program in the Department of Chemical and Biochemical Engineering, where he joined Dr. Al-Dahhan's research group to expand his research interests. During his Ph.D., he received a Certificate in Lean Six Sigma from Missouri S&T in May 2018. Humayun presented his research in many conferences and published a paper in the Catalysis Journal. In May 2020, Humayun Shariff received his Ph.D. in Chemical Engineering from Missouri University of Science and Technology.